ALLOCENTRIC VERSUS EGOCENTRIC REPRESENTATIONS FOR VISUAL MEMORY AND ACTION IN HUMAN CORTEX

YING CHEN

A DISSERTATION SUBMITTED TO THE FACULTY OF GRADUATE STUDIES
IN PARTIAL FULFILLMENT OF THE REQUIREMENTS
FOR THE DEGREE OF
DOCTOR OF PHILOSOPHY

Graduate Program in
KINESIOLOGY & HEALTH SCIENCE
YORK UNIVERSITY
TORONTO, ONTARIO
June, 2016

ABSTRACT

In daily life, people frequently perform various aiming movements, such as reaching or making a saccade toward a cellphone. The early stage for executing such movements is to localize the target location precisely. A visual target can be represented and maintained in memory in two main reference frames: egocentric (body-fixed) or allocentric (world-fixed). However, the neural mechanisms for the allocentric spatial processing are poorly understood and for the Allo-Ego conversion are still unknown in humans.

This thesis investigated the allocentric and egocentric mechanisms with a focus on target memory coding for reaching (study 1) and saccades (study 2) in healthy humans using event-related functional magnetic resonance imaging (fMRI) designs where the phase of memorized target representation was separated from the phase of motor planning and execution. I further examined neural substrates for Allo-Ego conversion of targets for reach in study 3 using different types of cues to specify reach target direction for two reach tasks before delay or response phases.

I observed widely overlapping cortical areas in the egocentric and allocentric reach tasks as compared to the control, but higher activation in parietofrontal areas for the former, and higher activation in early visual areas for the latter. Further, directional selectivity in egocentric coordinates (target relative to gaze/midline) was observed in superior occipital and inferior occipital gyrus; on the other hand, directional selectivity in allocentric coordinates (target relative to a landmark) was revealed in inferior temporal gyrus and inferior occipital gyrus. These results indicate that different cortical mechanisms are involved in the representations of remembered reach targets. I found similar pattern of task-relevant

activation and egocentric directional selectivity in the saccade study. However, different areas from those observed in the reach study showed allocentric directional selectivity of remembered saccade targets including precuneus and midposterior intraparietal sulcus, suggesting effector-specific (eye vs. hand) neural mechanisms. In study 3, I identified four areas in parietal and frontal cortex, i.e., posterior precuneus, angular gyrus, supramarginal gyrus and medial frontal gyrus that are specifically involved in converting allocentric target coding to egocentric representation as soon as the final target location for reach is specified.

This dissertation is dedicated to my beloved husband Hong.
I am truly thankful for having you in my life.
This work is also dedicated to my parents, Huamin and Jing.

Thank all of you for your love, support and inspiration.
I could not have made this without you all.

ACKNOWLEDGEMENTS

First and foremost, I would like to extend great and special thanks to my graduate supervisor, Dr. Doug Crawford. Thank you for accepting me as your PhD student, and for your always support, encouragement and trust throughout those years in your laboratory. I have not only learned broad knowledge and skills from you, but more importantly, obtained different perspectives to think about how to lead and conduct research on my own in the future. You have been my role model to be an excellent researcher and mentor.

I thank the members of my thesis committee – Melvyn Goodale, Shayna Rosenbaum, Denise Henriques, Lauren Sergio, and William Gage – for your carefully reading and valuable feedback on my thesis that have improved my project and provided insights into what needs to be thought about in my future research in neuroscience.

Thank you to Joy Williams for your help with fMRI data collection. Without your support, I would have had more challenges to complete my experiments. To Bianca-Ruxandra Baltaretu, I appreciate your help whenever I needed, and your time spending on reading my thesis.

TABLE OF CONTENTS

LIST OF TABLES

LIST OF FIGURES

CHAPTER ONE

GENERAL INTRODUCTION

To perform an aiming movement at a remembered object, one must encode and maintain its location in memory. In principle, the location of an object in space can be represented in two main reference frames: egocentric and allocentric (Howard and Templeton, 1966; Vogeley and Fink, 2003). A reference frame can be defined as a means of representing the locations of objects in space (Klatzky, 1998). In the egocentric (body-fixed, viewer-fixed) frames, the locations of targets are coded relative to the axes (left-right, front-back, up-down) of the observer's body part, such as the eyes, head, or arm. On the other hand, in the allocentric (world-fixed, earth-fixed) frames where the world can be assumed to be stable, typically there are three orthogonal axes outside the viewer, one corresponding to the gravitational axis of the world and the other two in the horizontal directions along the current plane (Wexler, 2003; Coluccia et al., 2007). There are at least two types of allocentric coding of visual targets associated with allocentric frames: the location of a target represented relative to an external landmark in the scene where the origin and the set of axes are centered on the landmark (allocentric cue), and the target location of the subpart of an object represented relative to the object itself where the origin and the set of axes are centered on the intrinsic sides of the object (Marr and Nishihara, 1978; Humphreys, 1983; Deneve and Pouget, 2003; Wexler, 2003; Coluccia et al., 2007). The former is usually referred to allocentric representation / coding, whereas the latter is referred to object-centered representation / coding.

Here I take an example close to a real situation to demonstrate the two types of spatial coding of a visual target: egocentric and allocentric. As illustrated in Figure 1.1, a person is sitting at his desk and reading a book; there are a laptop and a cup of coffee on his desk. He is reaching to the cup of coffee (the target). The location of the cup can be defined in

egocentric frames of reference, such as his eyes (gaze) and his hand. Alternatively, the cup can be represented in an allocentric frame of reference, e.g., relative to his laptop (an allocentric cue), independent of his eyes and hand orientation and position. Accordingly, as shown in Figure 1.1, the cup is located right of his gaze in the egocentric reference frame, but left of his laptop in the allocentric reference frame. It would be better to indicate that the book can be also used as an allocentric cue to represent the cup so that the cup is located to right of the book, similar to its egocentric direction in the eye-centered coordinates. In most natural cases, there are multiple objects in the scenes, and sometimes the target location in the egocentric reference frames is overlapping with that in the allocentric ones. It has been suggested that the two types of cue can be combined in a real-world environment, based on their reliability and stability (Byrne and Crawford, 2010).

Likewise, a number of behavioral studies have shown that visual targets can be represented and maintained in memory for a delayed movement in egocentric (McIntyre et al., 1997; Henriques et al., 1998; Vindras and Viviani, 1998; Burnod et al., 1999; Pouget et al., 2002; Crawford et al., 2004; Lemay and Stelmach, 2005; Brouwer and Knill, 2007) and allocentric frames of reference (Goodale and Haffenden, 1998; Carrozzo et al., 2002; Obhi and Goodale, 2005; Chen et al., 2011). The next questions are how and where this egocentric or allocentric spatial coding is processed in the brain. Over the past years, neurophysiological studies and human neuroimaging studies have explored the neural mechanisms for egocentric target coding and motor planning (Andersen et al., 1993; Batista et al., 1999; Connolly et al., 2000; DeSouza et al., 2000; Astafiev et al., 2003; Connolly et al., 2003; DeSouza et al., 2003; Medendorp et al., 2003; Prado et al., 2005; Connolly et al., 2007; Fernandez-Ruiz et

al., 2007; Beurze et al., 2010). However, the neural substrates for allocentric coding of remembered targets for movements are essentially unknown.

My doctoral dissertation focused on the neural mechanisms for the allocentric coding of reach and saccade targets, and distinguished between allocentric versus egocentric mechanisms. In addition, the brain areas involved in the conversion of allocenric to egocentric target representations for reaching were investigated as well. I completed three studies using functional magnetic resonance imaging (fMRI).

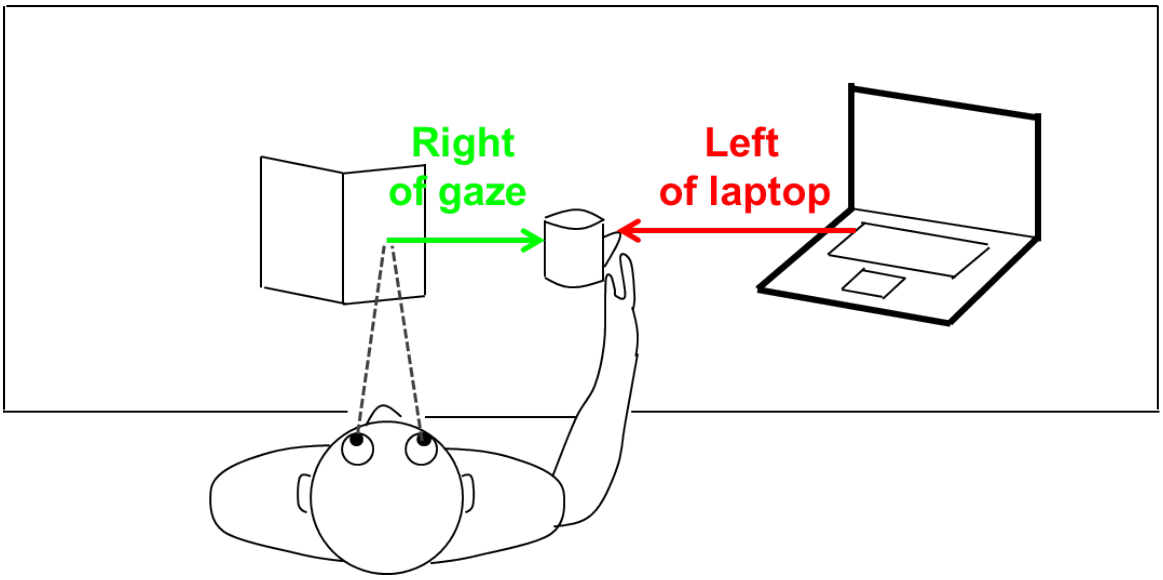

Figure 1.1 Demonstration of the two reference frames for target coding. As depicted in this example, a person is sitting at his desk and reading a book; there are a cup of coffee and a laptop on his desk. He is reaching to his cup. As shown here, the location of this cup (reaching target) can be represented right relative to his gaze, which is in an egocentric reference frame, or defined left relative to the laptop, which is in an allocentric reference frame where the laptop is used as an allocentric landmark.

1.1 Two visual streams

To better understand the neural mechanisms for allocentric versus egocentric spatial coding, it is important to describe the two cortical visual streams, the ventral stream and the dorsal stream (Figure 1.2). The two streams arise from the early visual areas (V1), but the ventral stream projects to the infero-temporal cortex through areas V2, V3, V4, TE and TEO, whereas the dorsal stream terminates in the posterior parietal cortex via a number of routes involving areas V2, MT and MST (Ungerleider and Mishkin, 1982).

In 1992 Milner and Goodale proposed a highly influential perception- action model for cortical visual processing related to these two streams (Goodale and Milner, 1992; Milner and Goodale, 1995, 2006, 2008). The important point in this model is that both streams process information about the property of objects including size, shape and spatial location, but they process visual information in different ways. According to this model, both streams can contribute to spatial coding of targets, but the dorsal stream computes the absolute metrics of the target in egocentric reference frames to perform a goal-directed movement that requires a moment-to-moment update. In contrast, the ventral stream must take into account the spatial relations between targets and the relevant allocentric visual cues, i.e., defining the target in allocentric reference frames that can be retained in memory over long time intervals (Goodale and Milner, 1992; Milner and Goodale, 1995, 2006, 2008). Behavioral studies have looked at the rates of decay in these two types of spatial representations for arm movements (Elliott and Madalena, 1987; McIntyre et al., 1997; Hu et al., 1999; Bradshaw and Watt, 2002). The results showed that egocentric representations of targets degrade after a memory delay of 2 s. In comparison, the target location represented in allocentric reference

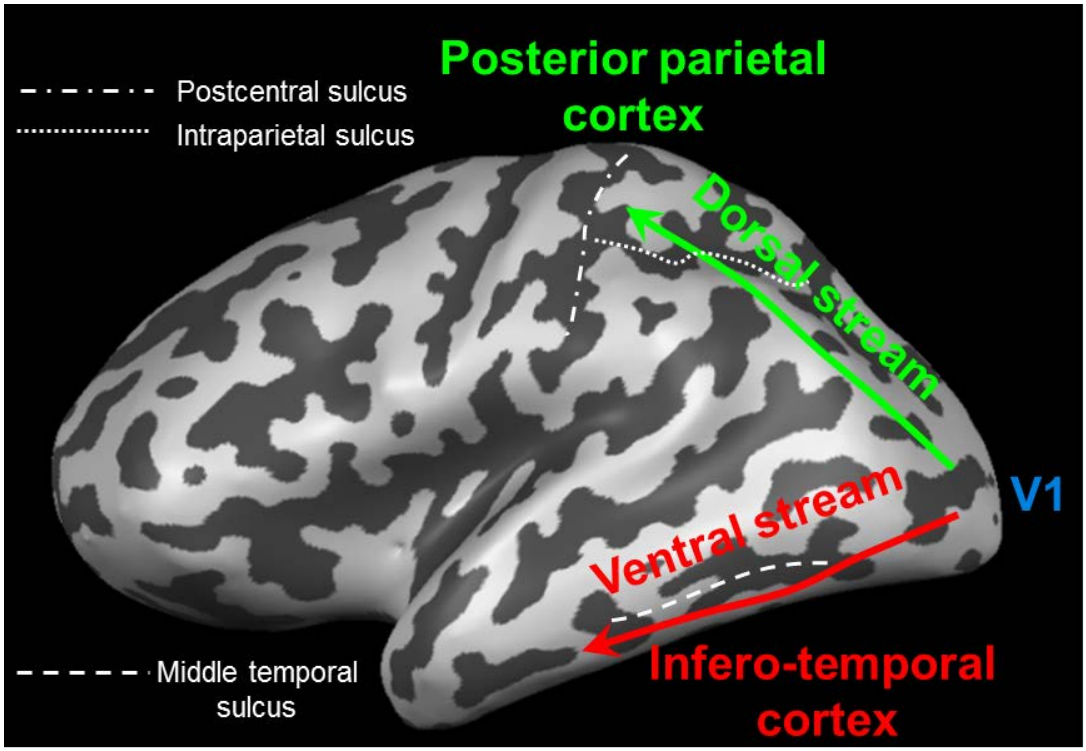

Figure 1.2 The two visual streams in the human brain. As illustrated in the left hemisphere of the inflated brain, both dorsal and ventral streams arise from primary visual cortex (V1). The dorsal stream (green) projects to the posterior parietal cortex. The ventral stream (red) terminates in the infero-temporal cortex.

frames can be maintained over longer memory intervals (Krigolson and Heath, 2004; Obhi and Goodale, 2005; Hay and Redon, 2006; Chen et al., 2011), for example, a memory delay of 5 s (Hay and Redon, 2006), or even a longer time of 8.5 s (Chen et al., 2011). These results have suggested that the two visual streams process vsuospatial information in different ways, relying on a corresponding frame of reference.

Further, in a recent neuropsychological study (Schenk, 2006) the patient (D.F.), who had an extensive bilateral lesion to the lateral occipital complex (LOC) in the ventral stream following anoxia (Milner et al., 1991), performed motor and perception tasks in two conditions (target-directed and allocentric). In the target-directed condition of the motor task, participants moved their finger from the starting point toward the target, thus the target was defined in egocentric coordinates. In contrast, in the allocentric condition of the motor task, a reference target was displayed along with the aiming target, and participants were instructed to move their finger from the starting point toward a location so that this position relative to the starting position matched the vector of the reference target to the aiming target. D.F.'s performance was as good as normal participants in the egocentric motor task, suggesting that the egocentric target coding is associated with the dorsal stream. However, D.F.'s performance in the allocentric motor task was obviously impaired as compared to the normal participants, suggesting that the allocentric target representation is associated with the ventral stream. Although the author also challenged that it would be allocentric-egocentric models rather than the perception-action model for visuospatial processing in the ventral and the dorsal stream, Milner and Goodale have addressed this issue and clarified the model in more detail in their review paper (Milner and Goodale, 2008). In particular, Milner and Goodale point out that the allocentric motor task in Schenk's study was still testing spatial perception

since what D.F. did was to manually report her perceived position of the target relative to the reference point, similar to what she did in the allocentric perceptual task using a verbal report. As Milner and Goodale indicated, realizing the distinction between task and process is very important to understand the related mechanisms, for instance, performing an "action" task (like the allocentric "action" task in Schenk's study) actually requires the process of vision for perception, not vision for action. Taken together, with respect to the spatial coding of targets, the critical point in the two visual systems theory is that egocentric and allocentric representations are associated with the dorsal and ventral streams, respectively. In the following sections, I will discuss evidence for egocentric and allocentric neural mechanisms for spatial coding from neurophysiological studies, and human neuroimaging and transcranial magnetic stimulation (TMS) studies.

1.2 Egocentric visuomotor systems for reaching/pointing and saccades

The visuomotor systems for egocentric reaching/pointing and saccades have been investigated in neurophysiology and human imaging studies (Andersen et al., 1993; Colby, 1998; Batista et al., 1999; DeSouza et al., 2000; Sereno et al., 2001; Andersen and Buneo, 2002; Munoz, 2002; Medendorp et al., 2003; Munoz and Everling, 2004; Medendorp et al., 2005a; Prado et al., 2005; Schluppeck et al., 2005; Curtis and D'Esposito, 2006; Medendorp et al., 2006; Kastner et al., 2007; Van Pelt et al., 2010; Crawford et al., 2011; Gertz and Fiehler, 2015). The main brain areas involved in the two parietofrontal networks (reaching/pointing, saccades) in humans are shown in Figure 1.3. It has been indicated that posterior parietal cortex (PPC) plays a critical role in movement control (Andersen et al., 1998; Batista et al., 1999; Medendorp et al., 2003; Crawford et al., 2004; Medendorp et al.,

2005b). The PPC is situated between the visual cortex in the occipital lobe and the somatosensory cortex in the parietal lobe, which makes PPC able to receive visual and somatosensory input, and then send output to premotor and motor areas in the frontal lobe to generate movements. More specifically, PPC is anterior to the parieto-occipital sulcus (POS) and posterior to the postcentral sulcus (PCS). Anatomically, PPC is divided into the superior parietal lobule (SPL) and inferior parietal lobule (IPL) by the intraparietal sulcus (IPS) that ends posteriorly in the transverse occipital sulcus (TOS). IPL is segregated into two regions, supramarginal gyrus (SMG, anterior) and angular gyrus (AG, posterior) in humans. The medial component of the parietal lobe is precuneus, located anterior to POS. As illustrated in Figure 1.3, besides PPC, some other areas in the frontal lobe are also involved in the control of either reaching/pointing or saccades. Next, I will discuss the role of these brain areas in further detail.

1.2.1. Neurophysiological studies of reaching/pointing movements

Electrophysiological studies from monkeys have identified a number of effector-related regions within IPS. For instance, the anterior intraparietal sulcus (AIP) encodes targets for grasping, the lateral intraparietal sulcus (LIP) encodes targets for saccades**,** and a more medial cluster, parietal reach region (PRR) encodes targets for reaching. PRR is situated more medial and posterior to LIP, and consists of medial intraparietal area (MIP) and V6A (within the superior parietal cortex near the junction of the dorsal POS). The premotor cortex in frontal lobe is divided into two main regions: dorsal premotor cortex (PMd) and ventral premotor cortex (PMv) (Barbas and Pandya, 1987; Kurata, 1991, 1994). PMd receives projection from SPL, including MIP, indicating its role in reach control, whereas

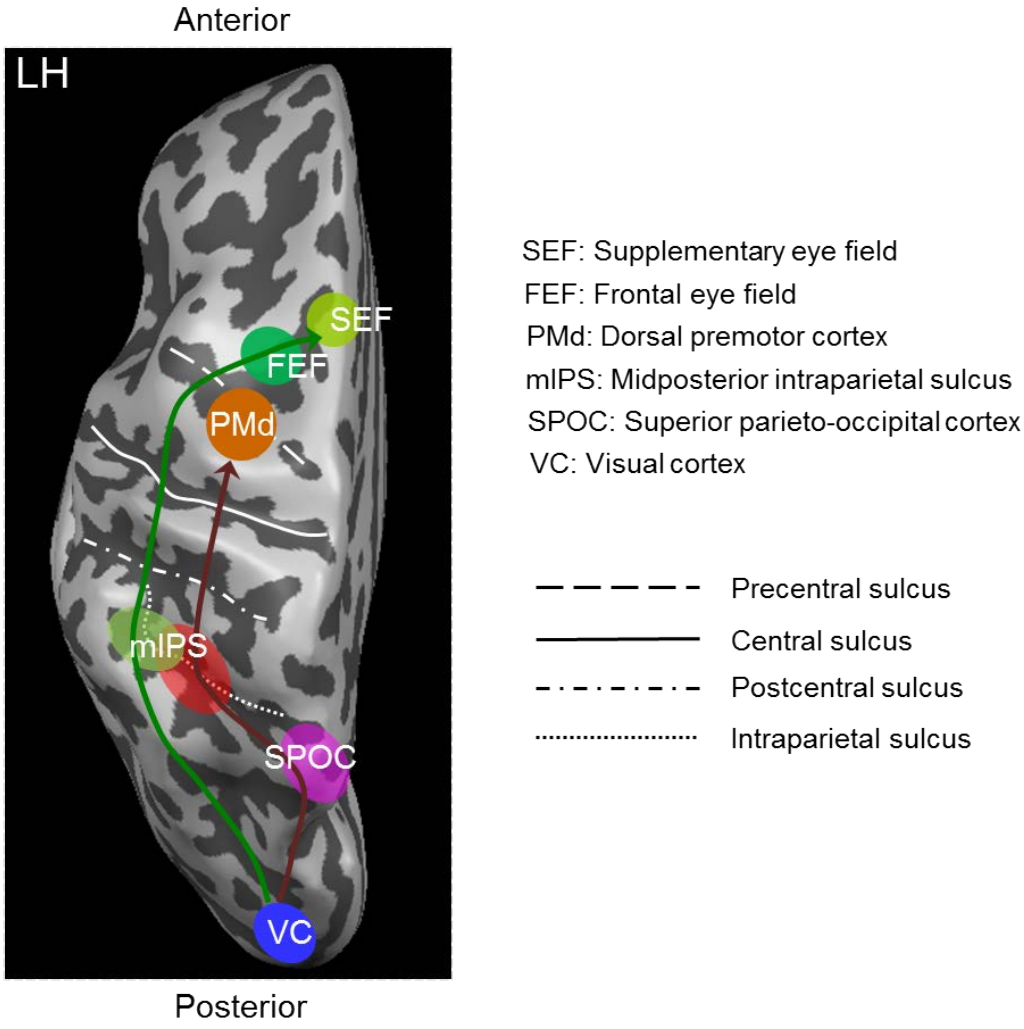

Figure 1.3. Egocentric visuomotor systems for reaching/pointing and saccades. The main brain areas are labeled on the left hemisphere of the human inflated brain.

PMv receives main projections from AIP, suggesting its function in grasping (Weinrich and Wise, 1982; Gentilucci et al., 1988; Kurata, 1994; Tanne-Gariepy et al., 2002).

Areas PRR and PMd are interconnected in the parietofrontal egocentric reach network and involved in the spatial representation of reach goals and reach planning (Hartje and Ettlinger, 1973; Mountcastle et al., 1975; Seal and Commenges, 1985; Wise et al., 1986; Murata et al., 1996). Although they play a similar role in reach control, the way they process spatial information still differ to some extent. In particular, remembered reach targets are mainly encoded in gaze-centered coordinates in the PRR, which must be updated across eye movements to maintain the accurate spatial coding for the upcoming reaches (Duhamel et al., 1992b; Batista et al., 1999). Further, it has been showed that hand position signals, even without vision (i.e., arising from proprioceptive signals), are also represented in gaze-centered reference in PRR (Buneo et al., 2002) so that the hand-target comparison is carried out in PRR. This suggests that PRR plays a critical role in the early visuomotor transformation in gaze-centered coordinates for reach. In comparison, PMd encodes reach targets in a combination of eye-, hand- (Pesaran et al., 2006; Batista et al., 2007) and shoulder-centered coordinates (Fogassi et al., 1996; Scott et al., 1997; Kakei et al., 2003), suggesting a later visuomotor transformation for reach planning. During the late stage at the cortical level, primary motor cortex (M1) executes reach movements in muscle-centered coordinates and determines forces and torques for each set of muscles (Scott and Kalaska, 1997; Sergio and Kalaska, 1998; Kakei et al., 1999; Sergio and Kalaska, 2003) (not discussed in this dissertation). The difference in egocentric reference frames between PRR, PMd and M1 possibly implicate the gradual spatial transformation of vision to motor for

reach control (Caminiti et al., 1991; Crammond and Kalaska, 1996; Kalaska et al., 1997; Sergio et al., 2005)

By using pro-reach (reaching directly to a cued target) and anti-reach tasks (reaching to the mirror location opposite to the cued target, also referred as an inferred target), the differences in the coding of spatial directional selectivity during planning and response phases between PRR and PMd are observed (Gail et al., 2009). In particular, PRR showed stronger directional selectivity to the pro-reach target than the inferred anti-reach target during reach planning, whereas PMd showed stronger activity to the inferred anti-reach target than the pro-reach target during reaches. This result suggests that PRR has a preference for encoding "automatic", visual-relevant movement goals (pro-reach), but PMd is involved in representing "inferred" rule-based movement goals (anti-reach). A recent neurophysiology study further suggests the important role of PRR, not PMd, in spatial working memory relative to movement goals by testing synchronization patterns in each of the two areas (Chakrabarti et al., 2014).

The findings from monkey neurophysiology studies have provided important insights into egocentric network for reach control. However, the fundamental question related to humans still remains. That is, are the identified egocentric reach network and its function in monkeys supported in humans? The development of advanced neuroimaging techniques, especially fMRI, and TMS has enabled researchers to address this question to some extent with various experimental designs.

1.2.2. Human neuroimaging and TMS studies of reaching/pointing movements

In humans, a parietofrontal reach network (Fig. 1.3) including the connected regions of PPC and PMd has been showed to be involved in the coding of reach targets and motor planning (Medendorp et al., 2003; Prado et al., 2005; Beurze et al., 2007; Tomassini et al., 2007; Busan et al., 2009; Lindner et al., 2010). A number of human imaging studies have revealed two distinct reach-related sub-regions in human PPC: one medial to intraparietal sulcus, along its anterior-posterior axis (midposterior IPS: mIPS) (DeSouza et al., 2000; Medendorp et al., 2003; Grefkes et al., 2004; Medendorp et al., 2005b; Prado et al., 2005; Hagler et al., 2007; Levy et al., 2007; Beurze et al., 2009), and the other further more medial-posterior, within precuneus situated in superior parieto-occipital cortex (SPOC) (Astafiev et al., 2003; Connolly et al., 2003; Fernandez-Ruiz et al., 2007; Beurze et al., 2009; Filimon et al., 2009; Bernier and Grafton, 2010a; Cavina-Pratesi et al., 2010), which represent reach targets in gaze-centered reference frames with a contralateral left-right topography. Compared to monkey PPC, mIPs might be homologous to macaque MIP (Johnson et al., 1996; Eskandar and Assad, 1999; Galletti et al., 2003; Pitzalis et al., 2006; Fattori et al., 2009), whereas SPOC possibly be homologous to macaque V6A (Galletti et al., 2003; Pitzalis et al., 2006; Fattori et al., 2009).

It has been reported that mIPS can be activated whether the target appeared in central or peripheral vision, whereas SPOC only responds to peripherally presented targets (Prado et al., 2005). Moreover, an fMRI study using left-right reversing prisms to dissociate the visual reach goal from physical reach direction showed that the reach goal, not motor commands is primarily encoded in SPOC, whereas AG is involved in the coding of reach direction (Fernandez-Ruiz et al., 2007). A TMS study further showed that mIPS as well as AG are

involved in the coding of reach direction (Vesia et al., 2010). Results from a recent fMRI study, where a pro-/anti-reach design was used to disentangle the location of reach goal from the location of a visual cue during movement planning, suggest that precuneus encodes the movement goal rather than the visual cue (Gertz and Fiehler, 2015). Taken together, these studies indicate a distinction between the coding of reach goals in the more medial region of PPC (precuneus, more specifically SPOC) and reach vector in the more lateral-anterior region (mIPS, AG).

Previous human neuroimaging studies have shown that both IPS and PMd represent the reach goal and the selected effector (e.g., left vs. right arm) during reach planning with an interaction of the hemispheric lateralization between hand and visual hemifield (Medendorp et al., 2005b; Beurze et al., 2007). For example, higher activation was observed in left IPS when the right hand, as compared to the left hand, was used to point to the target presented in the right hemisphere (Medendorp et al., 2005b). On the other hand, although in general anti-reaches recruited additional areas as compared to pro-reaches when the task did not separate the planning phase from execution (Connolly et al., 2000), both precuneus and PMd were involved in the planning of anti- and pro-reaches with no difference in activity strength between these two types of reaches during the planning period (Connolly et al., 2003; Gertz and Fiehler, 2015).

1.2.3 Neurophysiological studies of saccadic eye movements

The main cortical regions in the saccadic system include LIP, sometimes referred as the “parietal eye fields” (PEF), and other two in frontal cortex, frontal eye fields (FEF) and supplementary eye fields (SEF) (Gaymard et al., 1998; Schall and Thompson, 1999; Sparks

et al., 2001; Munoz, 2002). Area LIP projects directly to FEF and SEF, and FEF and SEF are interconnected. All these three cortical oculomotor areas show projections to the superior colliculus (SC) (not the topic in this dissertation) that generates the motor commands for saccadic eye movements (Wurtz and Albano, 1980; Sparks, 1986; Munoz, 2002). FEF corresponds to Brodmann's area 8 and lies in the rostral bank of the arcuate sulcus in macaque monkeys (Bruce et al., 1985). SEF in the macaque monkey is defined as a discrete region of dorsomedial frontal cortex, just anterior the supplementary motor area (Schlag and Schlag-Rey, 1985, 1987).

It has been shown that saccade targets are mainly represented in gaze-centered reference frames in monkey LIP, and the initial representations are spatially updated before and during intervening eye movements (Duhamel et al., 1992a; Colby et al., 1995; Duhamel et al., 1997; Gottlieb et al., 1998). Some other studies have shown that FEF uses gaze-centered reference frames to encode saccade targets in head-fixed monkeys (Bruce et al., 1985; Goldberg and Bruce, 1990; Schall, 1991). However, when saccades are made in a natural head-unrestricted condition, coexistence of eye- and head-fixed frames in FEF are reported, suggesting that FEF might be involved in complex reference frame transformation before the spatial information is sent to the SC to initiate saccade movements (Martinez-Trujillo et al., 2004; Monteon et al., 2013). SEF can encode saccade target in gaze-centered (Russo and Bruce, 1996) or object-centered (Olson and Gettner, 1995, 1999; Olson and Tremblay, 2000) reference frames. It has been reported that SEF is involved in coding temporally ordered saccades, suggesting SEF plays an important role in motor programs for single and sequence saccades (Isoda and Tanji, 2002).

1.2.4 Human neuroimaging and TMS studies of saccadic eye movements

Human studies using fMRI and TMS have revealed the parietofrontal network for saccadic eye movements, including human parietal eye field (hPEF, mIPS), SEF and FEF (Figure 1.3) (Sereno et al., 2001; Cornelissen et al., 2002; Pierrot-Deseilligny et al., 2003; Pierrot-Deseilligny et al., 2004). The hPEF (mIPS) is thought to be homologous to monkey LIP, but located medial to IPS (Muri et al., 1996).The FEF is located at the intersection of the precentral sulcus and the superior frontal sulcus (Paus, 1996).The SEF is located on the medial aspect of the superior frontal gyrus in the upper region of the paracentral sulcus (Grosbras et al., 1999).

It has been shown that all the three cortical oculomotor areas encode saccade targets in gaze-centered reference frames during saccade planning (Van Pelt et al., 2010). However, only areas IPS and FEF showed a preference for contralateral left-right topography (Kastner et al., 2007; Van Pelt et al., 2010). Further, similar to activation observed in mIPS for reach, the spatial coding of saccade goals in mIPS is also updated after an eye movement (Medendorp et al., 2003; Medendorp et al., 2005a, 2006). It has been reported that the mechanisms of IPS and FEF involved in the coding of saccade targets in memory are different, i.e., the former is more related to sensory representations, but the latter is more tied to the selection and coding of saccade goals (Curtis and D'Esposito, 2006). Previous fMRI studies where the preparatory phase was isolated from execution found that FEF (DeSouza et al., 2003), not IPS (Connolly et al., 2002; DeSouza et al., 2003) is involved in preparatory set. Together with the result from Curtis and D'Esposito's study, these findings suggest that IPS and FEF play a different role in the saccade generation, i.e., the former is closer to the sensory aspect and the latter is involved in preparatory set for intention and readiness to

perform a saccadic eye movement (Connolly et al., 2002). Some fMRI and TMS have shown that SEF is involved in saccade sequences, suggesting its specific role in motor programs for sequential saccades (Gagnon et al., 2002; Tobler and Muri, 2002; Pierrot-Deseilligny et al., 2003).

1.3 Allocentric mechanisms for spatial coding

Previous behavioral studies have suggested that both egocentric and allocentric cues can be used to encode spatial locations of visual targets in memory (Goodale and Haffenden, 1998; Henriques et al., 1998; Carrozzo et al., 2002; Crawford et al., 2004; Lemay and Stelmach, 2005; Hay and Redon, 2006). However, in contrast to egocentric coding, neutral substrates involved in allocentric coding for visuomotor control are much less studied. Instead, some human neuroimaging studies investigated allocentric coding of targets for spatial judgments (Fink et al., 1997; Honda et al., 1998; Fink et al., 2000; Galati et al., 2000; Committeri et al., 2004; Neggers et al., 2006; Zaehle et al., 2007). On the other hand, some neurophysiological studies have examined spatial coding of targets in object-centered reference frames for saccades (Olson and Gettner, 1995, 1996; Olson and Tremblay, 2000; Olson, 2003). I will discuss this topic in more detail in the following subsections.

1.3.1 Behavioral/computational studies of allocentric vs. egocentric reach target coding

It has been suggested that in normal conditions the brain likely uses both egocentric and allocentric cues to encode spatial locations of remembered reach targets on the basis of the relative weighting of the two cues determined by their reliability and stability (Byrne and Crawford, 2010). Some behavioral studies have indicated that this weighting seems to

depend on the proximity, number, and perhaps size of background objects (Diedrichsen et al., 2004; Krigolson et al., 2007; Uchimura and Kitazawa, 2013; Fiehler et al., 2014). Other behavioural studies investigating the influence of visual landmarks on reach performance have shown that landmarks can improve reaching accuracy and precision in both real-time and delayed movements (Krigolson and Heath, 2004; Obhi and Goodale, 2005; Krigolson et al., 2007). On the other hand, it has been shown that reach target location is still represented and updated in a gaze-dependent egocentric reference frame for movements after a delay up to 12 s when allocentric cues are available, but with a combination of the two types of spatial information (Schutz et al., 2013).

In a recent study by Chen et al. (2011), the time course of allocentric and egocentric decay, and allocentric-to-egocentric conversion were investigated. In particular, three delay intervals, short delay (2.5 s), medium delay (5.5 s) and long delay (8.5 s) were used in each of the three experimental conditions, Egocentric (reaching to the remembered target location after the variable delay), Allocentric (reaching to the remembered target location relative to the shifted landmarks which briefly re-appeared twice right after the variable delay) and Allo-to-ego conversion. The novelty of the design was the Allo-to-ego conversion condition where the shifted landmarks first re-appeared right before the variable delay, then again after the delay, just before response. In this situation, participants were free to convert allocentric coding into egocentric representation either early (during the variable delay after the first re-appearance of the shifted landmark) or later (during response after the second re-appearance of the shifted landmark). Using such a design, the questions of when (early or late) allocentric representations are transformed to egocentric commands, and how the allocentric and egocentric coding degrade were examined. The results showed that memory of reach

target location encoded in egocentric reference frames continued to decay over the time course of 2.5-8.5 s, whereas memory of target location represented in allocentric reference frames remained relatively stable over the same time scale. Most importantly, despite the stable allocentric coding, they found early allo-to-ego conversion. i.e., the brain converts the allocentric representation into egocentric representation at the first possible opportunity.

1.3.2 Neural mechanisms for allocentric coding

Some neuroimaging studies in humans have investigated allocentric mechanisms for target coding in spatial cognitive tasks (Fink et al., 1997; Honda et al., 1998; Fink et al., 2000; Galati et al., 2000; Committeri et al., 2004; Neggers et al., 2006; Zaehle et al., 2007). Those studies demonstrated that allocentric spatial coding for judgments tasks requires an additional involvement of the ventral stream and/or the hippocampus. More specifically, the lateral occipital complex (LOC) in the ventral stream has shown more activity during allocentric as compared to egocentric spatial judgments in some of those studies (Honda et al., 1998; Committeri et al., 2004; Neggers et al., 2006; Zaehle et al., 2007). Consistent with those findings, another fMRI study in recognition task has indicated that the processing of visual information in the LOC would take place in an allocentric frame of reference (McKyton and Zohary, 2007).

More recently, an fMRI study using the same experimental design as that in the previous neuropsychological study (Schenk, 2006) directly compared the neural mechanisms involved in the target coding for the two types of manual distance judgment tasks, the egocentric (target directed) versus the allocentric condition (Thaler and Goodale, 2011b). In brief, in the former, subjects just moved their hand from the starting position toward a target

location, whereas in the latter, they were instructed to move their hand to a location so that the distance between that location and the starting position matched that between the target location and the allocentric target. The result showed that LOC is essential for allocentric visual coding of targets in the allocentric task. Moreover, a contralateral preference for a target presented in the contralateral visual field was observed in LOC in the allocentric condition. However, in that design the target was not systematically manipulated to be presented to either the right or left with respect to the allocentric reference target. Instead, the target appeared along with the allocentric reference target in either the right or left visual field, thus the allocentric directional selectivity could not be examined. Moreover, as noted, unlike an actual reaching movement to the target represented relative to an allocentric cue, the manual movements using allocentric information in the Thaler and Goodale's study (2011) are to copy or draw matched vectors using hands. Thus, it is possible that neural mechanisms for the allocentric target coding in this type of tasks is different from those for the actual reaching movements to the goal, which has not been explored yet.

Regarding allocentric mechanisms involved in target coding for motor control, neurophysiological studies have examined target representation in object-centered reference frames for saccades (Olson and Gettner, 1995, 1996; Olson and Tremblay, 2000; Olson, 2003). For example, in a study by Olson and Gettner (1995), monkey were trained to make a saccade to the right or left side of the target bar after a delay while neuron activity in supplementary eye field (SEF) was recorded. Their results showed that neurons in SEF were selective for a particular side of the object, suggesting that SEF is involved in object-centered coding of saccade targets. However, as discussed before, although object-centered

representation is non-egocentric, it is still different from the allocentric coding using an external landmark in the environment.

In summary, although allocentric mechanisms for spatial coding of targets in cognitive tasks in humans and neural mechanisms for object-centered representations of saccade targets in primates have been examined, the allocentric cortical mechanisms for reach and saccades are still unknown. Investigating these mechanisms is very important to understand how and where the allocentric spatial information is used in the human brain for such arm and eye movements, and how the allocentric mechanisms are different from the egocentric mechanisms.

1.4 Functional magnetic resonance imaging (fMRI)

In order to identify the brain areas involved in a certain task so that the function of those areas can be investigated, the fMRI technique is crucial. In the early 1990s, researchers started to use MRI scanner to measure changes in the blood oxygenation of the brain over time rather than differences between tissues in structural MRI (Kwong et al., 1992; Ogawa et al., 1992). The advantages of this technique include that it is non-invasive, it has higher spatial resolution compared to other techniques such as magnetoencephalography (MEG) and electroencephalogram (EEG) and it can be used to various experimental tasks (Huettel et al., 2008). Spatial resolution of an fMRI study refers to its ability to distinguish differences between nearby locations, and is measured by the size of voxels (three-dimensional volume element, usually around 3 mm in each dimension).

The principle of fMRI is based on the relationship between neuronal activity and blood flow and oxygen consumption. Increased neuronal activity in a certain brain area leads

to an increased demand for oxygen with more blood flow supplied to that brain region. Oxygen is delivered to neurons by haemoglobin in capillary red blood cells. Haemoglobin is diamagnetic when oxygenated but paramagnetic when deoxygenated. This difference in magnetic properties gives rise to small differences in the MR signal of blood depending on the degree of oxygenation, known as blood oxygenation level dependent (BOLD) signal, which can be measured using MRI (Bandettini et al., 1992; Disbrow et al., 2000; Ances et al., 2008; Logothetis, 2008). The earlier fMRI studies used a blocked design where each experimental condition had a long block interval (10 - 30 s) because the magnitude of the BOLD change related to neuronal activity was still unknown at that time (Belliveau et al., 1991; Kwong et al., 1992; Ogawa et al., 1992). For instance, a simplest blocked-design can be two blocks, one for an experimental condition, and one for the control condition with a block interval of 30 s. The result of BOLD signal contrast between these two conditions then is translated into activation map with a color code, which is displayed on an anatomical MRI image to visualize. The significant step of fMRI uses in research is the development of event-related designs in the mid-1990s (Buckner et al., 1996; Dale and Buckner, 1997; Bandettini and Cox, 2000). Since then, this type of designs has been adopted in a wide of range of fMRI research fields to investigate the function of brain areas related to a specific event. Unlike blocked-designs, event-related designs measure transient changes in brain activity associated with discrete events, and the trials for experimental conditions can be presented in an unpredictable order. For instance, as seen in the following sections, I used an event-related design in my fMRI studies that included different phases (events) to allow me to examine the neural substrates involved in a certain time period (e.g., the delay phase in most of my studies). Based on the hypothesis of an experiment, some fMRI studies used a mixed design

where blocked and event-related approaches are combined so that each regular block includes different type of events whose order and timing can be randomized.

The analysis performed in the most fMRI experiments is hypothesis-driven. That is, the researcher designs their experiments with certain hypotheses about what type of differences to be observed between the experimental conditions. Statistical analyses then are conducted on the collected fMRI data to determine if the expected differences exist, not due to chance. There are two main approaches used on the fMRI data analysis: voxelwise and region of interest (ROI) analysis. In the voxelwise analysis, the statistical comparison is performed between the experimental conditions on an individual-voxel basis, often throughout the entire brain so that the brain functions that have not discovered in previous research can be revealed. This is a powerful approach to identify areas involved in certain information process. ROI analysis, on the other hand, focuses on the function of previously identified brain region in a specific task. For instance, the fusiform face area (FFA) is a common ROI that responses more strongly to faces than non-face objects (Kanwisher et al., 1997; Gauthier et al., 2000).In the fMRI studies of hand movements, grasping an object elicits higher activation in the defined ROI, aIPS, than reaching toward it by using knuckle (Culham et al., 2003; Cavina-Pratesi et al., 2007). When the ROI analysis is adopted, a localizer based on prior studies is used to identify the ROI, following by further analysis using independent experiments to test some new hypothesis related to that ROI. Therefore, the choice of using ROI analysis will depend on the purpose of the experiment, i.e., if the researcher is interested in investigating some unknown function in a given brain region. Since these two approaches have their own advantage and are not exclusive, sometimes they are combined in the analysis.

Over the past two decades, the fMRI technique has contributed greatly to understand human brain functions. As stated before, using fMRI has enabled researchers to identified functionally-specific brain areas in humans, such as PPC so that the similarities and differences of their functions between humans and macaque monkeys can be compared (Duncan and Owen, 2000; Culham and Kanwisher, 2001). However, knowing the limitations with fMRI is also important for researchers to properly design an fMRI study. First, the activation observed in fMRI data only can reflect neuronal activity, not a causal link. Second, although fMRI has high spatial resolution, its low temporal resolution (around seconds) will limit some use in studies where time as well as space is the considered elements. To overcome these limitations, some other techniques, such as TMS and MEG have been combined with fMRI in some research according to the experimental purpose (Paus et al., 1997; Ruff et al., 2008). In addition, a combination of neuroimaging in monkeys and humans can benefit in better evaluating differences between human and monkey brains (Paus et al., 1997; Logothetis et al., 1999; Orban et al., 2004; Ruff et al., 2008).

1.5 Overall objectives

As stated in previous sections, both egocentric and allocentric cues can be used to encode target location for aiming movements such as reaching and saccades, and the egocentric mechanisms have been relatively well-studies in human cortex. However, the allocentric cortical mechanisms are still not explored yet. My doctoral project overall was focused on the neural substrates involved in allocentric coding of remembered targets for two types of effector-specific movements, i.e., reaching (hand) and saccades (eye), and the cortical mechanisms for allocentric to egocentric conversion of remembered reach targets

using fMRI. The novel findings from this thesis provide more understanding of spatial coding in movements, especially how and where visual allocentric cues available in the external environment are used in processing the remembered goals for actions.

Chapter Two: I investigated the brain areas involved in allocentric coding of remembered targets for reach, and directly compared the allocentic mechanisms versus egocentric mechanisms, which has not been studied before. I used an experimental paradigm consisting of three tasks (Ego reach, Allo reach and Color control) with an event-related fMRI design where the target memory was isolated from reach planning and execution, enabling me to examine the neural mechanisms for target memory in the two types of coordinates. In addition, I systematically manipulated the target location relative to an allocentric landmark as well as to the fixation point. This allowed me to further investigate the directional selectivity in allocentric as well as in egocentric reference frames. First, I hypothesized that brain areas involved in the coding of remembered targets for both reach tasks would elicit higher activation compared to the control task. Second, I expected that brain areas involved in egocentric target coding would show higher activation in the Ego reach task than the Allo reach task and vice versa. Further, I hypothesized that brain areas involved in egocentric directional selectivity would show a preference for contralateral target coding relative to gaze / midline, whereas allocentric directional selectivity (target location relative to landmark location) would be revealed by higher activation for target contralateral than ipsilateral to the landmark.

Chapter Three: I used a similar experimental design to my first study (Chapter Two) to investigate and compare the allocentric neural mechanisms to egocentric ones for the coding of remembered targets for saccades. First, I expected a similar pattern of task-related

brain activity to the first study, i.e., higher activation in the two saccade tasks (Ego, Allo) than the Color control with different brain areas involved in egocentric versus allocentric target coding. Second, regarding the directional selectivity, if the cortical mechanisms for saccade target memory are similar to those for reach target memory, I expected the same brain areas as my first study showing directional specificity. Otherwise, different areas from those for reach target coding and/or from those for object-centered saccade target representations would be expected.

Chapter Four: As we know, the allocentric coding of reach targets has to be converted to egocentric representations since reaching movements eventually are performed in egocentric coordinates using hands. It has been indicated that reach targets encoded in allocentric reference frames are converted to egocentric representations at the first possible opportunity, i.e., as early as the reach target location is specified (Chen et al., 2011). My third fMRI study aimed to examine the neural substrates for this early allocentric to egocentric conversion of reach target representation. The experimental paradigm included two allocentric reach tasks (Same cue and Different cue) in which the target location was initially coded relative to an allocentric landmark. A verbal cue then was used to inform that the landmark would re-appear at the same location as before for the Same cue task so that the final location of the reach target was provided for the early allo-ego conversion in the following delay phase. In comparison, later on before the response phase, a visual cue of the re-displayed landmark at a different location for the Different cue task would specify the target location for reach so that the allo-ego conversion would happen for the Different cue task during the response. First, I hypothesized that the early allo-ego conversion would occur during the delay in the Same cue task, but only during the response in the Different cue task.

Second, I hypothesized that areas involved in the allo-ego conversion would show higher activation for the Same cue versus the Different cue task in the delay, but a reverse pattern in the response. Finally, with a use of the two types of modalities (verbal and visual, which are closer to the natural environment) as the cue of early allo-ego conversion, I expected to identify the common brain areas for the allo-ego conversion of reach targets, regardless of the type of available cues and the time points.

Overall, I used event-related fMRI designs in my doctoral project to answer the questions about allocentric mechanisms for the coding of target memory for reaches and saccades, and the cortical mechanisms for allo-ego conversion of target representation for reaching. My studies will provide insights into the understanding of neural mechanisms underlying spatial coding using allocentirc cues in healthy brain that will further be applied to patients with a lesion to only one of the two cortical substrates (allcentric or egocentric).

CHAPTER TWO

ALLOCENTRIC VERSUS EGOCENTRIC REPRESENTATION OF REMEMBERED REACH TARGETS IN HUMAN CORTEX

Authors: Ying Chen, Simona Monaco, Patrick Byrne, Xiaogang Yan

Denise Y.P. Henriques and J. Douglas Crawford

Published: *The Journal of Neuroscience, 34 (37): 12515-12526, 2014*

2.1 ABSTRACT

The location of a remembered reach target can be encoded in egocentric and/or allocentric reference frames. Cortical mechanisms for egocentric reach are relatively well described, but the corresponding allocentric representations are essentially unknown. Here, we utilized an event-related fMRI design to distinguish human brain areas involved in these two types of representation. Our paradigm consisted of three tasks with identical stimulus display but different instructions: *Egocentric reach* (remember absolute target location), *Allocentric reach* (remember target location relative to a visual landmark) and a non-spatial control, *Color report* (report color of target). During the *Delay phase* (when only target location was specified) the *Egocentric* and *Allocentric* tasks elicited widely overlapping regions of cortical activity (relative to the control), but with higher activation in parieto-frontal cortex for *Egocentric* task and higher activation in early visual cortex for *Allocentric* tasks. In addition, egocentric directional selectivity (target relative to gaze) was observed in the superior occipital gyrus (SOG) and the inferior occipital gyrus (IOG), whereas allocentric directional selectivity (target relative to a visual landmark) was observed in the inferior temporal gyrus (ITG) and IOG. During the *Response phase* (after movement direction had been specified either by re-appearance of the visual landmark or a pro/anti reach instruction), the parieto-frontal network resumed egocentric directional selectivity, showing higher activation for contralateral than ipsilateral reaches. These results show that allocentric and egocentric reach mechanisms use partially overlapping but different cortical substrates, and that directional specification is different for target memory versus reach response.

2.2 INTRODUCTION

To reach for a remembered object one must maintain an internal spatial representation of its location, either relative to some egocentric (body-fixed) frame of reference, such as the eyes, head or shoulder, or some allocentric (world-fixed) frame of reference, such as a stable visual landmark (Bridgeman et al., 1997; Burnod et al., 1999; Carrozzo et al., 2002; Olson, 2003; Crawford et al., 2011). Behavioral studies have investigated the influence of visual landmarks on reach (Krigolson and Heath, 2004; Obhi and Goodale, 2005; Krigolson et al., 2007) and the interactions between egocentric and allocentric representations for memory-guided targets (Byrne et al., 2010; Byrne and Crawford, 2010; Chen et al., 2011; Schutz et al., 2013). However, the cortical mechanisms for egocentric reach are still debated, and the neural mechanisms for allocentric reach are essentially unknown.

Neuropsychological studies of vision and action suggest that egocentric coding is associated with parietal cortex (which is closely associated with frontal cortex), and allocentric coding is associated with temporal cortex (Goodale and Haffenden, 1998; Milner and Goodale, 2006; Schenk, 2006; Milner and Goodale, 2008). Primate neurophysiological studies and human functional magnetic resonance imaging (fMRI) studies have investigated the neural substrates of egocentric reaching/pointing in considerable detail (Andersen et al., 1993; Andersen et al., 1998; Batista et al., 1999; Connolly et al., 2000; DeSouza et al., 2000; Andersen and Buneo, 2002; Astafiev et al., 2003; Connolly et al., 2003; Medendorp et al., 2003; Medendorp et al., 2005a; Prado et al., 2005; Fernandez-Ruiz et al., 2007; Beurze et al., 2010). These studies have shown that posterior parietal cortex (PPC) and dorsal premotor cortex (PMd) are involved in egocentric representation of reach targets, with a contralateral left-right topography in human cortical areas such as midposterior intraparietal sulcus

(mIPS), and superior parieto-occipital cortex (SPOC) (Vesia and Crawford, 2012). In comparison, allocentric mechanisms have only been studied for spatial judgements in cognitive tasks (Fink et al., 2000; Galati et al., 2000; Committeri et al., 2004; Neggers et al., 2006; Zaehle et al., 2007), saccade coding (Olson and Gettner, 1995; Olson and Tremblay, 2000; Sabes et al., 2002; Olson, 2003), and manual distance judgements (Thaler and Goodale, 2011a). To our knowledge, the neural substrates for allocentric coding of reach targets (i.e., target direction relative to a visual landmark: allocentric directional selectivity) have never been studied or directly compared to egocentric mechanisms (i.e., target direction in an egocentric frame: egocentric directional selectivity).

Here, we used an event-related fMRI paradigm to 1) explore brain regions involved in spatial coding of remembered reach targets in egocentric and allocentric frames of reference 2) establish which brain areas show directional selectivity when encoding target location in egocentric vs. allocentric coordinates, and 3) compare this to egocentric directional selectivity during the response phase. The results showed that, although allocentric and egocentric mechanisms for reach target coding show considerable overlap, they differ in key areas, both from each other and from the cortical activity during the reach response.

2.3 MATERIALS AND METHODS

Participants

Thirteen right-handed participants (9 females and 4 males, aged 23-40 years) took part in this study and gave informed consent. All had normal or corrected to normal vision and had no known neuromuscular deficits. This study was approved by the York Human Participants Review Subcommittee.

Experimental stimuli and apparatus

Visual stimuli consisted of dots of light produced by fiber optic cables that were embedded in a custom-built board mounted atop a platform. The platform was placed above the abdomen of the participant and affixed to the scanner bed through notches. The height and tilt of the platform could be adjusted to allow participants to reach comfortably to the stimuli (Fig. 2.1 A). A computer controlled touch screen (Keytec Inc, dimensions 170 (h) × 128 (v) mm) was attached on the custom-built board to allow the recording of reaching endpoints. An eye-tracking system (iView X) was used in conjunction with the MRI-compatible Avotec Silent Vision system (RE-5701) to record gaze movements from the right eye during fMRI experiments.

The head of the participant was slightly tilted (~20 deg) in order to allow direct viewing of the stimuli without using mirrors. The board was approximately perpendicular to the direction of gaze on the central fixation point and was placed about ~60 cm away from the eyes of the participants. The upper arm was strapped to the bed to avoid artifacts due to the motion of the shoulder and the head, therefore reaching consisted of movements of the

forearm and hand. A button pad was placed on the left side of the participant's abdomen. The button pad was used as a response key for the *Color report* task as well as the starting position for the right hand for the *Egocentric* and *Allocentric* reach tasks (see Experimental paradigm and timing). Participants wore headphones to hear audio instructions about the upcoming trial. During the experiment, participants were in complete darkness with the only exception of dots of light that served as visual stimuli. The dots of light were bright enough to be seen by the participant but too dim to allow viewing of the workspace. The hand was never visible to subjects, even during reaching.

Each dot of light had a diameter of 3mm and different colors were associated with different stimuli: yellow for the fixation dot, green or red for the target to be reached, blue for the visual landmark, and white for the mask. There were seven possible fixation points horizontally separated from each other by one degree, with the central one aligned to the participant's body midline. The dots of light corresponding to targets and relative visual landmarks were located to the left and the right of the fixation point. They were also separated from each other by a visual angle of one degree. There were four dots on the left and four dots on the right of the fixation point. Since these dots could be red, green or blue, they could be used as a target or a visual landmark in different trials. This allowed us to have 40 different combinations of target and visual landmark locations, in which the target could be located one or two visual degrees to the left or to the right of a visual landmark. Initial target and visual landmark were both presented either to the left or to the right of the fixation point. Therefore, the target could be displayed from one to nine visual degrees to the left or to the right of the initial fixation. The target presented to the right or left of the gaze was also

to the right or left of body midline (for instance: target right of gaze = target right of body midline, target left of gaze = target left of body midline).

The mask consisted of 20 dots of light organized in two rows, one above and one below the targets. The location of each dot for the mask was aligned with the midpoint between dots serving as targets and visual landmarks. The purpose of having a mask was to avoid potential after effects created by the illumination of the target and the landmark in the dark. Since our analyses focused mainly on the *Delay phase*, it was critical that participants were using memory information to recruit the location of the target rather than exploiting the afterimage of the target for the upcoming reach.

Experimental paradigm and timing

We used an event-related design to investigate three main questions. First, we examined the cortical circuits involved in processing the location of a reach target in egocentric and allocentric coordinates during the memory delay. Second, we investigated the areas showing directional selectivity when encoding target location in an egocentric vs. an allocentric representation during the memory delay. Third, we examined the brain areas involved in processing the reach direction for action planning and execution.

The paradigm included three tasks: *Egocentric reach* (*Ego*), *Allocentric reach* (*Allo*), and *Color report* (*Color*) (Fig. 2.1 B). In the *Allocentric reach* task, participants had to remember and later reach toward the location of the target relative to a visual landmark. The target and the landmark were initially presented together, then the landmark re-appeared at the same or at a different location (see Fig. 2.1 B and below for details). Since the landmark could re-appear to the left or right of the midline, the horizontal position of the reach could

not be predicted during the initial memory period (the *Delay phase*). In the *Egocentric reach* task, participants had to remember and reach toward the remembered location of the target, either at the location it initially appeared (*pro-reach*) or toward its mirror location in the opposite hemi-field (*anti-reach*). The *anti-reach* condition was included to equalize the motor aspects of the *Ego* and *Allo* tasks, i.e., in both cases the horizontal reach position could only be computed when the instruction to perform a reach or an anti-reach was given. Therefore, in both tasks the activation elicited during the *Delay phase* could only be related to the encoding horizontal target location, rather than reach planning (although other types of directionally non-specific motor preparation for a forward reach might occur during this phase). The *Color report* task served as a control and participants had to press a button one or two times depending on whether the target was green or red.

Prior to each trial, a recorded voice instructed the participant about the upcoming task: “Reach to target” (in *Egocentric reach* tasks), “Reach relative to cue” (in *Allocentric reach* tasks), “Report target color” (in *Color report* tasks). Although the audio cue occurred 8 s before presentation of the target, participants performed the actual movement upon the go instruction only at the end of the same trial.

Each trial started with the presentation of a fixation point that participants were required to fixate throughout the experiment. After 2 s, a target was presented for 2 s along with a landmark. Depending on the initial instruction, after the target and landmark disappeared, participants had to remember the location of the target regardless of the landmark (*Egocentric reach*), the location of the target relative to the landmark (*Allocentric reach*) or the color of the target (*Color report*). After the brief presentation of target and landmark, the fixation point shifted to the centre and was followed by a 12 s delay during

which a mask appeared. By shifting the fixation point before the delay period, the possibility of using the fixation point as an allocentric cue in the *Ego* task was removed. In order to keep all tasks as similar as possible, the fixation shift was retained in the *Allo* and *Color* tasks as well. After the delay, the landmark re-appeared for 2 s either at its original location or at another location in the same or opposite hemifield relative to its first appearance. Subsequently, an auditory signal cued the participant to reach towards the instructed egocentric target location (audio: "Target"), the location opposite to the egocentric target location (audio: "Opposite") or the allocentric target location (audio: "Reach"). In the *Color report* task participants were informed to press the button corresponding to the color of the previously presented target (audio: "Color"). Our paradigm consisted of five phases (*Fixation point, Stimulus presentation, Delay, Landmark presentation, Response*) (Fig. 2.1 B). A gap of 16 s was inserted between each trial to allow the hemodynamic response to return to baseline. Each run consisted of 18 trials, and each task was repeated six times in a random order yielding a run time of ~ 12 min. Each participant performed six runs. Our design consisted of three factors: 3 Tasks (*Ego, Allo, Color*) x 2 Target relative to gaze (*Left of Gaze: LG* and *Right of Gaze: RG*) x 2 *Target relative to landmark* (*Left of Landmark: LL* and *Right of Landmark: RL*). This design gave rise to 12 conditions in total: *Ego: LG:LL, Ego: LG:RL, Ego: RG:LL, Ego: RG:RL, Allo: LG:LL, Allo: LG:RL, Allo: RG:LL, Allo: RG:RL, Color: LG:LL, Color: LG:RL, Color: RG:LL, Color: RG:RL*. The 12 conditions were counterbalanced in each run. The "*Left of Gaze*" and "*Right of Gaze*" conditions included targets located to the left or right of the fixation point regardless of their distance from it. Similarly, the "*Left of Landmark*" and "*Right of Landmark*" conditions included targets located to the left or right of a visual landmark regardless of their distance from it,

i.e., we did not include a target distance-from centre covariate in our GLM. For the purpose of the analyses, we collapsed target locations into “Left” and “Right” relative to either gaze or visual landmark. Participants were trained to perform the tasks one day prior to the scanning session.

Behavioural recordings

Following our fMRI experiments, we inspected eye and hand position data for every trial to ensure that subjects correctly followed all instructions. Errors in eye movements were defined as trials in which subjects made a saccade toward the target or the visual landmark, or were not able to maintain fixation during the delay phase. Errors in reaching movements were defined as trials in which the location of the reaching endpoint and the actual reach target location were on opposite sides relative to the midline on the touch screen. Trials that showed errors in eye and/or reach movements were modelled as confound predictors and excluded from further fMRI analyses (see Data analyses). All participants completed at least 95 correct trials (88% of the total trials).

In order to confirm that subjects actually used egocentric or allocentric visual information in the *Ego* or *Allo* task to encode target location as instructed, and to exclude the possibility that they simply reached toward the correct side of the screen midline, we performed a correlation analysis. First, we calculated the absolute distance between a subject's reaching response for a given trial and the screen midline, then we calculated the distance between the proper target location (whether egocentrically or allocentrically defined) and the screen midline. If subjects were attempting to reach to the correct location, as instructed, these two values should be well-correlated in both the *Ego* and *Allo* tasks.

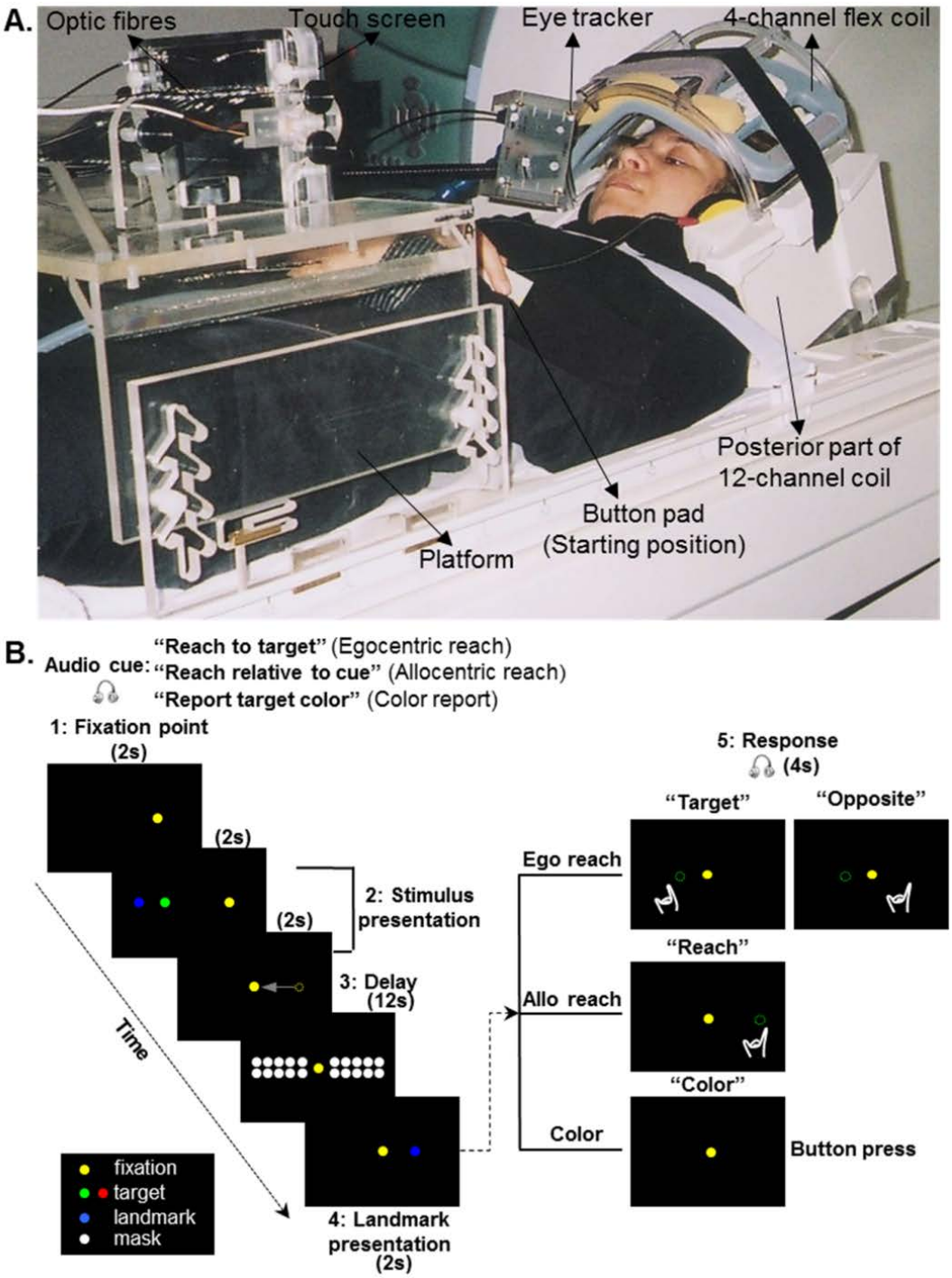
A.
Optic fibres
Touch screen
Eye tracker
4-channel flex coil
Posterior part of
12-channel coil
Button pad
(Starting position)
Platform
B.
Audio cue:
"Reach to target" (Egocentric reach)
"Reach relative to cue" (Allocentric reach)
"Report target color" (Color report)
1: Fixation point
(2s)
(2s)
(2s)
2: Stimulus
presentation
3: Delay
(12s)
Time
4: Landmark
presentation
(2s)
fixation
target
landmark
mask
5: Response
(4s)
"Target"
"Opposite"
Ego reach
"Reach"
Allo reach
"Color"
Color
Button press

Figure 2.1 Experimental setup and paradigm. ***A,*** Picture of the participant's setup from a side view. ***B,*** Illustration of the experimental paradigm. The display of the visual targets is the same for the three tasks (Egocentric reach, Allocentric reach and Color report). The critical difference between the two reach tasks is the frame of the reference used by the participant to encode target location for the upcoming action. In the Egocentric reach task, target location is encoded relative to the self. In the Allocentric reach task, target location is encoded relative to the landmark. In the Color report task, target color, rather than location, is being remembered and reported.

The across-subject means of these correlation coefficients were 0.31 ± 0.04 for the *Ego* task and 0.45 ± 0.04 for the *Allo* task. We then applied Fisher's r-to-z transformation to the individual subject correlation coefficients (r) so that we could use standard t-tests to compare the between-subjects means of z values to zero. If subjects were using the egocentric or allocentric spatial information for target coding, then these coefficients should have been significantly greater than zero. Standard t-tests showed that mean of correlation coefficient was significantly greater than zero in both tasks (p_{ego} = 0.00001, p_{allo} = 0.000002). Thus, both target location and allocentric cue location influenced behavior.

To further quantify participants' performance, we calculated the absolute error (AE) and the variable error (VE) in the horizontal dimension for each participant and each reach task (*Ego* or *Allo*), respectively. The AE is the absolute value of the distance between the target position and the endpoint of a reach movement and represents the amount by which the target was missed. The VE was computed by taking the standard deviation of the constant reaching errors and represents the variability of reach endpoints around the average endpoint. The across-subject means of AE were 1.42 ± 0.09 cm for the *Ego* task and 1.48 ± 0.07 cm for the *Allo* task. The across-subject means of VE were 1.65 ± 0.08 cm for the *Ego* task and 1.63 ± 0.05 for the *Allo* task.

Imaging parameters

The experiment was conducted at the neuroimaging centre of York University with a 3-T whole body MRI system (Siemens Magnetom TIM Trio, Erlangen, Germany). The posterior half of a 12-channel head coil (6 channels) was placed at the back of the head in conjunction with a 4-channel flex coil over the anterior part of the head (Fig. 2.1 A). The

former was tilted at an angle of 20° to allow a reach-to-touch movement to the touch screen as well as the direct viewing of the stimuli.

Functional data were acquired using an EPI (echo-planar imaging) sequence (repetition time [TR] = 2000 ms; echo time [TE] = 30 ms; flip angle [FA] = 90°; field of view [FOV] = 192 mm × 192 mm, matrix size = 64 × 64 leading to in-slice resolution of 3 mm × 3 mm; slice thickness = 3.5 mm, no gap; 35 transverse slices angled at approximately 25° covering the whole brain). The slices were collected in ascending and interleaved order. During each experimental session, a T1-weighted anatomical reference volume was acquired using a MPRAGE sequence (TR = 1900 ms; TE = 2.52 ms; inversion time TI = 900ms; FA = 9°; FOV=256 mm× 256 mm× 192 mm, voxel size = 1 × 1 × 1 mm^3).

Preprocessing

Data were analyzed using the Brain Voyager QX 2.2 software (Brain Innovation, Maastricht, the Netherlands). The first 2 volumes of each fMRI scan were discarded to avoid T1 saturation effects. For each run, slice scan time correction (cubic spline), temporal filtering (to remove frequencies < 2 cycles/run) and 3D motion correction (trilinear/sinc) were performed. The 3D motion correction was performed aligning each volume to the volume of the functional scan closest to the anatomical scan. Following inspection of the 3D motion correction parameters, we discarded runs showing abrupt head motion exceeding 1 mm or 1°. The whole data set (six runs) of one participant was discarded from the analyses due to head motion exceeding our set threshold; therefore data from twelve participants were included in the group GLM. The functional runs were co-registered to the anatomical image. Functional data were then transformed into standard Talairach space, using the spatial

transformation parameters from each participant's anatomical image. Functional data was spatially smoothed using a FWHM of 8mm.

Data analyses

For each participant, we used a GLM (general linear model) that included 21 predictors in total. In particular, one predictor was used for the eye movement to the *Fixation point* (2 s or 1 volume). In the *Stimulus presentation phase*, we used one predictor for target-landmark presentation and gaze shift (4 s or 2 volumes). In the *Delay phase*, we used 12 predictors (12 s or 6 volumes), one for each experimental condition (see "Experimental paradigm and timing"). In the *Landmark presentation phase*, we used one predictor (2 s or 1 volume). In the *Response phase* (4 s or 2 volumes), we considered two factors: 3 Tasks (*Ego, Allo, Color*) x 2 Target relative to gaze (*Left of Gaze: LG* and *Right of Gaze: RG*), which gave rise to six predictors: *Ego Reach: LG, Ego Reach: RG, Allo Reach: LG, Allo Reach: RG, Color: LG, Color: RG*. This allowed us to explore the brain areas involved in processing the direction of the movement during reach response. Each predictor was derived from a rectangular wave function convolved with a standard hemodynamic response function (HRF: Brain Voyager QX's default double-gamma HRF). In addition, we added six motion correction parameters and errors made in eye and reach data as confound predictors.

Voxelwise analyses

We performed contrasts on beta weights (β) using a RFX (group random effects) GLM where percent signal change transformation had been performed. Our questions were aimed at exploring brain areas that encode the target location during the *Delay phase* prior to

the movement (See Fig. 2.2 for predictions). First, we expected that areas involved in coding of target location and/or motor preparation for reach during the *Delay phase* would show higher activity in the *Egocentric* and *Allocentric reach* tasks as opposed to the *Color report* task. This was tested with Contrast no. 1: [(Delay Ego + Delay Allo) > Delay Color], in which we collapsed the left and right locations of target relative to gaze and landmark in the *Delay phase*. Second, we hypothesized that areas involved in egocentric coding of target location would show higher activation for the *Egocentric* vs. *Allocentric* task. In contrast, areas involved in allocentric coding of target location would show higher activation for the *Allocentric* vs. *Egocentric* task. Therefore, to further distinguish brain areas processing target location during the *Delay phase* in egocentric vs. allocentric coordinates, we performed Contrast no. 2: [Delay Ego > Delay Allo]. Third, we expected that egocentric directional selectivity (target location relative to gaze) would be revealed by higher activation for targets located to the left or to the right relative to the gaze. In order to explore areas showing egocentric directional selectivity, we performed Contrast no. 3: [Delay Ego (Target Right of Gaze) > Delay Ego (Target Left of Gaze)], in which we collapsed left and right target locations relative to landmark. Fourth, we expected that allocentric directional selectivity (target location relative to landmark) would be revealed by higher activation for target location to the left or to the right of the landmark. In order to investigate brain areas involved in allocentric directional selectivity, we performed Contrast no. 4: [Delay Allo (Target Right of Landmark) > Delay Allo (Target Left of Landmark)], in which we collapsed left and right target locations relative to gaze. Finally, we tested whether areas in the parieto-frontal network of each hemisphere are involved in processing the location of the target in the contralateral visual hemifield for reaching movements during the *Response phase*.

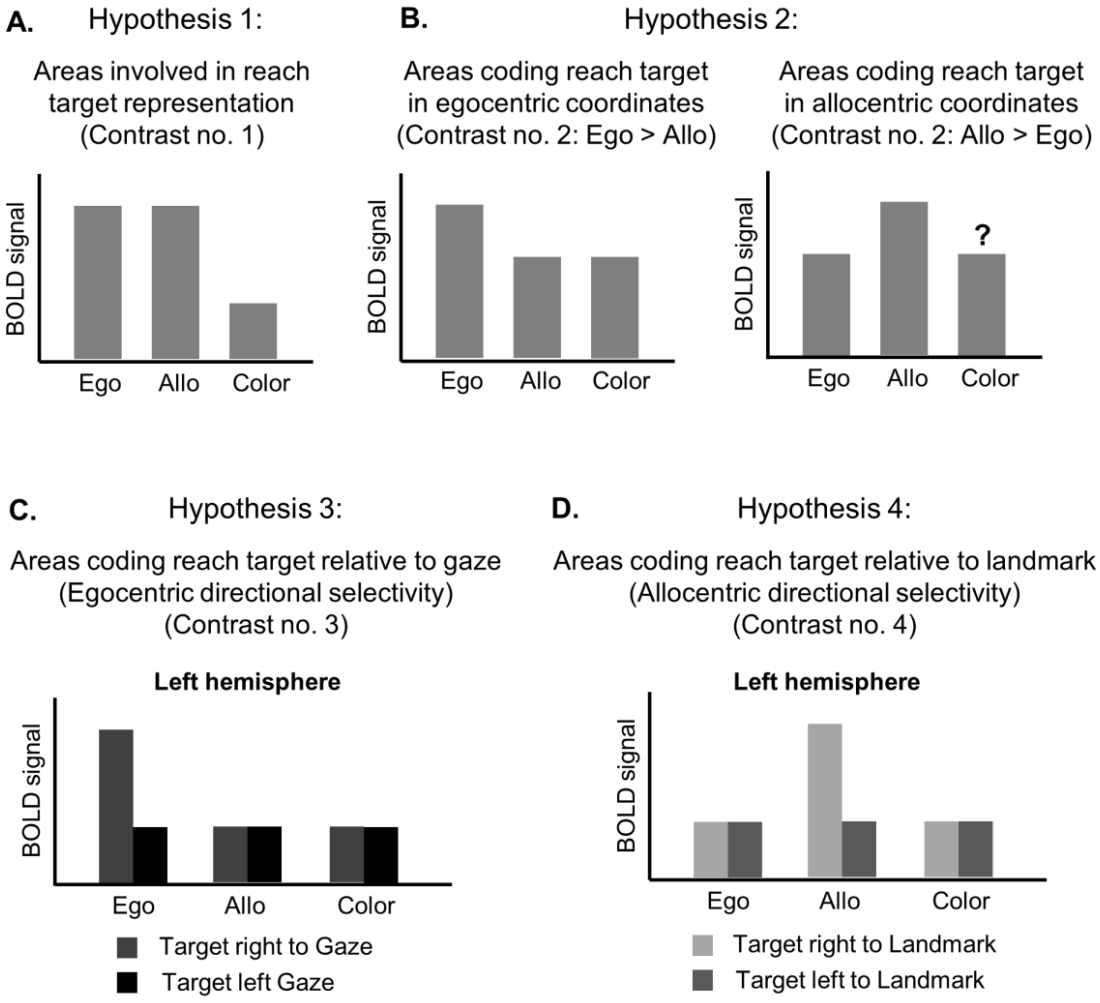
A.
Hypothesis 1:
Areas involved in reach target representation (Contrast no. 1)
BOLD signal
Ego
Allo
Color
B.
Hypothesis 2:
Areas coding reach target in egocentric coordinates (Contrast no. 2: Ego > Allo)
BOLD signal
Ego
Allo
Color
Areas coding reach target in allocentric coordinates (Contrast no. 2: Allo > Ego)
BOLD signal
?
Ego
Allo
Color
C.
Hypothesis 3:
Areas coding reach target relative to gaze (Egocentric directional selectivity) (Contrast no. 3)
Left hemisphere
BOLD signal
Ego
Allo
Color
Target right to Gaze
Target left Gaze
D.
Hypothesis 4:
Areas coding reach target relative to landmark (Allocentric directional selectivity) (Contrast no. 4)
Left hemisphere
BOLD signal
Ego
Allo
Color
Target right to Landmark
Target left to Landmark

Figure 2.2 Predicted BOLD signal changes based on our four contrasts during the delay phase. ***A,*** We expected that areas involved in reach target representation for Egocentric (Ego) and Allocentric (Allo) reach tasks would elicit higher activation as compared to the Color report (Color) task. ***B,*** Areas involved in coding reach target in egocentric coordinates would elicit higher activation in the Ego task as opposed to the Allo task and vice versa. We did not have any specific prediction about the level of activation in the Color task as compared to the Allo task for allocentric coding areas. ***C,*** We expected egocentric directional selectivity (target location relative to gaze) would be revealed by higher activation for target to the right vs. left of the gaze in the left hemisphere. ***D,*** We expected allocentric directional selectivity (target location relative to landmark location) would be revealed by higher activation for target to the right vs. left of the landmark in the left hemisphere.

This was tested by Contrast no. 5: [Reach (Target Right of Gaze) > Reach (Target Left of Gaze)] in *Egocentric* and *Allocentric reach* tasks, respectively. For this contrast, direction was defined according to the direction of the actual reach (i.e., reach direction relative to gaze).

Activation maps for group voxelwise results were overlaid either on the inflated anatomical image of one representative participant (Fig. 2.3, 2.8) or on the average anatomical image from twelve participants (Fig. 2.4, 2.5, 2.6, 2.7). In order to correct for multiple comparisons, we performed a cluster threshold correction (Forman et al., 1995) using BrainVoyager's cluster-level statistical threshold estimator plug-in. This algorithm uses Monte Carlo simulations (1000 iterations) to estimate the probability of a number of contiguous voxels being active purely due to chance while taking into consideration the average smoothness of the statistical maps. Areas that did not survive a cluster threshold correction were excluded from further analyses. The estimated minimum cluster size was 11 voxels (3 mm^3) for a total volume of 297mm^3. Subsequently, a Bonferroni correction was applied to paired-sample t-tests on β weights extracted from the areas that survived the cluster threshold correction. The Bonferroni correction was performed for three comparisons (corrected $p = 0.0167$) aimed at answering our main questions. The first group of comparisons performed on the results of Contrasts no. 1 and 2 was aimed at exploring differences between brain areas involved in egocentric and allocentric target coding. Therefore we performed the following comparisons: *Ego* vs. *Color, Allo* vs. *Color, Ego* vs. *Allo*. The second group of comparisons performed on the results of Contrasts no. 3 was aimed at investigating whether the coding of left and right target location relative to gaze was specific to the egocentric task or if it applied also to other tasks. Therefore we performed the

comparison *RG* vs. *LG* in *Ego, Allo* and *Color* tasks, respectively. The third group of comparisons performed on the results of Contrasts no. 4 was aimed at assessing whether the coding of target location relative to the landmark was specific to the allocentric task or it applied also to other tasks, therefore we performed the comparison *RL* vs. *LL* in *Ego, Allo* and *Color* tasks, respectively. The results on β weights are plotted in bar graphs in Figures 2.3 - 2.7 to illustrate significant differences between conditions at the corrected p-value, unless specified (see Results). Results that are non-independent of the selection criteria are indicated in square brackets in the β weight plots.

2.4 RESULTS

The main purpose behind our experimental design was to compare cortical activity related to egocentric and allocentric reach coding during the *Delay phase,* illustrated in Fig. 2.1 B. In this phase of our tasks, only target direction was specified (in Egocentric or Allocentric coordinates), while reach direction was specified only at the end of the *Landmark presentation phase* through the re-appearance of the landmark in the *Allocentric reach* task, or the *pro/anti-reach* instruction in the *Egocentric reach* task. We will begin with a detailed analysis of the *Delay phase* followed by a brief analysis of egocentric directional coding during the *Response phase.*

Task-Related Activation during the Delay Phase

We used Contrast no. 1 [(Delay Ego + Delay Allo) > Delay Color] to investigate the brain areas showing higher activation in the two experimental reach tasks (*Ego, Allo*) relative to the non-spatial control task *(Color).* The activation map for this contrast is shown on an

inflated cortical surface and the β weights are plotted in bar graphs (Fig. 2.3). The Talairach coordinates for the brain areas shown in Table 2.1. The activations shown by this contrast might be related to any aspect of target coding (not necessarily direction), cue location coding, and/or general motor preparation in anticipation of an oncoming reach movement.

This contrast revealed activation in dorsal premotor cortex (PMd), midposterior intraparietal sulcus (mIPS) and superior parieto-occipital cortex (SPOC) bilaterally, middle frontal gyrus (MFG), inferior frontal gyrus (IFG), pre-supplementary motor area (PreSMA) and extrastriate cortex in the left hemisphere. Post hoc comparisons revealed higher activation for *Ego* vs. *Color* in all these areas. In particular, this pattern was revealed in bilateral PMd [LH: $t(11) = 5.37$, $p = 0.001$; RH: $t(11) = 4.82$, $p = 0.001$], mIPS [LH: $t(11) = 4.29$, $p = 0.001$; RH: $t(11) = 4.34$, $p = 0.001$], SPOC [LH: $t(11) = 5.93$, $p = 0.001$; RH: $t(11) = 5.30$, $p = 0.001$], left MFG [$t(11) = 2.94$, $p = 0.013$], IFG [$t(11) = 2.84$, $p = 0.016$], PreSMA [$t(11) = 2.96$, $p = 0.013$], and extrastriate cortex [$t(11) = 4.61$, $p = 0.001$]. In addition, some of these areas also showed higher activation for *Allo* vs. *Color*. In particular, we found this pattern in bilateral PMd [LH: $t(11) = 4.23$, $p = 0.001$; RH: $t(11) = 2.60$, $p = 0.02$], SPOC [LH: $t(11) = 5.22$, $p = 0.001$; RH: $t(11) = 3.36$, $p = 0.006$], left MFG [$t(11) = 3.11$, $p = 0.010$], IFG [$t(11) = 3.20$, $p = 0.008$], PreSMA [$t(11) = 3.26$, $p = 0.008$], mIPS [$t(11) = 2.92$, $p = 0.014$] and extrastriate cortex [$t(11) = 3.11$, $p = 0.010$]. Moreover, the post hoc t-tests also revealed higher activation for *Ego* than *Allo* in bilateral SPOC [LH: $t(11) = 3.68$, $p = 0.004$; RH: $t(11) = 3.64$, $p = 0.004$], right PMd [$t(11) = 3.47$, $p = 0.005$] and mIPS [$t(11) = 2.63$, $p = 0.02$].

In summary, there was considerable overlap between areas showing higher activation in each of the two experimental reach tasks as opposed to the non-spatial control task. In

particular, these areas include bilateral PMd and SPOC, as well as left MFG, IFG, PreSMA, mIPS, and extrastriate cortex. Among these areas, bilateral SPOC, right PMd and mIPS also show higher activation for *Ego* vs. *Allo* tasks.

In order to investigate possible additional areas showing higher activation for *Ego* vs. *Allo* tasks and vice versa, we used Contrast no. 2, in which we directly compared *Ego* and *Allo* activation in the *Delay phase* (Fig. 2.4). The Talairach coordinates for the brain areas found with this contrast are shown in Table 2.2. The results confirmed higher activation for *Ego* vs. *Allo* tasks in bilateral SPOC, and PMd in the right hemisphere, and did not reveal any additional area with this pattern of activation. These 'Egocentric' areas also showed significantly higher activation in the *Allocentric* task versus the *Color* control task, suggesting that they were always active to some degree when a reach was being prepared. Several other areas in the early visual cortex showed higher activation for the *Allo* vs. *Ego* tasks (Fig. 2.5). In particular, we found bilateral lingual gyrus (LG) [LH: $t(11) = 4.04$, $p = 0.002$; RH: $t(11) = 3.75$, $p = 0.003$], calcarine sulcus [LH: $t(11) = 3.32$, $p = 0.007$; RH: $t(11) = 3.38$, $p = 0.006$], and cuneus [LH: $t(11) = 3.78$, $p = 0.003$; RH: $t(11) = 3.71$, $p = 0.003$]. In addition, these areas also showed higher activation for *Color* vs. *Ego*, including bilateral LG [LH: $t(11) = 3.22$, $p = 0.008$; RH: $t(11) = 2.97$, $p = 0.013$], calcarine sulcus [LH: $t(11) = 3.21$, $p = 0.008$; RH: $t(11) = 3.78$, $p = 0.003$], and cuneus [LH: $t(11) = 3.45$, $p = 0.005$; RH: $t(11) = 3.57$, $p = 0.004$] and no difference between *Allo* vs. *Color* tasks. This might be because early visual cortex was not selective for spatial memory in our experiment (see Discussion).

Contrast no. 1:
(Delay Ego + Delay Allo) > Delay Color

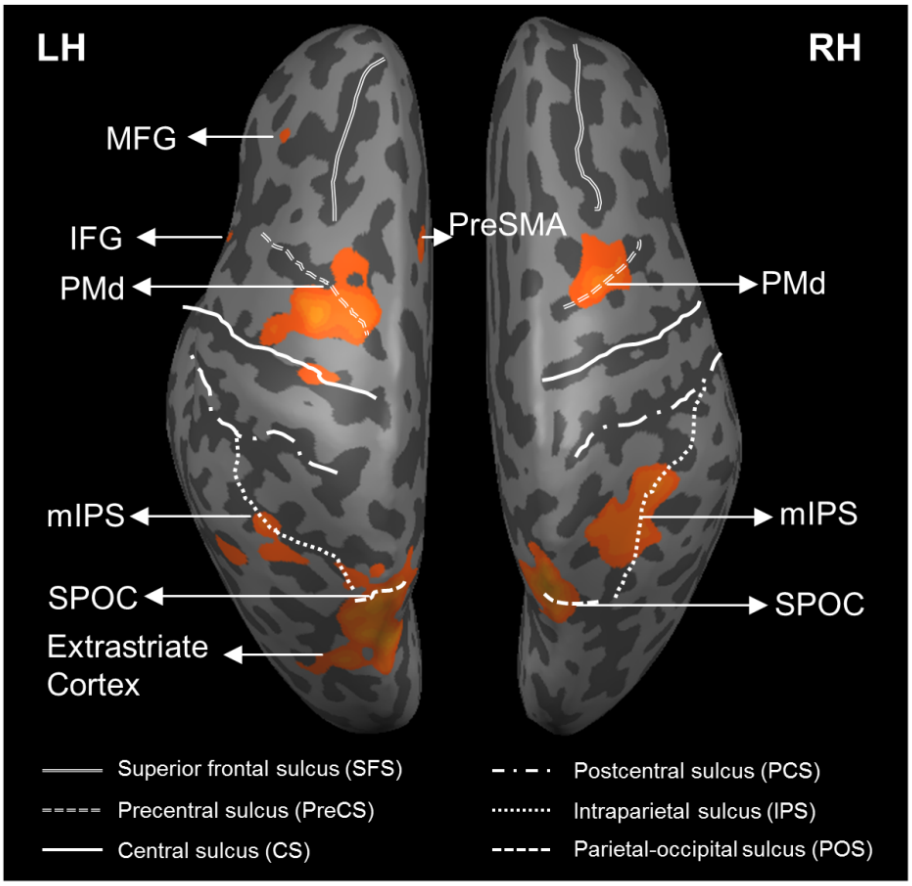

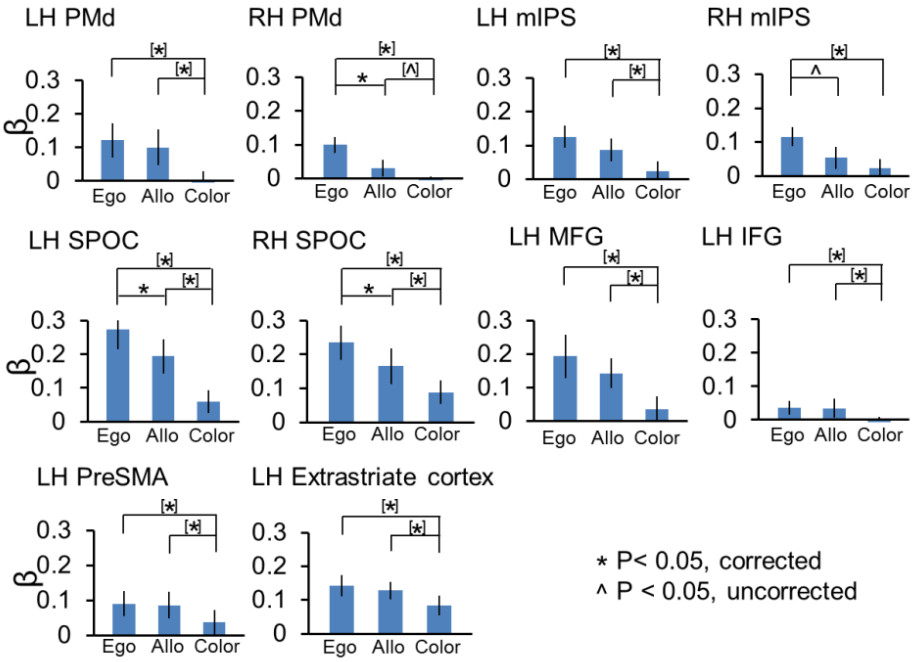

* P< 0.05, corrected
^ P < 0.05, uncorrected

Figure 2.3 Voxelwise statistical map and activation levels for each area using Contrast no. 1. [(Delay Ego + Delay Allo) > Delay Color], Top panel: activation map displayed on the inflated brain of one representative participant. Bottom panel: The bar graphs indicate the β weights for the three tasks in each area. * Significant differences between two tasks for $p < 0.05$. ^ Significant difference between two tasks for $p < 0.05$, uncorrected. Error bars are 95% confidence intervals.

Table 2.1 Talairach coordinates and number of voxels for contrast no. 1

Brain areas	Talairach coordinates			No. of voxels
	x	y	z	
[(Delay Ego + Delay Allo) > Delay Color]				
LH PMd	-29	-4	50	992
RH PMd	25	-6	50	943
LH mIPS	-32	-48	42	388
RH mIPS	31	-48	42	917
LH SPOC	-18	-68	48	956
RH SPOC	19	-65	48	867
LH MFG	-41	32	34	426
LH IFG	-41	13	10	693
LH PreSMA	-4	12	48	496
LH Extrastriate Cortex	-26	-75	26	628

In summary, these results demonstrate a parieto-frontal network involved in spatial memory of target for reaching movements. In particular, we show the presence of allocentric target representation in early visual areas in addition to an overlapping parieto-frontal circuit recruiting egocentric as well as allocentric target representation. In particular, while egocentric target coding preferentially relies on areas of the parieto-frontal network, such as PMd, mIPS, and SPOC, allocentric target coding preferentially relies on early visual cortex, such as LG, calcarine and cuneus. However, this coding was not discretely separate; in our task design, 'Egocentric' areas also showed activity in the *Allocentric* task, and 'Allocentric' areas also showed activity in the *Color* task.

Egocentric Directional Selectivity: Target Location Relative to Gaze

Next, we examined the directional selectivity revealed by cortical activation during the *Delay phase* with the use of Contrast no. 3 [Delay Ego (Target Right of Gaze) > Delay Ego (Target Left of Gaze)]. The Talairach coordinates of the brain areas are reported in Table 2.3. As shown in Figure 2.6, this contrast revealed higher activation for right vs. left target location relative to the gaze in the left superior occipital gyrus (SOG) [$t(11) = 3.00$, $p = 0.012$] and inferior occipital gyrus IOG [$t(11) = 3.00$, $p = 0.012$]. Neither area showed significant egocentric direction specificity in either the *Allocentric* or *Color* tasks, suggesting that the egocentric coding scheme in SOG and IOG was task-dependent. There was no active voxel showing higher activation for targets presented to the left as compared to the right of the gaze in the *Egocentric reach* task.

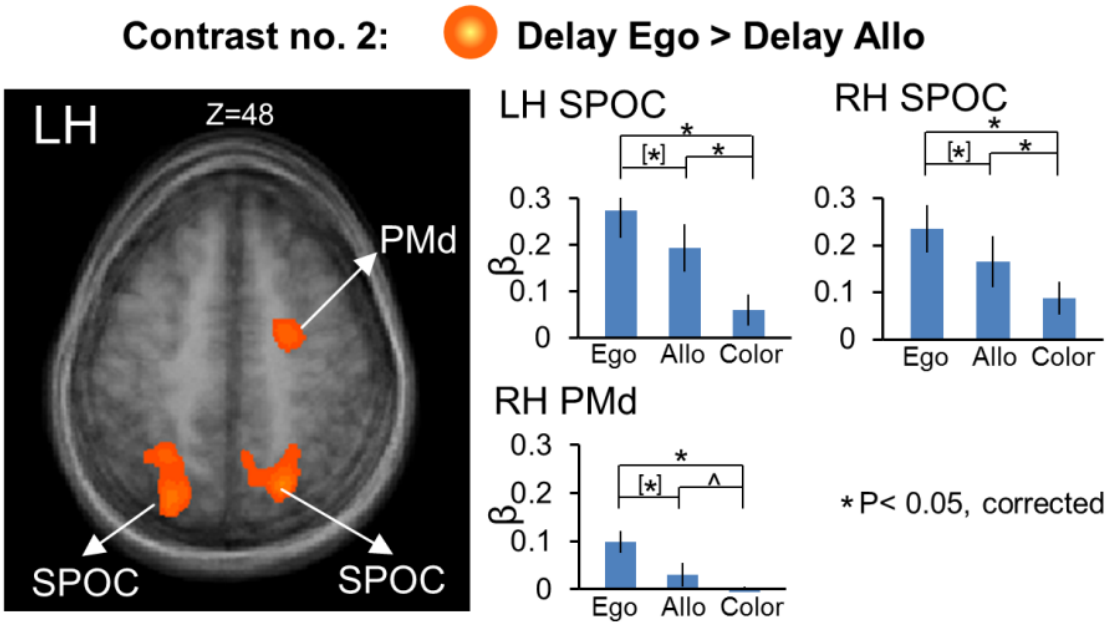

Figure 2.4 Voxelwise statistical map and activation levels for each area using Contrast no. 2 [Delay Ego > Delay Allo]. Left panel: activation map overlaid on the averaged anatomical image from all 12 participants. Right panel: The bar graphs indicate the β weights for the three tasks in each area. [*] Significant difference non-independent of the criteria used to select the area. Other legends as in Figure 2.3.

Contrast no. 2: **Delay Allo > Delay Ego**

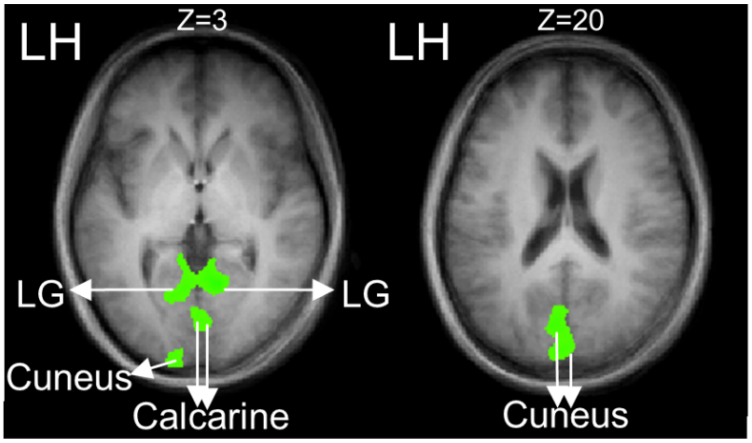

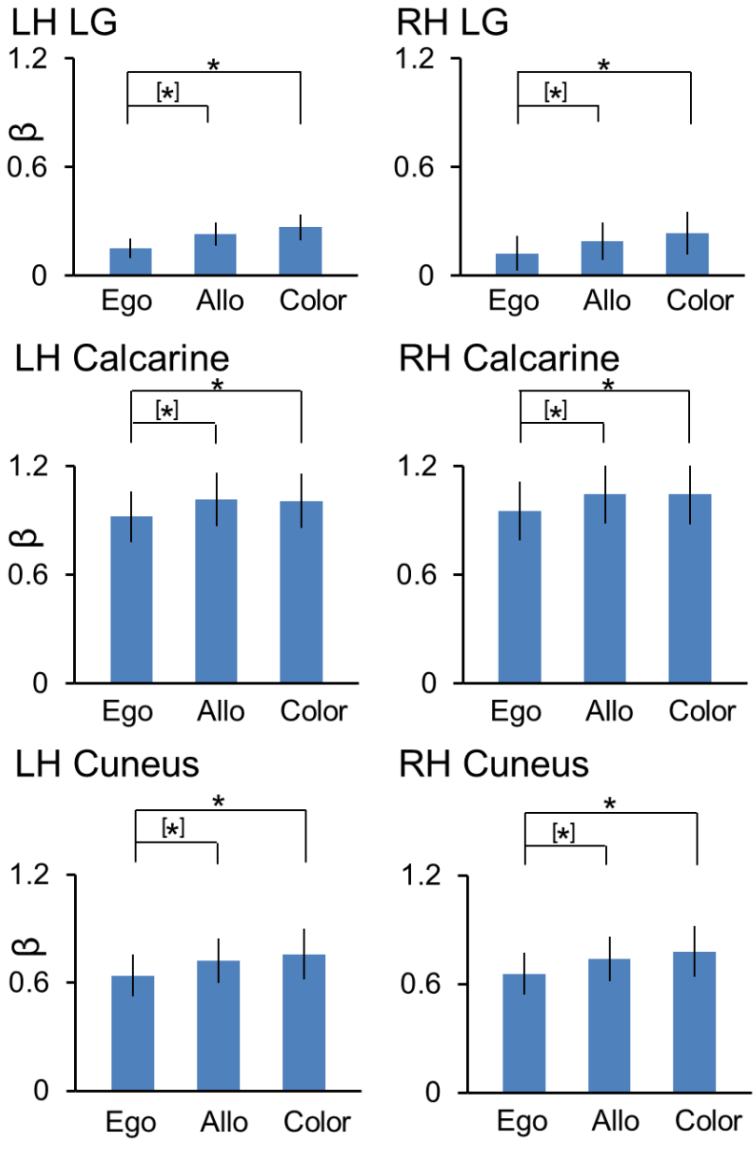

* P< 0.05, corrected

Figure 2.5 Voxelwise statistical map and activation levels for each area using Contrast no.2 [Delay Allo > Delay Ego]. Top panel: activation map overlaid on the averaged anatomical image from all 12 participants. Bottom panel: The bar graphs indicate the β weights for the three tasks in each area. Legends as in Figure 2.3.

Table 2.2 Talairach coordinates and number of voxels for contrast no. 2

Brain areas	Talairach coordinates			No. of voxels
	x	y	z	
Delay Ego > Delay Allo				
RH PMd	25	-6	50	943
LH SPOC	-18	-68	48	956
RH SPOC	19	-65	48	867
Delay Allo > Delay Ego				
LH LG	-6	-58	3	592
RH LG	4	-57	3	785
LH Calcarine	-2	-79	3	736
RH Calcarine	1	-77	3	857
LH Cuneus	-2	-87	20	869
RH Cuneus	1	-86	20	586

To investigate whether there were additional areas showing egocentric directional selectivity in the *Allocentric* task, we ran the contrast [Delay Allo (Target Right of Gaze) > Delay Allo (Target Left of Gaze)]. This analysis revealed an additional area (data not shown) in the right calcarine sulcus that showed higher activation for right vs. left target location relative to gaze in *Allo* [t (11) = 3.05, p = 0.011]. However, this area also showed egocentric directional specificity in *Color* [t (11) = 3.15, p = 0.009], suggesting that the egocentric directional specificity observed in this area was not specific for reach tasks.

Allocentric Directional Selectivity: Target Location Relative to Landmark

The key element to the design of this study was that it allowed us to analyze the neural coding of reach targets relative to visual landmarks in the *Allocentric reach* task. To determine which brain regions were involved in allocentric directional selectivity of target location relative to the landmark, independent of other visual features, we performed Contrasts no. 4 [Delay Allo (Target Right of Landmark) > Delay Allo (Target Left of Landmark)]. The brain areas revealed by this contrast are shown in Figure 2.7. Talairach coordinates are shown in Table 2.3.

As illustrated in Figure 2.7 A, area IOG [t (11) = 4.07, p = 0.002] in the left hemisphere showed higher activation for target to the right vs. left of the landmark. In addition, inferior temporal gyrus (ITG) in the left hemisphere [LH: t (11) = 3.13, p = 0.009] showed higher activation for target to the left vs. right of the landmark (Fig. 2.7 B). These regions showed no significant allocentric coding during the *Egocentric reach* and *Color report* tasks, suggesting that these allocentric coding results are task specific.

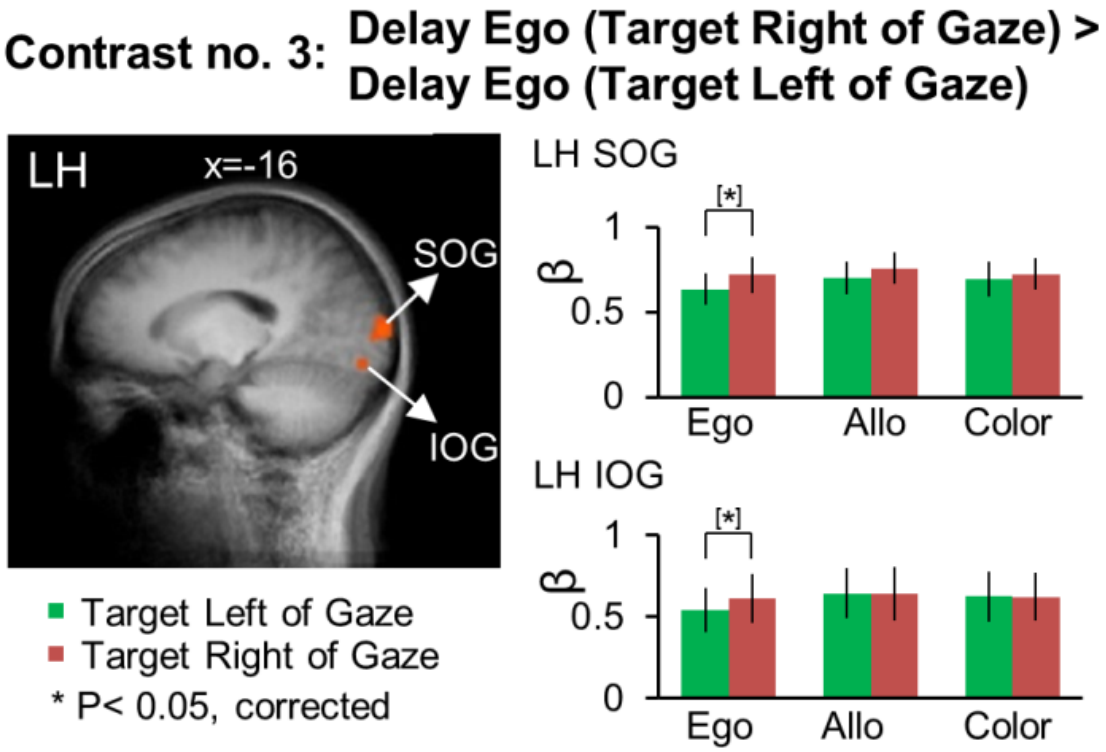

Figure 2.6 Voxelwise statistical map and activation levels for each area using Contrast no.3 Egocentric directional selectivity during delay. [Delay Ego: (Target Right of Gaze) > Delay Ego: (Target Left of Gaze)]. Left panel: activation map overlaid on the averaged anatomical image from all 12 participants. Right panel: The bar graphs indicate the β weights for each condition in each area. Legends as in Figure 2.3.

To investigate whether there were additional areas showing allocentric directional selectivity in the egocentric task, we ran the contrast [Delay Ego (Target Right of Landmark) > Delay Ego (Target Left of Landmark)]. We found no significant active voxel for this contrast.

To summarize, we found significant allocentric directional selectivity in ITG and IOG. These results suggest that temporal and early visual cortices are specifically involved in the allocentric coding of remembered target location in a task where allocentric landmark location is unpredictable.

Reach Direction during Movement Response

As noted above, we did not observe egocentric directional selectivity in parietal or frontal cortex during the *Delay phase*, unlike previous fMRI studies where reach direction could be planned during the delay phase (Medendorp et al., 2003; Medendorp et al., 2005b; Fernandez-Ruiz et al., 2007). This may have been because in our *Delay phase*, subjects could not yet plan the horizontal position of the actual reach. To test if this was the case, we performed Contrast no. 5 [Reach (Target Right of Gaze) > Reach (Target Left of Gaze)] during the *Response phase*, i.e., after reach direction was cued by either the reappearance of the landmark (*Allo* task) or the *pro/anti* instruction (*Ego* task). The hand was not visible to subjects during reach; therefore, these responses were not contaminated by visual feedback. The brain areas revealed by these contrasts are shown in Figure 2.8, and the Talairach coordinates are shown in Table 2.4.

Contrast no. 4:

A. Delay Allo (Target Right of Landmark) > Delay Allo (Target Left of Landmark)

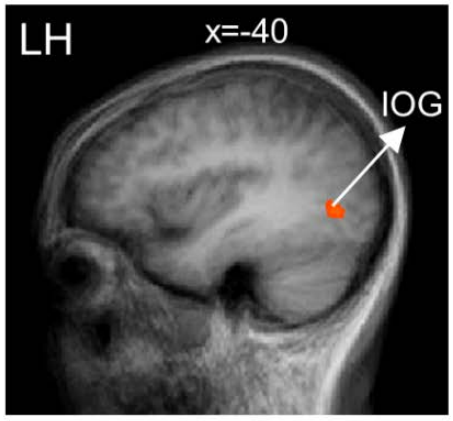

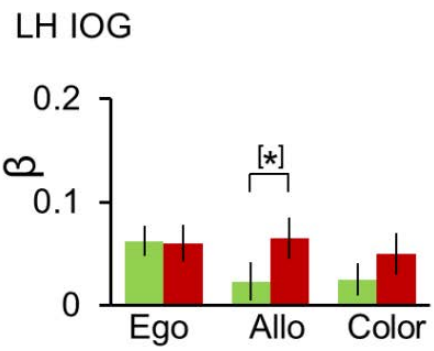

B. Delay Allo (Target Left of Landmark) > Delay Allo (Target Right of Landmark)

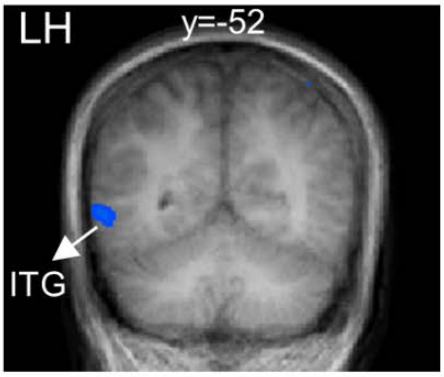

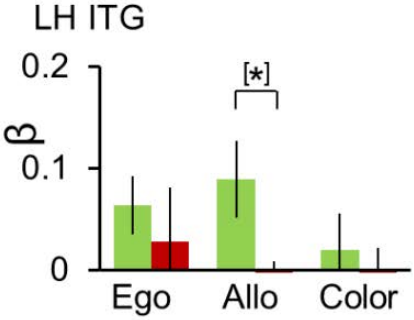

* P< 0.05, corrected

Target Left of Landmark

Target Right of Landmark

Figure 2.7 Voxelwise statistical map and activation levels for each area using Contrast no.4 Allocentric directional selectivity during delay. ***A,*** [Delay Allo (Target Right of Landmark) > Delay Allo (Target Left of Landmark)] ***B,*** [Delay Allo (Target Left of Landmark) > Delay Allo (Target Right of Landmark)]. Left panels: activation maps overlaid on the averaged anatomical image from all 12 participants. Right panels: The bar graphs indicate the β weights for each condition in each area. Legends as in Figure 2.3.

Table 2.3 Talairach coordinates and number of voxels for contrast nos. 3, 4

Brain areas	Talairach coordinates			No. of voxels
	x	y	z	
Delay Ego (Target Right of Gaze) > Delay Ego (Target Left of Gaze)				
LH SOG	-12	-95	4	380
LH IOG	-16	-86	-11	422
Delay Allo (Target Right of Landmark) > Delay Allo (Target Left of Landmark)				
LH IOG	-40	-68	2	386
Delay Allo (Target Left of Landmark) > Delay Allo (Target Right of Landmark)				
LH ITG	-56	-52	-3	413

This analysis revealed contralateral egocentric directional selectivity, primarily in the left hemisphere, including several parieto-frontal areas that did not show directional selectivity during the *Delay phase*. As shown in Figure 2.8, there was higher activation for reaching movements to the right vs. left of gaze in the *Ego* task in left PMd, supplementary motor area (SMA), M1, S1, superior parietal lobe (SPL), extrastriate cortex and lateral occipital complex (LOC). In addition, precentral gyrus, pIPS, extrastriate cortex, LOC, calcarine and LG showed higher activation for movements to the right as opposed to the left of gaze in the *Allo* task. Only three regions in the right hemisphere showed directional selectivity (this time preferring movements left vs. right of gaze) in the *Ego* and *Allo* tasks, respectively. Specifically, this pattern was revealed in mIPS, angular gyrus (AG) and pIPS for the *Ego* task, while in SPL, calcarine and LG for the *Allo* task.

In summary, during the *Response phase,* we found egocentric directional selectivity in occipital, parietal, and frontal cortex, with structures in both hemispheres showing a directional preference for reaches made to the contralateral side relative to gaze.

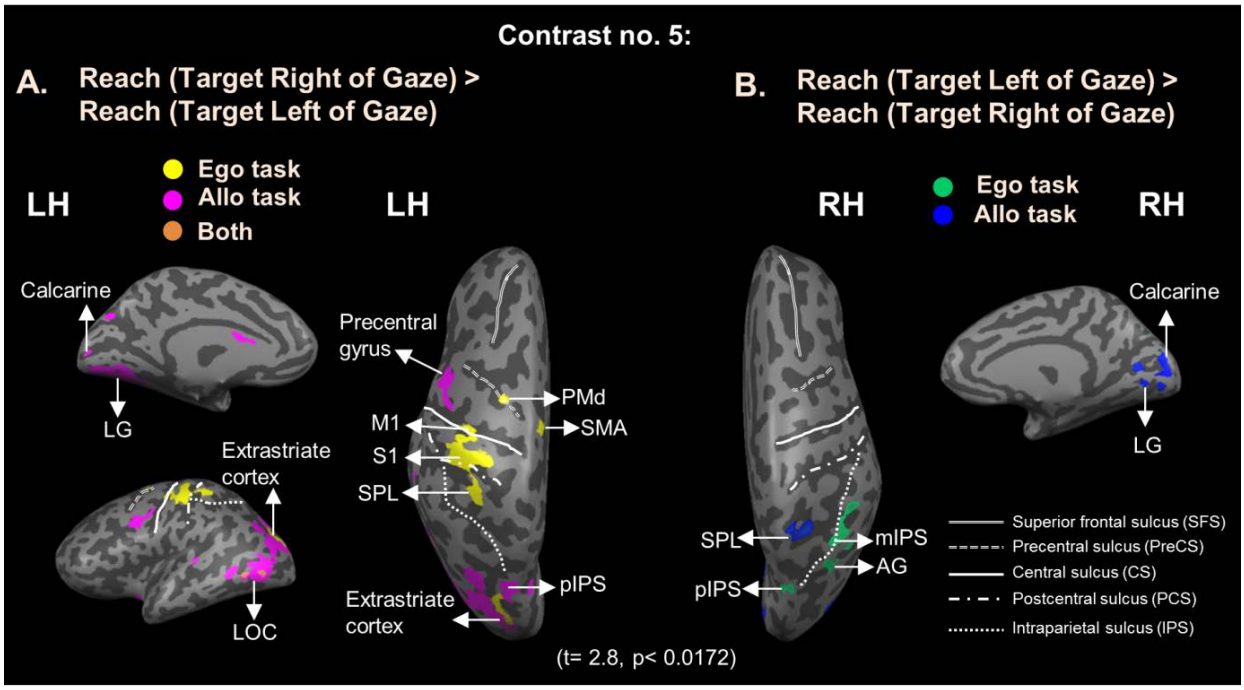

Figure 2.8 Voxelwise statistical map using Contrast no. 5 Egocentric directional selectivity during response. ***A,*** Reach (Target Right of Gaze) > Reach (Target Left of Gaze). Yellow, voxels activated in Ego task. Pink, voxels activated in Allo task. Orange, voxels activated in both tasks. ***B,*** Reach (Target Left of Gaze) > Reach (Target Right of Gaze). Green, voxels activated in Ego task. Blue, voxels activated in Allo task.

Table 2.4 Talairach coordinates and number of voxels for contrast no. 5

Brain areas	Talairach coordinates			No. of voxels
	x	y	z	
Reach (Target Right of Gaze) > Reach (Target Left of Gaze)				
Ego task:				
LH PMd	-22	-6	56	158
LH SMA	-4	-10	55	362
LH M1	-33	-18	47	249
LH S1	-38	-24	53	352
LH SPL	-39	-40	58	320
Allo task:				
LH Precentral Gyrus	-49	-2	41	358
LH pIPS	-23	-68	32	318
LH Calcarine	-7	-86	7	164
LH LG	-9	-76	3	234
Both tasks:				
LH Extrastriate Cortex	-21	-86	25	334
LH LOC	-45	-74	6	412
Reach (Target Left of Gaze) > Reach (Target Right of Gaze)				
Ego task:				
RH mIPS	40	-54	41	244
RH AG	35	-68	41	374
RH pIPS	30	-73	41	386
Allo task:				
RH SPL	27	-53	55	383
RH Calcarine	11	-86	9	313
RH LG	7	-72	3	457

2.5 DISCUSSION

In this study, we employed an experimental design that distinguished between egocentric vs. allocentric coding of a reach target during the *Delay phase*, and temporally separated target location memory from motor planning by only cuing reach direction at the start of the *Response phase*. This distinguishes our experiment both from imaging studies that tested allocentric memory through some type of spatial judgement and from reach tasks where movement direction was cued from the beginning of each trial. Further, our analysis discriminated between 1) cortical areas that were active during egocentric and allocentric target coding, 2) areas that were differentially active for egocentric versus allocentric target coding, and 3) areas that were spatially selective in either egocentric or allocentric coordinates. This analysis revealed widespread, partially overlapping patterns of cortical activation in the *Delay phase* with, most importantly, divergent occipital-temporal mechanisms for allocentric vs. egocentric target direction coding. Additional parieto-frontal mechanisms for reach direction coding emerged during the *Response phase*. We will consider each of these findings in detail.

Egocentric vs. Allocentric Activation during the *Delay Phase*

Numerous human imaging studies have implicated superior occipital-partietal-frontal cortex in reach and pointing planning (Astafiev et al., 2003; Connolly et al., 2003; Medendorp et al., 2003; Brown et al., 2004; Medendorp et al., 2005b; Medendorp et al., 2005a; Prado et al., 2005; Brown et al., 2006; Fernandez-Ruiz et al., 2007; Beurze et al., 2009; Cavina-Pratesi et al., 2010; Fabbri et al., 2012; Konen et al., 2013). Our study

generally agrees with their findings, but places a stronger emphasis on target coding during our *Delay phase*.

Our *Delay phase* analysis revealed considerable overlap in extrastriate, parietal and frontal areas involved in both allocentric and egocentric coding of reach targets as compared to the non-spatial control task (*Color*). However, bilateral SPOC and right PMd showed a preference for egocentric reach target coding, whereas early visual cortex (LG, calcarine and cuneus) showed a preference for allocentric reach target coding. This allocentric preference in early visual cortex might be because this type of task requires subjects to remember multiple visual stimuli, whereas subjects only have to remember one visual stimulus in an egocentric task. Further, early visual cortex also showed higher activation in the *Color* as compared to the *Ego* task, so it was not selective for spatial memory in our experiment. These results are consistent with imaging studies that have implicated occipital cortex in both spatial and feature-specific memory (Greenlee et al., 2000; Merriam et al., 2007; Harrison and Tong, 2009).

Unlike previous neuroimaging studies of allocentric coding that involved perceptual judgments (Galati et al., 2000; Committeri et al., 2004; Neggers et al., 2006; Zaehle et al., 2007) or manual judgements (Thaler and Goodale, 2011b), we did not find higher allocentric activation in lateral occipital complex (LOC) or posterior parietal cortex (PPC) in our *Delay phase*. This might be because our behavioral task separated the storage of target information during this phase from the response, whereas these processes were integrated in previous paradigms. Comparing across these studies suggests that the neural mechanisms used for allocentric coding are task-dependent.

Directional Coding during the *Delay Phase*

Previous imaging studies demonstrated a preference for contralateral reach coding in gaze-centered coordinates in PPC (Medendorp et al. 2003, 2005; Fernandez-Ruiz et al., 2007). Previous imaging studies of allocentric judgements did not specifically test for allocentric directional selectivity, i.e. target location relative to cue (Fink et al., 2000; Galati et al., 2000; Committeri et al., 2004; Neggers et al., 2006; Zaehle et al., 2007; Thaler and Goodale, 2011b). However, neurophysiological studies have shown that saccade-related responses in parieto-frontal neurons can code relative locations within an object (Olson and Gettner, 1995; Olson and Tremblay, 2000; Sabes et al., 2002; Olson, 2003). This analysis has not been done in a reach task.

Here, during the *Delay phase* we found a preference for contralateral reach targets (relative to gaze/midline) in left IOG and SOG during the *Egocentric* task, whereas IOG and ITG coded target direction relative to a visual landmark in the *Allocentric* task. These responses may represent the cumulative population activity of neurons with directional modulations similar to those reported in the previous oculomotor studies (e.g. Olson 2003). The involvement of IOG in both egocentric and allocentric directional selectivity may indicate that these structures form a common hub for different types of visuospatial memory, whereas the differentiation of SOG for egocentric memory vs. ITG for allocentric memory is consistent with previous theories of functional specialization within the dorsal and ventral visual streams (Milner and Goodale, 1995; Schenk, 2006). Again, these findings suggest a degree of task-specificity not evident in previous perceptual studies (Merriam et al., 2007; Harrison and Tong, 2009).

As in a previous study (Committeri et al., 2004), ours defined target locations relative to a mobile reference point, and both studies observed allocentric-specific activation in ventro-lateral occipital-temporal cortex. In natural circumstances, egocentric and allocentric cues are stable and agree with each other. Thus, they can be optimally integrated for reach (Byrne and Crawford, 2010), which likely involves cooperative network connections between the areas described in the current study. Finally, we employed an *explicit* allocentric task; different cortical mechanisms may be involved in tasks where allocentric information is *implicit* (Byrne and Crawford, 2010).

Parieto-frontal Direction Selectivity in *Delay* vs. *Response Phases*

We observed general activation of the parieto-frontal reach network in the *Delay phase* of both of our spatial tasks, presumably because our subjects were expecting to apply a rule-based visuomotor transformation upon the arrival of the subsequent go-signal for a reach movement (Hawkins et al., 2013). However, we were surprised that this activation was not directionally selective. This contradicts a study that reported ipsilateral direction preference in the monkey parietal reach region and PMd during a task very similar to our *Egocentric task* (Westendorff et al., 2010), but those responses may have been biased by lengthy training on the anti-reach task. Conversely, the lack of parieto-frontal direction selectivity in our *Delay phase* data appears to contradict studies that showed contralateral directional selectivity in PPC during the delay between viewing a target and reaching toward it (Medendorp et al., 2005a; Gail and Andersen, 2006). However, our subjects did not know what direction they would reach, relative to gaze/midline until the end of the *Delay phase*.

Thus, only target direction was coded in this phase, and our data suggest that this is not sufficient to evoke measureable parieto-frontal direction selectivity in the human.

The latter conclusion suggests that additional motor signals are required to evoke parieto-frontal direction selectivity. To test this, we analyzed egocentric directional selectivity during our *Response phase*, after movement direction was specified. As predicted, directional selectivity re-appeared through most of the expected components of the human parieto-frontal reach network, including mIPS, SPL, AG, and PMd (Filimon, 2010; Vesia and Crawford, 2012). This data likely contained signals related to transformation of target memory into motor plans, commands, motor execution, and propriopceptive (but not visual) feedback. However, comparing the current data to studies where planning was separated from motor execution suggests that the conversion of target coding into planning, or planning itself, is sufficient to produce directional tuning in parieto-frontal cortex (Medendorp et al., 2005a; Gail and Andersen, 2006).

These conclusions are harder to reconcile with studies that showed spatial selectivity in PPC in the absence of any overt movement (Duhamel et al., 1992b; Colby et al., 1995; Merriam et al., 2003). It is possible that those subjects implicitly use motor imagery to help remember target location. Conversely, it is possible that in our *Delay phase*, parieto-frontal target signals were masked by directionally non-specific reach plans. Otherwise, our findings generally agree with the literature on movement planning in parieto-frontal cortex (Kalaska and Crammond, 1992; Kalaska et al., 1997; Kakei et al., 2001; Andersen and Buneo, 2002; Beurze et al., 2009; Filimon et al., 2009).

Asymmetry of Cortical Responses

Overall, we found a greater propensity for left hemisphere activation (and concomitantly rightward target coding) in both the *Delay* and *Response* phases. This might be explained by interactions between hand lateralization and visual hemifield lateralization (Perenin and Vighetto, 1988; Rossetti et al., 2003; Medendorp et al., 2005b; Beurze et al., 2007; Blangero et al., 2007; Vesia and Crawford, 2012). This has been shown before in parietal cortex (Fernandez-Ruiz et al., 2007), but is somewhat surprising that it also occurred in occipital cortex. Possibly this reflects feedback of reach signals to these areas. For example, even though subjects could not see their hand in our task, they may have visualized it (Filimon et al., 2007). It is also possible that this is related to attentional enhancement of visual stimuli near the hand (di Pellegrino and Frassinetti, 2000; Reed et al., 2006; Abrams et al., 2008). Taken together with our main result that occipital cortex encodes reach targets in both egocentric and allocentric coordinates, these results support the notion that occipital cortex plays a more important role in the guidance of action than often assumed (Pasternak and Greenlee, 2005).

CHAPTER THREE

CORTICAL MECHANISMS FOR ALLOCENTRIC AND EGOCENTRIC REPRESENTATION OF REMEMBERED TARGETS FOR SACCADES IN HUMAN CORTEX

Authors: Ying Chen, J. Douglas Crawford

Currently Submitted / in review

3.1 ABSTRACT

A remembered saccade target could be encoded in egocentric (body-centered) coordinates or relative to some allocentric (world-centered) cue. In comparison to egocentric mechanisms, very little is known about allocentric representation. Here, we used an event-related fMRI design to identify brain areas supporting these two types of spatial coding for target memory during the *Delay phase* where only target location, not saccade direction, was specified. The paradigm included three tasks with identical display of visual stimuli but different auditory instructions: *Allocentric saccade* (remember target location relative to a visual landmark), *Egocentric saccade* (remember target location independent of the landmark), and a non-spatial control, *Color report* (report target color). During the *Delay phase,* the *Egocentric* and *Allocentric* tasks activated overlapping areas in posterior parietal cortex (PPC) and frontal cortex as compared to the control, but with higher activation in PPC for *Egocentric* coding and higher activation in temporal and occipital cortex for *Allocentric coding*. Egocentric directional selectivity (target relative to gaze fixation at midline) was observed in superior occipital gyrus and inferior occipital gyrus, whereas allocentric directional selectivity was observed in precuneus and midposterior intraparietal sulcus. During the *Response phase* after saccade direction was specified, the parietofrontal network in the left hemisphere showed higher activation for rightward than leftward saccades. Our results suggest that the cortical mechanisms for coding saccade target direction relative to an independent visual cue differ from purely egocentric mechanisms for target memory, from the mechanisms for other types of allocentric tasks, and from the directionally selective mechanisms for saccade planning and execution.

3.2 INTRODUCTION

To explore and interact with the visual world, people make frequent saccades toward both visible and remembered targets (Enright, 1995; Rayner, 1998; Henderson and Hollingworth, 1999; Henderson et al., 1999; Land et al., 1999; Land and Hayhoe, 2001; Henderson, 2003; Bays and Husain, 2007; Rayner, 2009). In the absence of additional cues, visual movement targets can be encoded in memory with respect to egocentric (body-centered) frames of reference, such as the eyes, head or body (Dassonville et al., 1995; Andersen, 1997; Karn et al., 1997; Colby, 1998; Henriques et al., 1998; Burnod et al., 1999; Cohen and Andersen, 2002). However, the addition of other stable visual stimuli provides potential cues for an allocentric (world-centered) frame of reference for coding target location (Carrozzo et al., 2002; Obhi and Goodale, 2005; Crawford et al., 2011; Tatler and Land, 2011; Sharika et al., 2014). These cues can be implicit, such as the influence of general background information on a memory-guided movement (Mohrmann-Lendla and Fleischer, 1991; Whitney et al., 2003; Uchimura and Kitazawa, 2013), or they can be explicit, such as the deliberate choice of remembering target location relative to another cue that is judged to be stable (Olson, 2003; Krigolson and Heath, 2004; Krigolson et al., 2007; Cordova et al., 2012). Psychophysical studies in the reach system suggest that when both egocentric and allocentric cues are present, human subjects use an optimal combination of both, weighted through a combination of reliability and subjective judgements of cue stability (Byrne and Crawford, 2010). However, such studies cannot reveal the functional neuroanatomy of these systems. The goal of the current study was to compare human cortical mechanisms for egocentric coding of remembered saccade targets versus the explicit coding of a saccade target relative to a specified visual landmark.

The neural correlates of egocentric mechanisms are relatively well known, based on findings from both neurophysiological and human imaging studies. It has been shown that posterior parietal cortex (PPC), frontal eye field (FEF) and supplementary eye field (SEF) are involved in the coding of remembered saccadic targets and planning in egocentric reference frames (Colby, 1998; Sereno et al., 2001; Andersen and Buneo, 2002; Munoz, 2002; Medendorp et al., 2003; Munoz and Everling, 2004; Medendorp et al., 2005b; Medendorp et al., 2005a; Schluppeck et al., 2005; Curtis and D'Esposito, 2006; Kastner et al., 2007; Van Pelt et al., 2010; Crawford et al., 2011; Kravitz et al., 2011). Among these studies a contralateral left-right topography (i.e., egocentric directional selectivity: target direction in an egocentric frame) was shown in human midposterior intraparietal sulcus (mIPS) and FEF (Sereno et al., 2001; Medendorp et al., 2003; Medendorp et al., 2005b; Medendorp et al., 2005a; Schluppeck et al., 2005; Curtis and D'Esposito, 2006; Kastner et al., 2007; Van Pelt et al., 2010). However, the egocentric mechanisms for saccade target memory were not directly investigated in those studies because there was no explicit separation between memory and movement planning / execution.

In comparison to egocentric mechanisms, overall the allocentric mechanisms for saccade target coding are very little known. Some neurophysiological studies for object-centered (target location relative to a part of the object itself) spatial coding of saccade targets revealed selective activity in SEF(Olson and Gettner, 1995, 1996; Olson and Tremblay, 2000; Olson, 2003). A recent fMRI study demonstrated that several areas in temporal and occipital cortex can explicitly code the direction of reach targets relative to an allocentric visual cue (Chen et al., 2014). Another recent fMRI study has identified regions of the human parietal and occipital cortex that are involved in an ‘automatic’ (task irrelevant)

allocentric coding of visual stimuli for judgment tasks, if the background cue is large enough (Uchimura et al., 2015). However, to our knowledge, the cortical mechanisms for the allocentric coding of memorized saccade targets (target location relative to another visual landmark) have not been investigated or directly compared with egocentric mechanisms, in terms of either general cortical activation patterns or the directional selectivity of specific areas.

Based on the previous literature from reach and cognitive tasks, one might expect that egocentric and allocentric mechanisms for saccade target memory might have both shared and distinct cortical mechanisms (Galati et al., 2000; Zaehle et al., 2007; Thaler and Goodale, 2011b; Chen et al., 2014). More specifically, one might expect the involvement of occipital cortex for the egocentric directional selectivity of saccade target memory as shown in a recent fMRI study for reach (Chen et al., 2014). If the cortical mechanisms for allocentric directional selectivity of saccade targets are similar to those in object-centered coordinates, one might expect higher activation in SEF, or other areas in frontal cortex as indicated in previous neurophysiological studies (Olson and Gettner, 1996; Olson and Tremblay, 2000). If the cortical mechanisms involved in the allocentric directional selectivity for the coding of saccade targets are similar to those for reach targets, one might expect an engagement of temporal cortex (Chen et al., 2014). However, if there are specific neural mechanisms involved in the allocentric directional selectivity for saccade targets relative to independent visual cues, i.e., effector-specific mechanisms, one might expect the activation of areas that differ from those involved in either the coding of allocentric reach targets or object-centered saccade targets.

To test these predictions, we used an event-related fMRI paradigm similar to our recent reach study (Chen et al., 2014) (1) to examine brain areas involved in spatial coding of remembered saccade targets in egocentric and allocentric frames of reference; (2) to investigate which brain areas show directional selectivity of remembered saccade targets in egocentric versus allocentric coordinates; (3) to compare egocentric directional selectivity for remembered saccade targets versus actual saccades during the motor response. Our results showed that cortical areas for the coding of remembered saccade targets in egocentric coordinates were different from those employed for coding in allocentric coordinates, in both general activation and direction specificity. The cortical areas showing egocentric directional selectivity during the delay phase differed from those during the response phase. The cortical areas showing allocentric directional selectivity of saccade target memory were different from those observed for reach targets and saccade targets represented in object-centered coordinates (Olson and Gettner, 1995; Olson and Tremblay, 2000; Chen et al., 2014), suggesting an effector- and coordinate-dependent mechanisms for allocentric coding of target direction.

3.3 MATERIALS AND METHODS

Participants

Twelve right-handed participants (9 females and 3 males, aged 22-42 years) participated in this study and gave informed consent prior to the experiment. All had normal or corrected to normal vision and had no known neuromuscular deficits. We chose this number of subjects based on precedents set in similar studies of visuomotor control in healthy subjects (Cavina-Pratesi et al., 2007; Gallivan et al., 2011). The resulting dataset was sufficient to yield statistically significant results that survived corrections for multiple comparisons (see Results). This study was approved by the York Human Participants Review Subcommittee.

Experimental apparatus and stimuli

We used a same apparatus as that in a previous reach study (Chen et al. 2014). The visual stimuli of light dots produced by optic fibers were embedded in a custom-built board mounted atop a platform. The platform was placed above the abdomen of the participant and affixed to the scanner bed. The board was approximately perpendicular to the direction of gaze on the central fixation point and was placed about ~60 cm away from the eyes of the participants. Participant's head was slightly tilted to allow direct viewing of the stimuli without using mirrors. An eye-tracking system (iView X) was used in conjunction with the MRI-compatible Avotec Silent Vision system (RE-5701) to record gaze position from the right eye during fMRI experiments. A button pad was placed on the left side of the participant's abdomen and used as a response key for the *Color report* task (see

Experimental paradigm and timing). Participants wore headphones to hear auditory instructions about the upcoming trial. During the experiment, participants were in complete darkness except for being able to see the visual stimuli.

There were four types of stimuli each presented in a different color: yellow for the central fixation point, green or red for the saccade targets, blue for the visual landmarks, and white for the mask (Fig. 3.1). The dots of light corresponding to targets and relative visual landmarks were located to the left and the right of the central fixation point with a visual angle of four to seven degrees on each side, and being separated from each other by one visual degree. These dots could be red, green or blue, therefore they could be used as a target or a visual landmark in different trials. This allowed us to create 40 different combinations of target and visual landmark locations where the target could be located one or two visual degrees to the left or to the right of a visual landmark. Initial target and visual landmark were both displayed either to the left or to the right of the central fixation point. Since participants' gaze and head positions were always aligned with their body midline, we used 'midline' as the zero point in a general egocentric coordinate system for the analyses of egocentric directional selectivity (i.e., target/saccade right of gaze = target/saccade right of midline, target/saccade left of gaze = target/saccade left of midline).

The mask consisted of 20 dots of light displayed in two rows, one above and one below the targets. The location of each dot for the mask was aligned with the midpoint between two adjacent targets dots. The purpose of using a mask was to avoid potential after effects arising from the illumination of the target and the landmark in the dark. Since our analyses focused mainly on the *Delay phase*, it was critical to ensure that the recruitment of

target location for the upcoming saccade was resulting from memory rather than utilizing the afterimage of the target.

Experimental paradigm and timing

We employed an event-related design to investigate three main questions. First, we contrasted the neural substrates involved in the general processing saccade target location in allocentric versus egocentric frames of reference during the *Delay phase*. Second, we determined the brain areas showing directional selectivity of spatial coding of saccade targets in egocentric vs. allocentric coordinates during the same *Delay phase*. Third, we investigated the areas involved in processing saccade direction during the *Response phase*.

The paradigm consisted of three tasks: *Egocentric saccade* (*Ego*), *Allocentric saccade* (*Allo*), and *Color report* (*Color*) (Fig. 3.1). In the *Allocentric saccade* task, participants had to remember and later make a saccade to the location of the target relative to a visual landmark. The saccade target and the additional landmark were initially presented together, then the landmark re-appeared at the same or at a different location (see Fig. 3.1 and below for details). The horizontal position of the saccade could not be planned during the memory period (i.e., the *Delay phase*) as the location of re-displayed landmark could not be predicted during this phase. In the *Egocentric saccade* task, participants had to remember and make a saccade to the remembered target, either at its initial location (*pro-saccade*), or at its mirror location in the opposite hemi-field (*anti-saccade*). The *anti-saccade* condition was used to equalize the motor aspects in the *Ego* and *Allo* tasks, i.e., so that in both tasks the horizontal saccade position could only be computed when the instruction to perform a saccade or an anti-saccade was given. Therefore, the activation observed during the *Delay phase* in both

tasks could only be related to the coding of horizontal target location, rather than saccade planning (although other types of directionally non-specific motor preparation for a forward saccade might exist during this phase). The *Color report* task was used as a non-spatial control where participants only reported the color of targets by pressing a button once or twice corresponding to the green or red saccade target.

Our paradigm consisted of five phases (*Fixation point, Target and Landmark presentation, Delay, Landmark presentation, Response*) (Fig. 3.1). Prior to each trial, a recorded auditory instruction signalled the participant about the upcoming task: "Saccade relative to cue" (for *Allocentric saccade* tasks), "Saccade to target" (for *Egocentric saccade* tasks), "Report target color" (for *Color report* tasks). Each trial started with the presentation of the central fixation for participants to fixate throughout the experiment. After 2 s, a target was presented along with a landmark for 2 s. Depending on the initial instruction, after the target and landmark disappeared, during the following 12 s *Delay phase* participants had to remember the location of the target relative to the landmark (*Allocentric saccade*), the location of the target regardless of the landmark (*Egocentric saccade*), or the color of the target (*Color report*). After the delay, the landmark re-appeared for 2 s either at its original location or at a novel location in the same or opposite hemifield of its first presentation. Subsequently, an auditory signal cued participants to saccade toward the allocentric target location (audio: "Saccade"), i.e., the target location relative to the re-presented landmark location for the *Allocentric saccade* task. In the *Egocentric saccade* task, participants were instructed to saccade toward the egocentric target location (audio: "Target" for *pro-saccade*), or the location opposite to the egocentric target location (audio: "Opposite" for *anti-*

saccade). In the *Color report* task, participants indicated the color of the previously presented target by pressing the button (audio: “Color”).

Each run contained 18 trials where each task was repeated six times in a random order. An intertrial interval of 16 s was added between each trial to allow the hemodynamic response to return to baseline yielding a run time of approximately 12 min. Each participant was tested in six runs. In addition to the three tasks, we considered directional selectivity of remembered saccade targets in egocentric (Left and Right relative to midline) and allocentric coordinates (Left and Right relative to the visual landmark). This gave rise to three factors in our design: 3 Tasks (*Ego, Allo, Color*) x 2 Target locations relative to midline (*Left of Midline: LM, Right of Midline: RM*) x 2 *Target locations relative to landmark* (*Left of Landmark: LL, Right of Landmark: RL*). Therefore, there were 12 conditions in total: *Ego: LM:LL, Ego: LM:RL, Ego: RM:LL, Ego: RM:RL, Allo: LM:LL, Allo: LM:RL, Allo: RM:LL, Allo: RM:RL, Color: LM:LL, Color: LM:RL, Color: RM:LL, Color: RM:RL*. These 12 conditions were counterbalanced in each run. Participants were trained to perform the tasks one day prior to scan.

Behavioral analysis

Following our fMRI experiments, we inspected eye position data for every trial to ensure that participants correctly followed all instructions. Errors in eye movements were defined as trials in which participants made a saccade toward the target or the visual landmark, or were not able to maintain central fixation during the delay phase, or the location of the saccade endpoint was on the opposite side of the actual target location relative to the midline on the touch screen. Trials that showed those errors were modelled as confound

predictors and excluded from further fMRI analyses (see Data analyses). All participants completed at least 96 correct trials (89% of the total trials).

In order to confirm that participants actually used egocentric or allocentric visual information in the corresponding task (*Ego* or *Allo*) to encode target location as instructed, and to exclude the possibility that they simply made saccades to the correct side of the screen midline, we performed a correlation analysis. First, we calculated the distance between a participant's saccade response for a given trial and the screen midline, then calculated the distance between the proper target location (whether egocentrically or allocentrically defined) and the screen midline. If participants made saccades toward the correct location, these two values should be well correlated in both *Ego* and *Allo* tasks. The across-subject means of these correlation coefficients were 0.85 ± 0.01 for the *Ego* task and 0.87 ± 0.01 for the *Allo* task. We then applied Fisher's r-to-z transformation to the individual subject correlation coefficients (r) so that we could use standard t-tests to compare the between-subjects means of z values to zero. If participants were using the egocentric or allocentric spatial information for target coding, then these coefficients should have been significantly greater than zero. Standard t-tests showed that mean of correlation coefficient was significantly greater than zero in both tasks ($p_{ego} = 0.0000001$, $p_{allo} = 0.0000001$). The correlations were still significant ($p_{ego} = 0.000003$, $p_{allo} = 0.000004$) when absolute values for the distance were used, showing that subjects also adjusted the amplitude of the saccades in response to different target amplitudes on each side.

To further quantify participants' performance, we calculated the absolute error (AE) and the variable error (VE) in the horizontal dimension for each participant in each saccade task (*Ego* or *Allo*), respectively. The AE is the absolute value of the distance between the

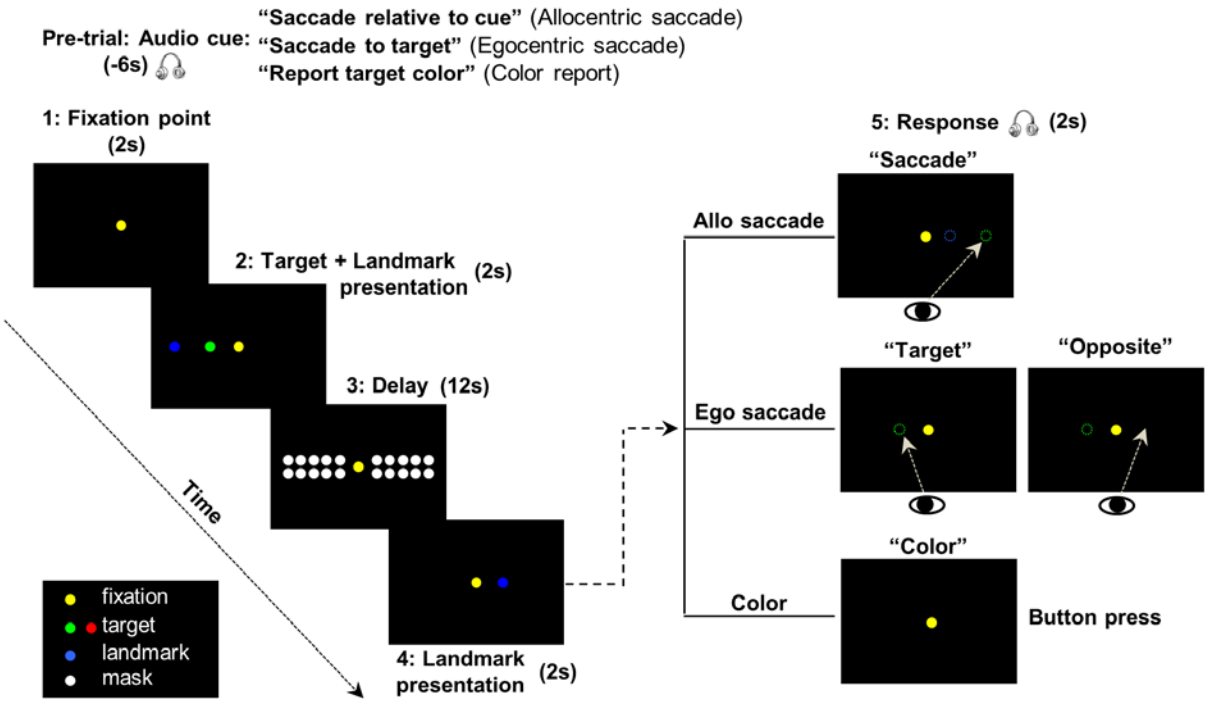

Figure 3.1. Experimental paradigm. The display of the visual stimuli is identical for the three tasks (Allocentric saccade, Egocentric saccade and Color report). The critical difference between the two saccade tasks is the reference frames used for the coding of target location for the upcoming saccade. In the Allocentric saccade task, target location is encoded relative to the landmark. In the Egocentric saccade task, target location is encoded relative to the self. In the Color report task, the color of the target, rather than location, is being remembered and reported.

target position and the endpoint of a saccadic movement and represents the amount by which the target was missed. The VE was computed by taking the standard deviation of the constant saccade errors and represents the variability of saccade endpoints around the average endpoint. The across-subject means of AE were 1.63 ± 0.07 cm for the *Ego* task and 1.58 ± 0.06 cm for the *Allo* task. The across-subject means of VE were 1.75 ± 0.06 cm for the *Ego* task and 1.73 ± 0.05 for the *Allo* task. There was no significant difference for AE [$t_{(11)}$ = 0.54, p = 0.60] and VE [$t_{(11)}$ = 0.39, p = 0.70] between the *Ego* and *Allo* tasks.

Imaging parameters

This study was conducted at the neuroimaging center at York University using a 3-T whole body MRI system (Siemens Magnetom TIM Trio, Erlangen, Germany). The posterior half of a 12-channel head coil (6 channels) was placed at the back of the head in conjunction with a 4-channel flex coil covering the anterior part of the head. The former was tilted at an angle of 20° to allow the direct viewing of the stimuli.

Functional data were acquired using an EPI (echo-planar imaging) sequence (repetition time [TR] = 2000 ms; echo time [TE] = 30 ms; flip angle [FA] = 90°; field of view [FOV] = 192 mm × 192 mm, matrix size = 64 × 64 leading to in-slice resolution of 3 mm × 3 mm; slice thickness = 3.5 mm, no gap; 35 transverse slices angled at approximately 25° covering the whole brain). The slices were collected in ascending and interleaved order. During each experimental session, a T1-weighted anatomical reference volume was acquired using a MPRAGE sequence (TR = 1900 ms; TE = 2.52 ms; inversion time TI = 900ms; FA = 9°; FOV=256 mm× 256 mm× 192 mm, voxel size = 1 × 1 × 1 mm^3).

Preprocessing

Data were analyzed using the Brain Voyager QX 2.2 software (Brain Innovation, Maastricht, the Netherlands). The first 2 volumes of each fMRI scan were discarded to avoid T1 saturation effects. For each functional run, slice scan time correction (cubic spline), temporal filtering (removing frequencies < 2 cycles/run) and 3D motion correction (trilinear/sinc) were performed. The 3D motion correction was performed aligning each volume to the volume of the functional scan closest to the anatomical scan. Following inspection of the 3D motion correction parameters, the runs showing abrupt head motion exceeding 1 mm or 1° were discarded. Two runs (one from each of two participants) were discarded from the analyses due to head motion exceeding our set threshold. The functional run closest to the anatomical image for each participant was co-registered to the anatomical image. Functional data were then mapped into standard Talairach space, using the spatial transformation parameters from each participant's anatomical image. Subsequently, functional data was spatially smoothed using a FWHM of 8mm.

Data analyses

For each participant, we used a general linear model (GLM) including 22 predictors in total. In particular, we used one predictor for the *Target and Landmark presentation phase* (2 s or 1 volume). We used 12 predictors (12 s or 6 volumes), one for each experimental condition for the *Delay phase*, (see Experimental paradigm and timing). We used one predictor (2 s or 1 volume) for the *Landmark presentation phase.* There were two factors in the *Response phase* (2 s or 1 volume): 3 Tasks (*Ego, Allo, Color*) x 2 Saccade direction relative to midline (*Left of Midline: LM, Right of Midline: RM*). This resulted in six

predictors: *Ego Saccade: LM, Ego Saccade: RM, Allo Saccade: LM, Allo Saccade: RM, Color: LM, Color: RM,* thus allowing us to explore the brain areas involved in processing the saccade direction during response. We used one predictor for keeping eyes on the saccade target (6 s or 3 volumes) for the current response to ensure stable saccade performance, and one predictor for shifting gaze back to the central fixation point for the next trial (2 s or 1 volume). Each predictor was derived from a rectangular wave function convolved with a standard hemodynamic response function (HRF), the Brain Voyager QX's default double-gamma HRF. In addition, we added six motion correction parameters and errors made in eye data as confound predictors.

Voxelwise analyses

We performed contrasts on beta weights (β) using a group random effects (RFX) GLM where percentage signal change transformation had been performed. Our study aimed to explore brain areas encoding the saccade target location during the *Delay phase* prior to the movement. First, we used Contrast no. 1: [(Delay Ego + Delay Allo) > Delay Color] to investigate areas involved in coding of target location for the *Egocentric* and *Allocentric* saccade tasks as compared to the *Color report* control task. We collapsed the target location left and right to midline and landmark in the *Delay phase*. Second, we performed Contrast no. 2: [Delay Ego > Delay Allo] to identify brain areas involved in processing target location in egocentric vs. allocentric coordinates during the *Delay phase*. Third, we performed Contrast no. 3: [Delay Ego (Target Right of Midline) > Delay Ego (Target Left of Midline)] to examine areas showing egocentric directional selectivity (target location relative to midline). We collapsed left and right target locations relative to landmark. Fourth, we

performed Contrast no. 4: [Delay Allo (Target Right of Landmark) > Delay Allo (Target Left of Landmark)] to investigate brain areas showing allocentric directional selectivity (target location relative to landmark). In this contrast, we collapsed left and right target locations relative to midline. Finally, we tested whether areas in the parieto-frontal saccade network show a preference for target location in the contralateral visual hemifield for movements during the *Response phase*. This was assessed by Contrast no. 5: [Saccade Right of Midline > Saccade Left of Midline] in *Egocentric* and *Allocentric* tasks, respectively, during the *Response phase*. For this contrast, direction was defined as saccade direction relative to midline.

Activation maps for group voxelwise results were rendered either on the inflated anatomical image of one representative participant (Fig. 3.2, 3.7) or on the average anatomical MRI from twelve participants (Fig. 3.3, 3.4, 3.5, 3.6). In order to correct for multiple comparisons, we performed a cluster threshold correction (Forman et al., 1995) using BrainVoyager's cluster-level statistical threshold estimator plug-in. This algorithm uses Monte Carlo simulations (1000 iterations) to estimate the probability of a number of contiguous voxels being active purely due to chance while taking into consideration the average smoothness of the statistical maps. Areas that did not survive a cluster threshold correction were excluded from further analyses. The estimated minimum cluster size was 28 voxels (3 mm^3) for a total volume of 756 mm^3. Subsequently, a Bonferroni correction was applied to paired-sample t-tests on β weights extracted from each area that survived the cluster threshold correction. The Bonferroni correction was performed for three comparisons (corrected $p = 0.0167$) aimed at answering our main questions.

For Contrasts no. 1 and 2, we performed the following comparisons on β weights: *Ego* vs. *Color*, *Allo* vs. *Color*, *Ego* vs. *Allo* to explore the difference of brain activity between tasks. For Contrasts no. 3, we performed three comparisons on β weights: *RM* vs. *LM* in *Ego*, *Allo* and *Color* tasks, respectively, to investigate whether the coding of left and right target location relative to midline was specific to the egocentric task or it also existed in other two tasks. For Contrasts no. 4, we performed three comparisons on β weights: *RL* vs. *LL* in *Ego*, *Allo* and *Color* tasks, respectively, to examine whether the coding of target location relative to the landmark was specific to the allocentric task or it also applied to other two tasks. For Contrasts no. 5, we performed three comparisons on β weights: Saccade *RM* vs. Saccade *LM* in *Ego*, *Allo* and *Color* tasks, respectively, to confirm that the coding of saccade direction relative to midline only emerged in the two saccade tasks, not in the *Color* control task. The results on β weights are plotted in bar graphs in Figures 3.2-3.7 to illustrate significant differences between conditions at the corrected p-value, unless specified (see Results). Results that are non-independent of the selection criteria are indicated in square brackets in the β weight plots.

3.4 RESULTS

The key question behind our design was to compare cortical activity involved in the coding of saccade targets in egocentric and allocenric coordinates during the *Delay phase.* As shown in Fig. 3.1, in this phase only target direction was specified (in Egocentric or Allocentric frames of reference), whereas saccade direction was informed only at the end of *Landmark presentation phase* through the re-presented landmark (*Allocentric saccade),* or the *pro/anti-saccade* instruction (*Egocentric saccade).* We performed a detailed analysis for

the *Delay phase*, followed by a brief analysis on saccade directional coding during the *Response phase.* Each of the figures (3.2 - 3.7) begins with a voxelwise analysis of whole brain activity, followed by further paired t-tests on β weights between conditions from each significant activity cluster. See Table 3.1 for a list of the cortical areas that were active in these analyses, and their acronyms.

Task-Related Cortical Activation during the Delay Phase

We performed Contrast no. 1 [(Delay Ego + Delay Allo) > Delay Color] to explore the brain areas showing higher activation in the two experimental saccade tasks (*Ego, Allo*), as opposed to the non-spatial control task *(Color).* Figure 3.2 shows the resulting activation map, superimposed on an inflated cortical surface, with the corresponding mean β weights for each task and area plotted beneath as bar graphs. The Talairach coordinates of these brain areas are reported in Table 3.2. Note that the activations revealed by this contrast might be related to any aspect of target coding, including landmark location coding, and/or general motor preparation with expectancy in an upcoming saccade, except target or movement direction (this is dealt with in subsequent sections).

Compared to the *Color report* task, the *Ego* and *Allo saccade* tasks elicited higher activation in: bilateral frontal eye field (FEF), midposterior intraparietal sulcus (mIPS) and superior parieto-occipital cortex (SPOC) in the left hemisphere, anterior (*a*mIPS) and posterior mIPS (*p*mIPS) in the right hemisphere (Fig. 3.2, upper panel). Paired t-tests on β weights (Fig. 3.2, lower panels) indicated higher *Ego* vs. *Color* activation in these areas:

Table 3.1 Acronyms for brain areas from voxelwise analyses

Acronyms	Names of brain areas
*a*IOG	anterior inferior occipital gyrus
*a*mIPS	anterior midposterior intraparietal sulcus
FEF	frontal eye field
IOG	inferior occipital gyrus
ITG	inferior temporal gyrus
LOtG	lateral occipitotemporal gyrus
MFG	middle frontal gyrus
mIPS	midposterior intraparietal sulcus
MOG	middle occipital gyrus
MTG	middle temporal gyrus
*p*IOG	posterior inferior occipital gyrus
*p*IPS	posterior intraparietal sulcus
*p*mIPs	posterior midposterior intraparietal sulcus
SEF	supplementary eye field
SMG	supramarginal gyrus
SOG	superior occipital gyrus
SPL	superior parietal lobule
SPOC	superior parieto-occipital cortex

bilateral FEF [LH: $t_{(11)} = 5.33$, $p = 0.00024$; RH: $t_{(11)} = 3.56$, $p = 0.0045$], left mIPS [$t_{(11)} = 2.95$, $p = 0.013$], left SPOC [$t_{(11)} = 3.30$, $p = 0.0071$], right *a*mIPS [$t_{(11)} = 3.27$, $p = 0.0075$] and right *p*mIPS [$t_{(11)} = 3.01$, $p = 0.012$]. We also found higher activation for *Allo* vs. *Color* in some of these areas: bilateral FEF [LH: $t_{(11)} = 4.66$, $p = 0.00070$; RH: $t_{(11)} = 2.76$, $p = 0.018$], left mIPS [$t_{(11)} = 4.17$, $p = 0.0016$] and left SPOC [$t_{(11)} = 3.24$, $p = 0.0079$]. In addition, the t-tests also indicated higher activation for *Ego* vs. *Allo* in right *a*mIPS [$t_{(11)} = 2.88$, $p = 0.015$]. In summary, this analysis mostly revealed overlapping activation in the *Ego* and *Allo* saccade tasks in bilateral FEF, left mIPS and left SPOC, except that right *a*mIPS showed higher activation for *Ego* vs. *Allo* tasks, and that right *p*mIPS showed higher activation for *Ego* vs. *Color* tasks.

Subsequently, we used Contrast no. 2 to directly compare *Ego* and *Allo* activation during the *Delay phase* to explore the areas showing higher activation for *Ego* vs. *Allo* tasks and vice versa. The Talairach coordinates for these brain areas are reported in Table 3.3. Figure 3.3 shows the areas that showed significantly higher activation in the *Ego* task, overlaid on horizontal brain slices and with the corresponding β-weights for each area and task plotted beneath. These areas included right *a*mIPS [$t_{(11)} = 2.88$, $p = 0.015$], and right supramarginal gyrus (SMG) [$t_{(11)} = 2.90$, $p = 0.014$]. The comparison of β-weights for these regions showed that they were also significantly activated less for the Color Task [*Ego* vs. *Color*: right *a*mIPS: $t_{(11)} = 3.27$, $p=0.0075$, right SMG: $t_{(11)} = 2.43$, $p = 0.033$]. This demonstrates that activation of amIPS and SMG showed specificity for the *Ego* task.

Figure 3.4 shows areas that showed significantly higher activation in the *Allo* task, using similar conventions to Figure 3.3 but showing the statistical map on both horizontal and sagittal brain slices. This analysis identified several areas in occipital cortex showing

Contrast no. 1:
(Delay Ego + Delay Allo) > Delay Color

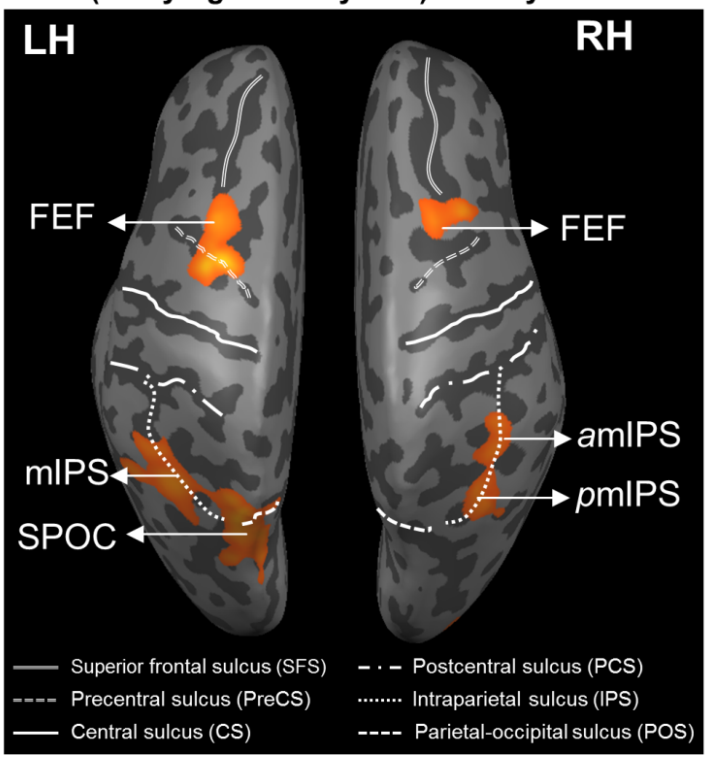

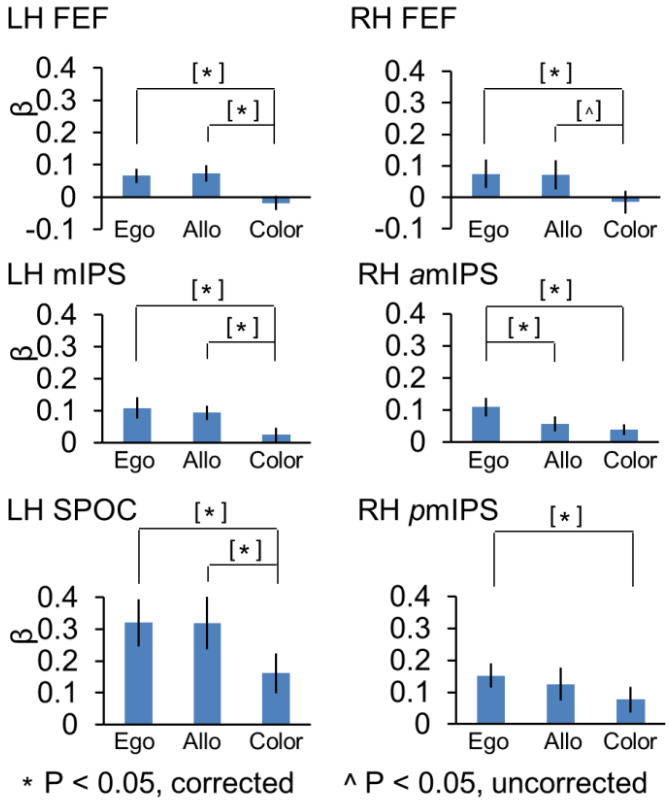

* P < 0.05, corrected

^ P < 0.05, uncorrected

Figure 3.2. Voxelwise statistical map and activation levels for each area using Contrast no.1. [(Delay Ego + Delay Allo) > Delay Color], Top panel: activation map rendered on the inflated brain of one representative participant. Bottom panel: bar graphs show the β weights for the three tasks in each area. [*] Significant difference between two tasks for $p < 0.05$, non-independent of the criteria used to select the area. [^] Significant difference between two tasks for $p < 0.05$, uncorrected, non-independent of the criteria used to select the area. Error bars indicate 95% confidence intervals.

Table 3.2 Talairach coordinates and number of voxels for contrast no. 1

Brain areas	Talairach coordinates			No. of voxels
	x	y	z	
[(Delay Ego + Delay Allo) > Delay Color]				
LH FEF	-24	-1	50	513
RH FEF	28	3	50	508
LH mIPS	-40	-48	42	512
RH *a*mIPS	33	-37	39	353
RH *p*mIPS	33	-57	39	392
LH SPOC	-18	-67	49	511

higher activation for the *Allo* vs. *Ego* tasks, including bilateral calcarine sulcus [LH: $t_{(11)} = 3.64$, $p = 0.0039$; RH: $t_{(11)} = 3.47$, $p = 0.0053$] and cuneus [LH: $t_{(11)} = 3.74$, $p = 0.0032$; RH: $t_{(11)} = 3.02$, $p = 0.012$], and middle occipital gyrus (MOG) in the right hemisphere [$t_{(11)} = 3.44$, $p = 0.0055$]. However, our t-test analysis on β-weights (lower panels) showed that these occipital areas also showed higher activation for *Color* vs. *Ego*, including bilateral calcarine sulcus [LH: $t_{(11)} = 2.96$, $p = 0.013$; RH: $t_{(11)} = 3.08$, $p = 0.010$] and cuneus [LH: $t_{(11)} = 3.01$, $p = 0.012$; RH: $t_{(11)} = 3.55$, $p = 0.0046$], and right MOG [$t_{(11)} = 3.15$, $p = 0.0093$]. This suggests that general activation of early visual cortex was not specific to any one of the tasks in the current experiment. In addition, this analysis (Figure 3.4) revealed higher *Allo* activation in left inferior temporal gyrus (ITG) [$t_{(11)} = 3.13$, $p = 0.0096$]. This area also showed higher activation in the *Allo* than the *Color* task, but this did not reach significance [$t_{(11)} = 1.61$, $p = 0.14$].

To summarize, these results showed overlapping parieto-frontal areas for spatial memory of egocentric and allocentric target representation for saccades. In addition, the *Ego task* evoked higher activation in parieto-frontal areas such as *a*mIPS and SMG. In contrast, the *Allo task* produced higher activation in temporal cortex (ITG) and early visual cortex areas such as calcarine and cuneus, although the latter areas also showed activity in the *Color* task.

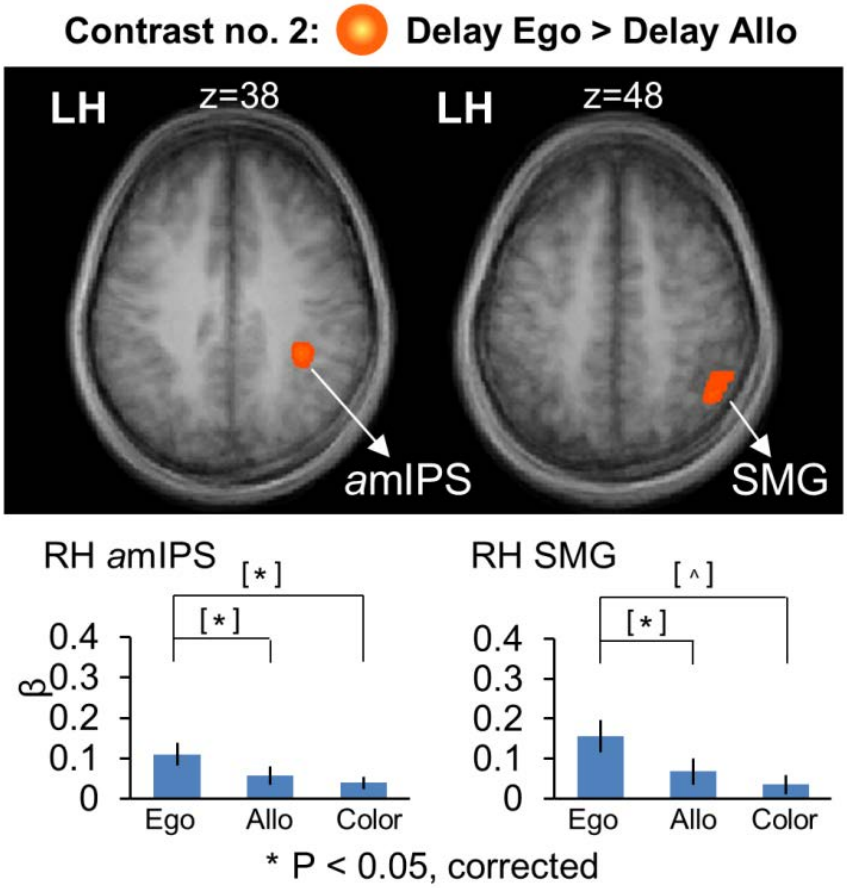

Figure 3.3. Voxelwise statistical map and activation levels for each area using Contrast no. 2 [Delay Ego > Delay Allo]. Top panel: activation map overlaid on the averaged anatomical image from all participants. Bottom panel: bar graphs show the β weights for the three tasks in each area. Legends as in Figure 3.2.

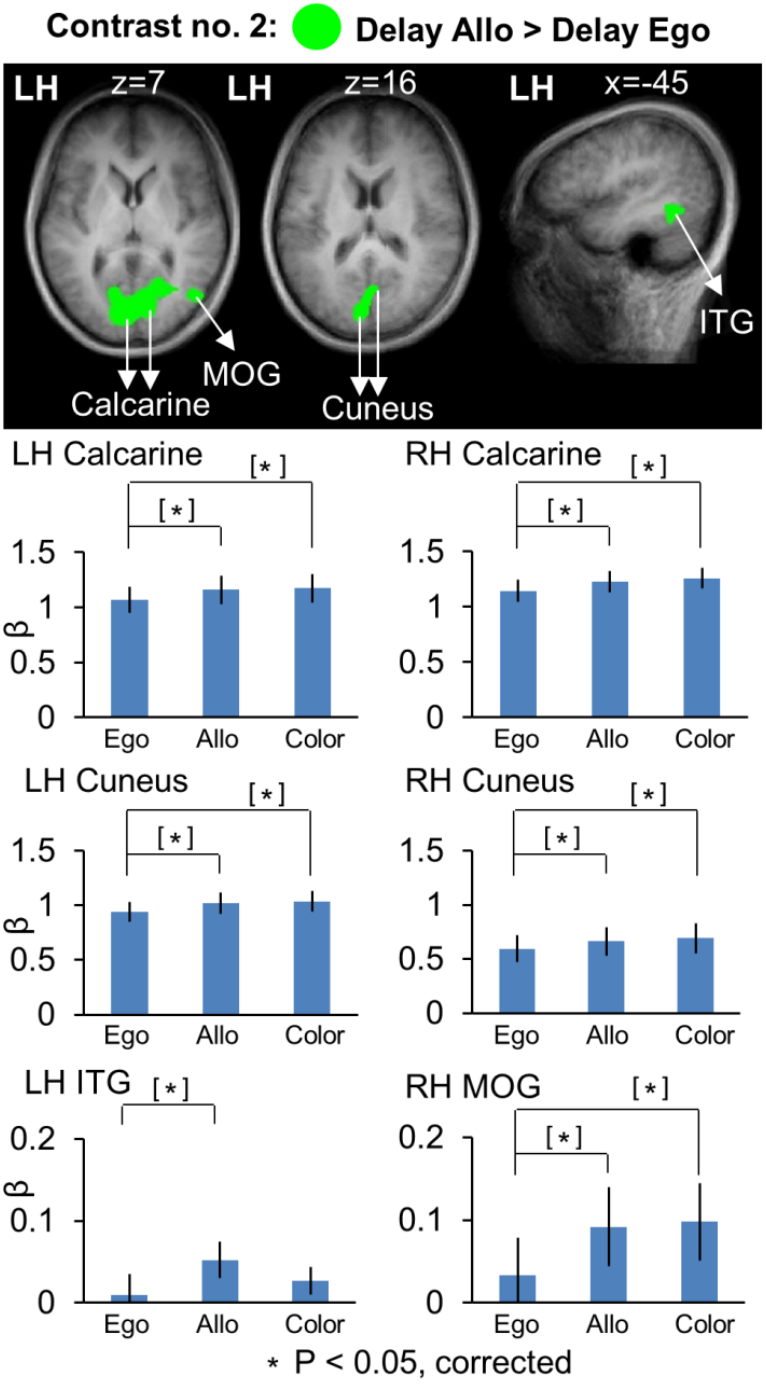

Figure 3.4. Voxelwise statistical map and activation levels for each area using Contrast no. 2 [Delay Allo > Delay Ego]. Top panel: activation map overlaid on the averaged anatomical image from all participants. Bottom panel: bar graphs show the β weights for the three tasks in each area. Legends as in Figure 3.2.

Table 3.3 Talairach coordinates and number of voxels for contrast no. 2

Brain areas	Talairach coordinates			No. of voxels
	x	y	z	
Delay Ego > Delay Allo				
RH *a*mIPS	33	-37	39	353
RH SMG	43	-49	48	431
Delay Allo > Delay Ego				
LH ITG	-45	-48	-8	400
LH Calcarine	-4	-82	5	512
RH Calcarine	5	-78	5	510
LH Cuneus	-2	-84	10	730
RH Cuneus	4	-67	10	323
RH MOG	46	-68	8	410

Egocentric Directional Selectivity: Target Location Relative to Midline during the Delay Phase

We used Contrast no. 3 [Delay Ego (Target Right of Midline) > Delay Ego (Target Left of Midline)] to investigate areas showing egocentric directional selectivity during the *Delay phase.* The Talairach coordinates of these brain areas are reported in Table 3.4. We found no active voxels showing higher activation for right vs. left target location. However, as illustrated in Figure 3.5, areas superior occipital gyrus (SOG) [$t_{(11)} = 4.21$, $p = 0.0015$] and inferior occipital gyrus (IOG) [$t_{(11)} = 3.92$, $p = 0.0024$] in the right hemisphere showed higher activation for target to the left vs. right of midline. Analysis of the β-weights for SOG and IOG (Fig. 3.5, right column) showed no egocentric directional selectivity in either the *Allo* or *Color* tasks. To confirm that the egocentric directional selectivity described above was specific to the egocentric task throughout the brain, we performed a full-brain voxelwise contrast [Delay Allo (Target Right of Midline) > Delay Allo (Target Left of Midline)] during the *Delay phase* in the *Allo* task (not shown). There were no significantly active voxels for this contrast.

In summary, we found significant egocentric directional selectivity in SOG and IOG during the *Ego* task, suggesting that these early visual areas are specifically involved in the egocentric coding of remembered target location for saccades.

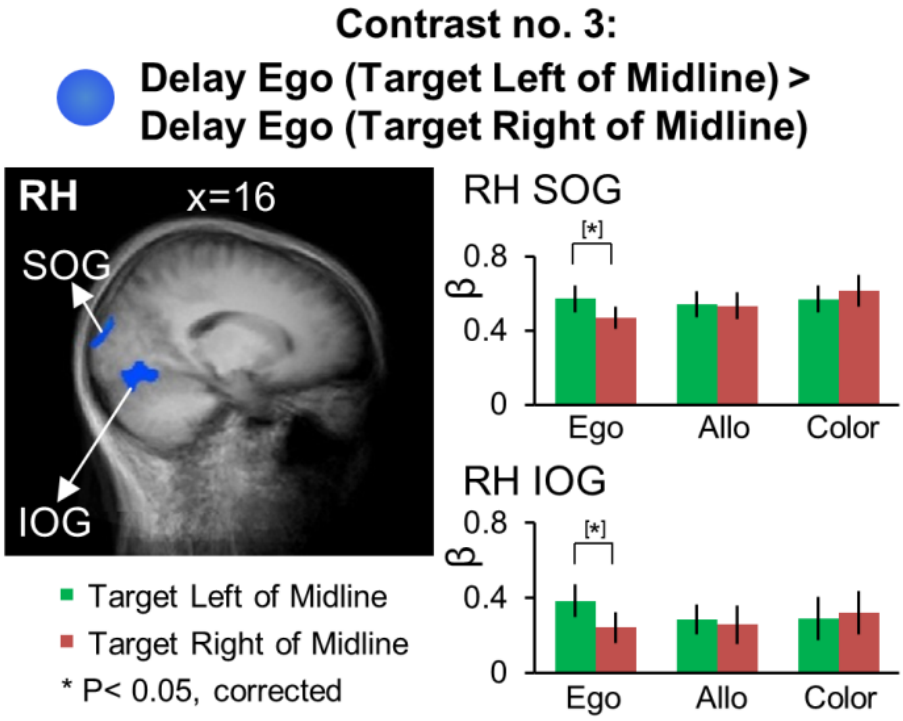

Figure 3.5. Voxelwise statistical map and activation levels for each area using Contrast no. 3 Egocentric directional selectivity during delay. [Delay Ego: (Target Left of Midline) > Delay Ego: (Target Right of Midline)], Left panel: activation map overlaid on the averaged anatomical image from all participants. Right panel: bar graphs show the β weights for each condition in each area. Legends as in Figure 3.2.

Allocentric Directional Selectivity: Target Location Relative to Landmark during the Delay Phase

The key point of this study was that our design allowed us to investigate neural substrates for the coding of saccade targets relative to a visual landmark in the *Allocentric saccade* task. We used Contrasts no. 4 [Delay Allo (Target Right of Landmark) > Delay Allo (Target Left of Landmark)] to identify the brain areas involved in allocentric directional selectivity (target location relative to landmark). Talairach coordinates of these brain areas are reported in Table 3.4. The results of this analysis are shown in Figure 3.6, with activation clusters superimposed on anatomical brain slices in the left column and the results of further t-test analysis of β weights on the right. This figure separates areas that show rightward (A) and leftward (B) allocentric tuning.

As shown in Figure 3.6 A, this contrast revealed significantly higher rightward allocentric activation in bilateral precuneus [LH: $t_{(11)} = 4.33$, $p = 0.0012$; RH: $t_{(11)} = 3.88$, $p = 0.0026$] and left mIPS [$t_{(11)} = 3.66$, $p = 0.0037$]. Our β weight comparisons (right column) revealed that in parietal cortex this directional selectivity was specific to the *Allo* task. This analysis also revealed higher leftward activation in the right calcarine sulcus (Fig. 3.6 B) for the *Allo saccade* task [$t_{(11)} = 3.28$, $p = 0.0074$] as well as for the *Ego saccade* task [$t_{(11)} = 2.95$, $p = 0.013$].

In order to examine the task-specificity of allocentric directional selectivity throughout the brain, we performed voxelwise contrast [(Target Right of Landmark) > (Target Left of Landmark)] for the *Egocentric* task during the *Delay phase*. This confirmed left vs. right allocentric directional selectivity in right calcarine sulcus [$t_{(11)} = 2.95$, $p = 0.013$], and revealed additional occipital areas (not shown) with allocentric directional

selectivity in the *Egocentric* task. These included right vs. left allocentric tuning in bilateral IOG [LH: $t_{(11)} = 3.49$, $p = 0.0051$; RH: $t_{(11)} = 3.23$, $p = 0.0080$], and left vs. right allocentric tuning in the left calcarine sulcus [$t_{(11)} = 2.59$, $p = 0.025$].

In summary, precuneus and mIPS showed significant allocentric directional selectivity only for the *Allocentric saccade* task, suggesting that dorsal-medial PPC and middle IPS are specifically recruited for the allocentric coding of remembered saccade targets (see Discussion). Occipital areas also showed allocentric directional selectivity, but this was not task specific.

Saccade Direction Coding during the Response Phase

As noted above, we did not observe egocentric directional selectivity in the parietal-frontal saccade circuit during the *Delay phase*. The reason may be that unlike previous fMRI studies where saccade direction could be planned during memory delay (Medendorp et al., 2005a; Kastner et al., 2007), participants in our study would not be able to plan the horizontal position of the actual saccade in the *Delay phase* until saccade direction was specified by either the reappearance of the landmark (*Allo* task) or the *pro/anti* instruction (*Ego* task) right before the *Response phase*. To confirm this, we performed Contrast no. 5 [Saccade Right of Midline > Saccade Left of Midline] in *Egocentric* and *Allocentric saccade* tasks, respectively, during the *Response phase*. The Talairach coordinates of brain areas were reported in Table 3.5.

Contrast no. 4:

A. Delay Allo (Target Right of Landmark) > Delay Allo (Target Left of Landmark)

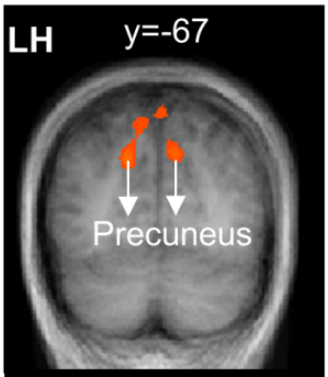

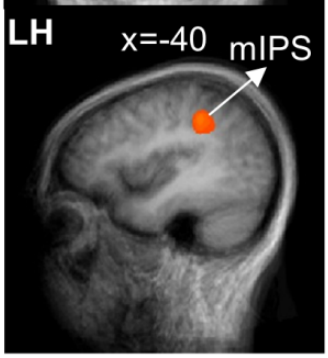

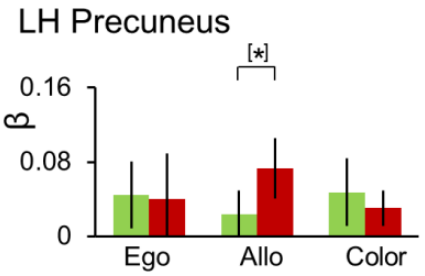

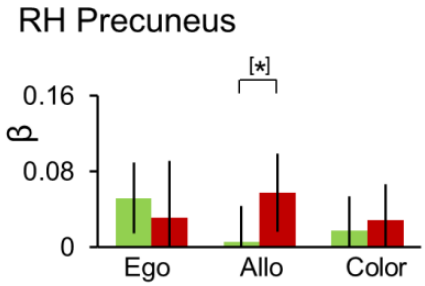

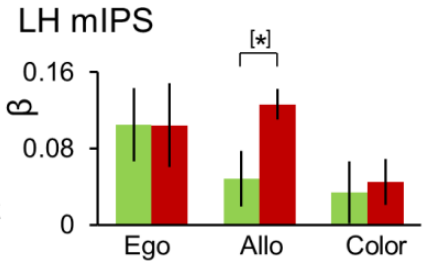

Target Left of Landmark

Target Right of Landmark

* P< 0.05, corrected

B. Delay Allo (Target Left of Landmark) > Delay Allo (Target Right of Landmark)

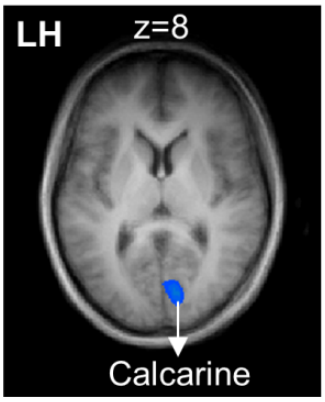

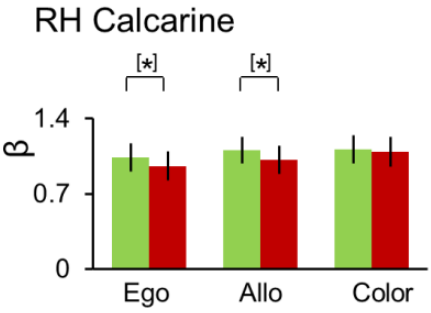

Figure 3.6. Voxelwise activation maps and activation levels for each area using Contrast no.4 Allocentric directional selectivity during delay. (A) [Delay Allo (Target Right of Landmark) > Delay Allo (Target Left of Landmark)]. (B) [Delay Allo (Target Left of Landmark) > Delay Allo (Target Right of Landmark)]. Left panels: activation maps overlaid on the averaged anatomical image from all participants. Right panels: bar graphs show the β weights for each condition in each area. Legends as in Figure 3.2.

Table 3.4 Talairach coordinates and number of voxels for contrast nos. 3, 4

Brain areas	Talairach coordinates			No. of voxels
	x	y	z	
Delay Ego (Target Left of Midline) > Delay Ego (Target Right of Midline)				
RH SOG	16	-97	7	236
RH IOG	16	-79	-13	467
Delay Allo (Target Right of Landmark) > Delay Allo (Target Left of Landmark)				
LH precuneus	-14	-68	36	247
RH precuneus	10	-63	36	230
LH mIPS	-40	-36	36	472
Delay Allo (Target Left of Landmark) > Delay Allo (Target Right of Landmark)				
RH calcarine	7	-78	8	360

As shown in Figure 3.7 (which superimposes activity clusters on an inflated brain in the upper row, and their task-specific β weights in the lower row), this analysis revealed contralateral egocentric directional selectivity, mainly in the left hemisphere. This includes several additional areas in the parieto-frontal network that did not show egocentric directional specificity during the *Delay phase.* In particular, we found higher activation for saccade toward right vs. left in left supplementary eye field (SEF) for both *Egocentric* [$t_{(11)}$ = 3.24, p = 0.010] and *Allocentric saccade* tasks [$t_{(11)}$ = 3.05, p = 0.014], middle frontal gyrus (MFG) [$t_{(11)}$ = 4.52, p = 0.0014], FEF [$t_{(11)}$ = 3.59, p = 0.0059] and posterior IPS (*p*IPS) [$t_{(11)}$ = 4.00, p = 0.0031] for the *Egocentric saccade* task. In addition, there was higher activation for saccade toward right vs. left for the *Allocentric saccade* task in superior parietal lobule (SPL) [$t_{(11)}$ = 4.19, p = 0.0023], middle temporal gyrus (MTG) [$t_{(11)}$ = 3.74, p = 0.0046], lateral occipitotemporal gyrus (LOtG) [$t_{(11)}$ = 4.13, p = 0.0026], anterior (*a*IOG) [$t_{(11)}$ = 4.05, p = 0.0029] and posterior IOG (*p*IOG) [$t_{(11)}$ = 4.18, p = 0.0024] in the left hemisphere. Insula in the right hemisphere [$t_{(11)}$ = 3.85, p = 0.0039] showed higher activation for saccades to left vs. right in the *Allocentric saccade* task.

In summary, during the *Response phase,* contralateral egocentric directional selectivity emerged in occipital, parietal, temporal, and frontal cortex, primarily in the left hemisphere (with the exception of insular cortex).

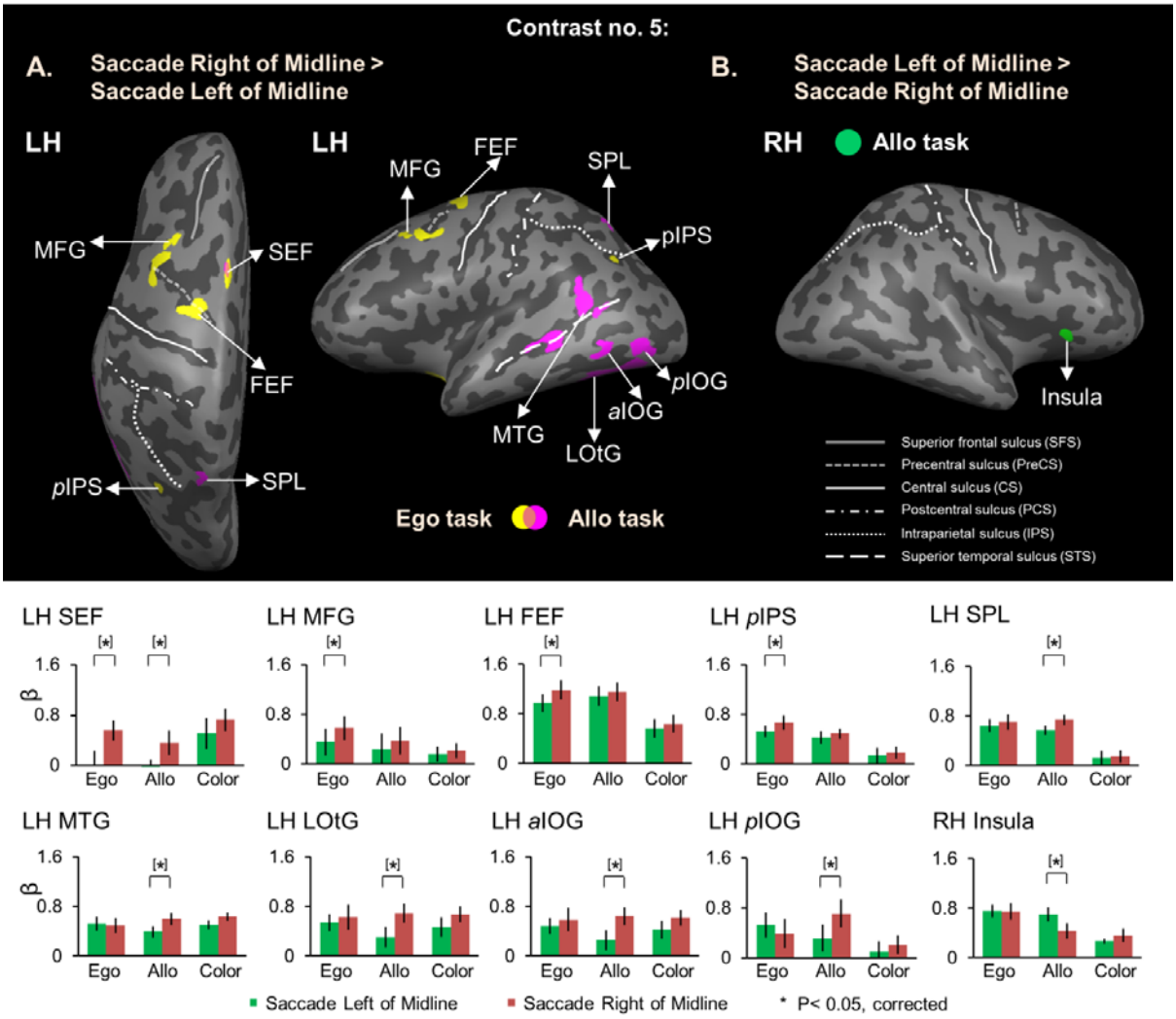
Contrast no. 5:
A.
Saccade Right of Midline >
Saccade Left of Midline
B.
Saccade Left of Midline >
Saccade Right of Midline
LH
LH
RH
Allo task
MFG
SEF
FEF
pIPS
SPL
MFG
FEF
SPL
pIPS
pIOG
aIOG
MTG
LOtG
Insula
Ego task
Allo task
Superior frontal sulcus (SFS)
Precentral sulcus (PreCS)
Central sulcus (CS)
Postcentral sulcus (PCS)
Intraparietal sulcus (IPS)
Superior temporal sulcus (STS)
LH SEF
LH MFG
LH FEF
LH pIPS
LH SPL
LH MTG
LH LOtG
LH aIOG
LH pIOG
RH Insula
β
1.6
0.8
0
Ego
Allo
Color
[*]
Saccade Left of Midline
Saccade Right of Midline
* P< 0.05, corrected

Figure 3.7. Voxelwise activation maps and activation levels for each area using Contrast no.5 Egocentric directional selectivity during response. Top panel: activation maps rendered on the inflated brain of one representative participant. (A) Saccade Right of Midline > Saccade Left of Midline. Yellow, voxels activated in the Ego task. Pink, voxels activated in the Allo task. Orange, voxels activated in both tasks. (B) Saccade Left of Midline > Saccade Right of Midline. Green, voxels activated in the Allo task. Bottom panel: bar graphs show the β weights for each condition in each area. Legends as in Figure 3.2.

Table 3.5 Talairach coordinates and number of voxels for contrast no. 5

Brain areas	Talairach coordinates			No. of voxels
	x	y	z	
Saccade Right of Midline > Saccade Left of Midline				
Both tasks:				
LH SEF	-5	6	62	440
Ego task:				
LH FEF	-24	-6	58	396
LH MFG	-40	9	47	319
LH *p*IPS	-30	-65	32	343
Allo task:				
LH SPL	-24	-65	54	394
LH LOtG	-33	-69	-11	392
LH *a*IOG	-47	-60	-1	498
LH *p*IOG	-47	-75	-2	441
Saccade Left of Midline > Saccade Right of Midline				
Allo task:				
RH Insula	31	25	8	462

3.5 DISCUSSION

In this study, we utilized an event-related fMRI design to discriminate between egocentric versus allocentric coding of remembered saccade targets during a *Delay phase* that was temporally and spatially separated (by a pro/anti saccade instruction or a re-presented landmark) from saccade planning and execution (during the *Response phase*). This design differed from saccade tasks where saccade direction was instructed from the beginning of the task. Thus our analysis could focus on the *Delay phase* to distinguish between cortical areas 1) that were differentially activated for egocentric versus allocentric target coding, or 2) that showed directional selectivity in either egocentric or allocentric coordinates. Since our design included explicit instructions for two different spatial tasks (*Ego* and *Allo*), it will allow us to contrast areas involved in explicit spatial coding versus areas involved in implicit spatial coding (Uchimura et al., 2015).

Our results showed partially overlapping patterns of cortical activation in the egocentric and allocentric saccade tasks during the *Delay phase*. Most importantly, different cortical mechanisms for directional coding of remembered saccade targets, i.e. occipital areas for egocentric directional selectivity vs. parietal areas for allocentric directional selectivity, were observed during the *Delay phase.* Egocentric saccade direction selectivity only appeared in parieto-frontal cortex during the *Response phase*, after movement direction was specified.

Explicit vs. Implicit Use of Allocentric Cues

Consistent with previous studies (Krigolson and Heath, 2004; Obhi and Goodale, 2005; Krigolson et al., 2007; Chen et al., 2014), here we showed that humans were able to

explicitly aim movements toward a location defined relative to a specific allocentric cue. In other situations, allocentric background information was used implicitly (Whitney et al., 2003; Chen et al., 2011; Uchimura and Kitazawa, 2013), although in these cases motor behavior seemed to only partially weighted toward the allocentric cue (Byrne and Crawford 2010). In particular, this weighting seemed to depend on the proximity, number, and perhaps size of background objects (Diedrichsen et al., 2004; Krigolson et al., 2007; Uchimura and Kitazawa, 2013; Fiehler et al., 2014).

Recently, in an fMRI study that used a non-spatial shape judgement task (that most closely resembles our *Color* control task as opposed to our saccade tasks), Uchimura et al. (2015) found adaptation effects for allocentric stimulus location in precuneus and MOG. These modulations disappeared when the allocentric cue was reduced to a size comparable to the cue that was used in the current study. It is difficult to directly compare this study with ours because of task differences (perceptual judgement vs. saccade response), but there are some common elements. In the current study, MOG showed higher activation in the *Color* and *Allo* tasks than in the *Ego* task, but did not show allocentric directional selectivity. Several other areas (including precuneus) did show allocentric directional selectivity in the explicit *Allo* task, none of these showed implicit allocentric directional selectivity in the *Color* task. Comparing the results of these two studies suggests that similar (or overlapping) cortical networks are partially activated during implicit allocentric coding (to a degree depending on the salience of the cue), and fully activated (independent of cue salience) in tasks that require explicitly allocentric coding. This could explain why cue proximity, number, and size have different influences on allocentric coding, depending on the task.

Egocentric vs. Allocentric Cortical Activation during the *Delay Phase*

In most previous fMRI studies of egocentric coding for saccades, movement direction was instructed from the beginning of each trial (Connolly et al., 2002; Medendorp et al., 2003; Schluppeck et al., 2005; Medendorp et al., 2006; Van Pelt et al., 2010). As noted above, our study differed in that participants did not know which way they would saccade until the *Response phase*, enabling us to focus our analysis on remembered target coding during the *Delay phase.*

We found overlapping areas in parietal and frontal cortex in the two saccade tasks (*Ego, Allo)* as opposed to the non-spatial control task (*Color)* during the *Delay phase*. However, right *a*mIPS and SMG were preferentially involved in egocentric saccade target coding. Area mIPS is thought to correspond to the human parietal eye fields (Muri et al., 1996; Sereno et al., 2001; Medendorp et al., 2003; Koyama et al., 2004; Pierrot-Deseilligny et al., 2004; Medendorp et al., 2005b; Hagler et al., 2007; Merriam et al., 2007; Vesia et al., 2010) and to correspond to monkey lateral intraparietal cortex (Andersen and Buneo, 2002; Culham et al., 2006; Vesia and Crawford, 2012), whereas SMG is thought to be involved in spatial memory (Moscovitch et al., 1995; Salmon et al., 1996; Faillenot et al., 1997; Silk et al., 2010).

In contrast, temporal cortex (ITG) and occipital cortex (calcarine, cuneus and MOG) were preferentially involved in allocentric saccade target coding. Although these occipital areas also showed higher activation in the *Color* as compared to the *Ego* saccade task, ITG only showed higher activation in the *Allo* vs. *Ego* saccades, suggesting temporal cortex was selective for spatial memory of allocentric saccade targets in our study. Temporal cortex has previously been implicated in allocentric coding in neuropsychological studies (Milner and

Goodale, 2006; Schenk, 2006), whereas occipital cortex (calcarine, cuneus, and MOG) is generally thought to be involved in stimulus-feature processing and visual working memory (Greenlee et al., 2000; Harrison and Tong, 2009).

Directional Selectivity for Saccade Target Coding during the *Delay Phase*

Previous neuroimaging studies indicated that human mIPS and FEF preferentially code contralateral saccade targets in egocentric coordinates (Medendorp et al., 2003; Medendorp et al., 2005a; Curtis and D'Esposito, 2006; Kastner et al., 2007). However, the design of those studies may have conflated saccade target memory and planning. Previous neurophysiological studies have shown that neurons in lateral intraparietal sulcus (LIP) and SEF can code saccade target location within an object relative to other parts of the same object (object-centered coordinates), with a weaker signal in the former (Sabes et al., 2002; Olson, 2003). But to our knowledge, the cortical mechanisms for spatial selectivity of saccade target memory in egocentric and allocentric (target relative to a separate visual landmark) reference frames have not been studied before the current investigation.

In the present study, during the *Delay phase* a preference for contralateral saccade targets relative to midline was observed in right SOG and IOG in the *Ego* task (note again that gaze, head, and body coordinates were aligned with midline; we made no attempt to distinguish between these egocentric frames in this experiment). Similar brain areas in occipital cortex for the egocentric directional selectivity of reach target memory were reported in our previous reach study (Chen et al., 2014), which used a similar design except for details of the fixation requirements, timing, and of course the effector used for the final action. We did not do a direct statistical comparison of the data from these two studies

because of these minor design differences and because different pools of participants were employed.

In comparison, we found allocentric directional selectivity (target location relative to the landmark) in bilateral precuneus and left mIPS. The involvement of PPC areas in allocentric directional selectivity of saccade targets is consistent with the suggestion of non-retinal representation of target location for saccades in PPC from neurophysiological (Galletti et al., 1993; Thier and Andersen, 1996; Mullette-Gillman et al., 2005) and human imaging studies (Pertzov et al., 2011). For instance, Pertizov et al. (2011) indicated that the multiple reference frames in mIPS for saccade target coding could be head-centered, body-centered, or even allocentric coordinates. However, that study did not distinguish between non-retinal and allocentric frames of reference. Alternatively, it may be that a single egocentric frame (such as gaze-centered coordinates) was used to code the relative locations of the cue and target in these areas, and that this is the underlying mechanism for solving our allocentric task (Filimon, 2015).

In contrast to our previous study (i.e. rather than observed allocentric directional selectivity in inferior occipital and inferior temporal gyrus for reach targets), we found precuneus and mIPS showing direction specificity for saccade targets in allocentric coordinates. This difference might have something to do with the speed and frequency of saccades relative to relatively sluggish reaches, perhaps requiring a more direct link between allocentric and egocentric coding mechanisms (Crowe et al., 2008). Unlike previous neurophysiological studies showing object-centered saccade target coding in SEF (Olson and Gettner, 1995, 1996; Olson and Tremblay, 2000), we did not observe allocentric directional specificity in SEF in our study. This could reflect the difference between the two non-

egocentric reference frames used in these studies (independent allocentric cue vs. object-centered), thus suggest the divergent neural mechanisms related to each of them for the coding of saccade target direction relative to an external landmark versus to a part of the object itself.

Direction Selectivity in *Delay* versus *Response Phases*

It is important to point out that the spatial details of saccade planning and execution could only occur in our *Response phase* after movement direction was specified by re-appearance of the landmark in the *Allo* task and by providing a *pro/anti-saccade* auditory cue in the *Ego* task right before the *Response phase*. This would explain why, unlike previous fMRI studies showing contralateral directional selectivity in parietal and frontal cortex for saccades (Medendorp et al., 2003; Kastner et al., 2007), we did not observe any egocentric directional selectivity in the parieto-frontal network during our *Delay phase*. As expected, we found directional selectivity contralateral to the direction of saccades in several parietal and frontal areas in the left hemisphere, such as SEF in both *Ego* and *Allo* tasks, FEF and *p*IPS in the *Ego* task and SPL in the *Allo* task. However, we were somewhat surprised by the additional recruitment of left occipital and temporal areas for directional selectivity of rightward saccades in the *Allo* task. These areas are not normally associated with control of saccades. This might reflect the greater degree of task complexity, and/or the maintenance of allocentric coding mechanisms during the *Response phase*. Likewise, we were somewhat surprised to find that only the right insula showed directional selectivity of leftward saccades in the *Allo* task. This directionally selective activation might be related to a role of right insula in more complex saccade tasks, like the *Allo* task in our study (Blurton et al., 2012).

We observed a similar pattern of contralateral directional selectivity for saccades to that for reaches during the *Response phase*, with more areas in the left hemisphere (Chen et al. 2014). This is easier to explain for reaches as interactions between visual directional selectivity and contralateral hand specificity (Perenin and Vighetto, 1988; Rossetti et al., 2003; Medendorp et al., 2005b; Beurze et al., 2007; Blangero et al., 2007; Vesia and Crawford, 2012), but hemispheric specialization for saccadic eye movements is still debated (Pierrot-Deseilligny et al., 1991; Muri et al., 2000; Leff et al., 2001; Muri et al., 2002; Yang and Kapoula, 2004). However, it has been suggested that saccade-related hemispheric asymmetry in PPC could be influenced by factors such as latency and dynamics (Yang and Kapoula, 2004; Vergilino-Perez et al., 2012).

In summary, other than the few exceptions noted above, the cortical activation observed during the *Response phase* was generally consistent with previous fMRI literature on egocentric movement selectivity for saccades and the ways this differs from reach direction selectivity (Beurze et al., 2007; Fernandez-Ruiz et al., 2007; Busan et al., 2009; Chen et al., 2014). This difference is in accordance with effector specificity for reach versus saccade planning and execution (Medendorp et al., 2005b; Connolly et al., 2007; Beurze et al., 2009; Vesia et al., 2010). Likewise, as noted above we found some detailed differences between directional selectivity for saccade and reach target memory in our current and previous studies (Chen et al. 2014). But the important common message from both our studies is that egocentric and allocentric target coding mechanisms differ, both from each other and from the cortical mechanisms used for the planning and execution of movements.

CHAPTER FOUR

NEURAL SUBSTRATES FOR ALLOCENTRIC-TO-EGOCENTRIC CONVERSION OF REMEMBERED REACH TARGETS IN HUMANS

Authors: Ying Chen, Simona Monaco, J. Douglas Crawford

Currently Submitted / in review

4.1 ABSTRACT

Targets for goal-directed action can be encoded in allocentric coordinates (relative to another visual landmark), but it is not known how these are converted into egocentric commands for action. Here, we investigated this using a novel event-related fMRI paradigm, based on our previous behavioral finding that the Allocentric to Egocentric (Allo-Ego) conversion for reach is done at the first possible opportunity. Participants were asked to remember (and eventually reach toward) the location of a briefly presented target relative to another visual landmark. After a 1st memory delay, participants were forewarned if the landmark would reappear at the same location, (potentially allowing them to plan a reach during the 2nd delay), or at a different location where they had to wait for the end of the 2nd delay to see the final landmark location, and then reach toward the remembered target location. As predicted, participants showed landmark-centered directional selectivity in occipital-temporal cortex during the first memory delay, only developed egocentric directional selectivity in occipital-parietal cortex during the second delay for the "same" task, and after the second delay for the "different" task. We then compared cortical activation between these two tasks at the times when the Allo-Ego conversion must have occurred, and found common activation in right precuneus, right supramarginal gyrus, left angular gyrus, and right mid-frontal gyrus. These results confirm that the brain converts allocentric codes to egocentric plans at the first possible opportunity, and identify the four most likely candidate sites specific to the Allo-Ego transformation for reaches.

4.2 INTRODUCTION

Various studies of spatial cognition have emphasized that visual locations can be specified in either egocentric (Ego: body-fixed) or allocentric (Allo: world-fixed) frames of reference (Philbeck et al., 1997; Galati et al., 2000; Schmidt et al., 2003; Burgess et al., 2004; Mou et al., 2006; Zaehle et al., 2007). Previous neuropsychological studies have suggested that allocentric and egocentric target representation is associated with the ventral and dorsal visual streams, respectively (Milner and Goodale, 2006; Schenk, 2006; Milner and Goodale, 2008). However, in many cases, transformations must occur between these two types of spatial coding (Burgess, 2006; Byrne and Becker, 2008). In particular, in order to aim a movement toward an allocentrically defined target, this information must be transformed into egocentric commands for motion of one body segment relative to another (Chen et al., 2011; Crawford et al., 2011; Chen et al., 2014). To our knowledge, the neural mechanisms for such an "Allo-Ego" transformation are completely unknown at this time.

It has been shown that the location of visual reach targets can be represented in either egocentric (McIntyre et al., 1997; Henriques et al., 1998; McIntyre et al., 1998; Pouget et al., 2002; Lemay and Stelmach, 2005), or allocentric frames of reference (Goodale and Haffenden, 1998; Carrozzo et al., 2002; Obhi and Goodale, 2005). Human neuroimaging studies investigating the neural substrates of egocentric reach plan have shown the recruitment of a parietofrontal network that includes superior parietal-occipital cortex (SPOC), midposterior intraparietal sulcus (mIPS) and dorsal premotor cortex (PMd) (Beurze et al., 2010; Vesia and Crawford, 2012), and a preference for contralateral left-right reach coding in posterior parietal cortex (PPC) (Medendorp et al., 2003; Medendorp et al., 2005b; Fernandez-Ruiz et al., 2007; Chen et al., 2014). Further, a recent fMRI study indicated

different cortical mechanisms for allocentric versus egocentric coding of remembered reach targets, including areas of temporal and occipital cortex that code the location of a reach target relative to an independent visual cue (Chen et al., 2014). While this study confirmed that egocentric cortical reach codes arose after the cue was used to specify reach direction, it could not show where this Allo-Ego transformation occurred.

Behavioral studies have shown that allocentric representations are more stable than egocentric representations (Krigolson and Heath, 2004; Heath, 2005; Obhi and Goodale, 2005; Hay and Redon, 2006; Krigolson et al., 2007). However, behavioral work has further shown that paradoxically the brain performs the conversion from allocentric to egocentric representations at the first possible opportunity for reach movements in the absence of visual feedback (Chen et al., 2011). These behavioral findings could not show where or how the brain computes the Allo-Ego conversion. In order to answer this question, we designed the current study, which is aimed at identifying the neural mechanisms of Allo-Ego conversion for reach.

The goal of the present study was (1) to confirm "first possible" hypothesis of Allo-Ego conversion for reach targets in a situation where either a visual or a verbal cue is available for this conversion, and (2) to investigate the brain areas involved in this conversion. We used an event-related fMRI paradigm where – based on our previous behavioral study (Chen et al., 2011) – the Allo-Ego conversion should be expected during the delay phase in our "*Same cue'* task, but only during the later response phase in our "*Different cue"* task (see Figure 4.1 for details). The brain imaging results of this study confirmed and extended our previous behavioral results by showing, at the neural level, that (after a period of allocentric coding) egocentric coding arose at the first opportunity (in the second delay for

the *Same cue* task and in the response for the *Different cue* task). More importantly, multiple comparisons between these two tasks narrowed down four specific candidate areas in PPC and frontal cortex for the Allo-Ego conversion, independent of the time of conversion or modality of available cues (verbal or visual).

4.3 MATERIALS AND METHODS

Participants

Twelve right-handed participants (8 females and 4 males, aged 24-42 years) participated in this study and gave informed consent prior to the experiment. All had normal or corrected to normal vision and had no known neuromuscular deficits. This size subject pool was chosen based on previous fMRI studies of visuomotor control in healthy subjects (Cavina-Pratesi et al., 2007; Gallivan et al., 2011) and proved sufficient to provide statistically significant results that survived corrections for multiple comparisons (see Results). This study was approved by the York Human Participants Review Subcommittee.

Experimental apparatus and stimuli

We used the same apparatus as that for our previous reach study on allocentric coordinates for remembered reach targets (Chen et al., 2014). In brief, visual stimuli of light dots produced by optic fibers were embedded in a custom-built board mounted atop a platform. The platform was placed above the abdomen of the participant and affixed to the bed of the scanner. The board was approximately perpendicular to the direction of gaze on the central fixation point and was placed about ~60 cm away from the eyes of the

participants. A computer controlled touch screen (Keytec Inc, dimensions 170 (h) × 128 (v) mm) was attached on the custom-built board to allow the recording of reaching endpoints. Participant's upper arm was strapped to the bed to avoid artifacts due to the motion of the shoulder and the head, therefore the reaching movements were performed by the forearm and hand. Participant's head was slightly tilted to allow direct viewing of the stimuli without using mirrors. An eye-tracking system (iView X) was used in conjunction with the MRI-compatible Avotec Silent Vision system (RE-5701) to record gaze position from the right eye during fMRI experiments. Participants wore headphones to hear verbal instructions about the reach task to be performed. During the experiment, participants were in complete darkness except for dots of lights corresponding to the visual stimuli, which were dim enough to prevent the illumination of the workspace.

There were four types of stimuli each presented in a different color: yellow for the central fixation point, red for the reach targets, blue for the visual landmarks, and white for the mask (Figure 4.1 A). The dots of light corresponding to the targets and the relative visual landmarks were located to the left and the right of the central fixation point with a visual angle of four to seven degrees on each side, and were separated from each other by one visual degree. These dots could be red or blue, therefore they could be used as a target or a visual landmark in different trials. This allowed us to create 20 different combinations of target and visual landmark locations where the target could be located one or two visual degrees to the left or to the right of a visual landmark. Since participants' gaze and head positions were always aligned with their body midline, we used "midline" as the zero point in a general egocentric coordinate system for the analyses of egocentric directional selectivity (i.e., target right of gaze = target right of midline, target left of gaze = target left of midline).

The mask consisted of 20 dots of light displayed in two rows, one above and one below the targets. The location of each dot for the mask was aligned with the midpoint between two adjacent target dots. The purpose of using a mask was to avoid potential after effects arising from the illumination of the target and the landmark in the dark.

Experimental paradigm and predictions

The paradigm consisted of two allocentric reach tasks (*Same cue* and *Different cue)*, in which an allocentric cue was initially used to encode target location for reach. We employed an event-related design to identify the brain areas involved in the Allo-Ego conversion that we have previously observed behaviorally (Chen et al., 2011). To do this, we designed a paradigm that prompted the participants to perform this conversion at one of two different stages of the trial, depending on the task instruction. Each participant was tested in five runs. Each run included 16 trials and each task was repeated eight times in a randomized order. An inter-trial interval of 14 s was added between each trial to allow the hemodynamic response to return to baseline and yield a run time of approximately 11 min.

As illustrated in Figure 4.1 A, the paradigm consisted of seven phases (fixation point, target and landmark presentation, first delay, audio instruction, second delay, landmark presentation, response). Each trial started with the presentation of the central fixation that participants fixated throughout each run. After 2 s, a target was presented along with an allocentric landmark for 2 s, followed by a 6-s delay phase. After the first delay phase, a verbal instruction, either "*Same cue*", or "*Different cue*" indicated whether the landmark would re-appear at the same location or at a different location. This was followed by a 10-s second delay phase. In the *Same cue* and *Different Cue* tasks during the first delay,

participants could encode the target in allocentric coordinates (target direction relative to the landmark) as observed in in our previous study (Chen et al., 2014), but no egocentric directional selectivity, as the movement direction was not specified yet.

Once the verbal cue was given, the *Same cue* instruction implicitly informed participants that at the end of the trial they were reaching toward the same target location indicated in the target and landmark presentation phase. This allowed participants to immediately convert the allocentrically-defined target location into an egocentric representation (specifying reach direction and amplitude) during the second delay phase (Chen et al., 2011). In contrast, the *Different cue* instruction indicated that the landmark was re-displayed at a new location after the second delay, so that the Allo-Ego conversion could be processed only then. This part of the design led to our first two predictions during the second delay (Figure 4.1 B). First, areas involved in the Allo-Ego conversion would be more active in the *Same Cue* task than the *Different cue* task in the second delay, as the *Same* but not the *Different cue* task allowed the conversion of the Allocentric target into an Egocentric representation (see "Voxelwise Analysis" below for details of these tests). Second, as a result of this conversion, contralateral directional selectivity would appear in brain areas involved in egocentric coding in the *Same Cue* task (Medendorp et al., 2003; Medendorp et al., 2005; Fernandez-Ruiz et al., 2007; Chen et al., 2014), but not in the *Different Cue* task, as the movement direction was explicit in the *Same* but not in the *Different Cue* task.

After the second delay, the landmark re-appeared for 2 s at a novel location in the same or opposite hemifield of its first presentation in the *Different cue* task, or at its original location in the *Same cue* task. During the following response phase, participants reached toward the remembered target location relative to the re-displayed allocentric landmark.

Therefore, the Allo-Ego conversion for the *Different cue* task could only occur in the response phase. We made two more predictions for the response phase (Figure 4.1 C): areas directly involved in producing the Allo-Ego conversion would now be more active in the *Different Cue* task (because the cue for this conversion was now present in this task) than in the *Same cue* task (as the conversion had happened earlier, see Figure 4.1C, right panel), and as a result egocentric cortical directional selectivity should now be present in both the *Same* and *Different Cue* tasks (because the Allo-Ego conversion had now occurred in both tasks, see Figure 4.1C, left panel). Therefore, we further predicted that cortical areas that passed both Allo-Ego comparisons (Figures 4.1 B, C right panels) would be the best candidates for the conversion, i.e., independent of the timing and nature of the cue (verbal before the second delay, visual before the response).

In summary, we made the following predictions: an early Allo-Ego conversion in the *Same Cue* task producing egocentric coding in the second delay (Figure 4.1B), and a late Allo-Ego conversion in *Different Cue* task (Figure 4.1C) with egocentric directional coding in the final response phase for the *Different Cue* task and with continued egocentric coding in the *Same Cue* task (Figure 4.1C, left panel). These were tested as follows in Results.

To confirm that there was allocentric coding of remembered target location, and that there was no egocentric directional selectivity of reach direction during the first delay, we tested allocentric target directional specificity (Left and Right relative to landmark) and egocentric reach directional selectivity (Left and Right reach relative to midline). This gave rise to three factors in the first delay phase: 2 Tasks (*Same cue, Different cue*) x 2 Reach direction relative to midline (*Left of Midline: LM, Right of Midline: RM*) x 2 Target direction relative to landmark (*Left of Landmark: LL, Right of Landmark: RL*). Therefore, there were 8

conditions in total: First delay: *Same cue: LM:LL,* First delay *Same cue: LM:LR,* First delay *Same cue: RM:LL,* First delay *Same cue: RM:LR,* First delay: *Different cue: LM:LL,* First delay *Different cue: LM:LR,* First delay *Different cue: RM:LL,* First delay *Different cue: RM:LR.* In order to test the Allo-Ego conversion we examined egocentric directional selectivity of reach direction (Left and Right reach relative to midline) in the second delay phase and response phase, respectively. This gave rise to two factors in each of these two phases: 2 Tasks (*Same cue, Different cue*) x 2 Reach direction relative to midline (*Left of Midline: LM, Right of Midline: RM*). Therefore, there were 8 conditions in total: 4 for *Second delay* (Second delay: *Same cue: LM,* Second delay: *Same cue: RM,* Second delay: *Different cue: LM,* Second delay: *Different cue: RM),* and 4 for *Response (*Response: *Same cue: LM,* Response: *Same cue: RM,* Response*: Different cue: LM,* Response: *Different cue: RM).* These conditions were counterbalanced in each run. Participants were trained to perform the tasks one day prior to scan.

Behavioral analysis

Following our fMRI experiments, we inspected eye position data for every trial to ensure that participants fixated the central fixation. Errors in eye position were defined as trials in which participants made a saccade toward the target or the visual landmark, or were not able to maintain central fixation. Errors in reaching performance were defined as trials in which the location of the reaching endpoint and the actual reach target location were on opposite sides relative to the midline on the touch screen. Trials that showed errors in eye and/or reach were modeled as confound predictors and excluded from further fMRI analyses

(see Data analyses). All participants completed at least 72 correct trials (90% of the total trials).

In order to confirm that participants actually used allocentric visual information to encode target location, and to exclude the possibility that they simply reached to the correct side of the screen midline, we performed a correlation analysis between the correct target location and the corresponding reaching endpoint for each of the two tasks. First, we calculated the distance between a participant's reach response for a given trial and the screen midline. Second, we calculated the distance between the reach target location and the screen midline. If participants reached to the correct location, these two values should be well correlated in both *Same cue* and *Different cue* tasks. The across-subject means of these signed correlation coefficients were 0.89 ± 0.01 for the *Same cue* task and 0.91 ± 0.01 for the *Different cue* task. We then applied Fisher's r-to-z transformation to the individual subject correlation coefficients (r) so that we could use standard t-tests to compare the between-subjects means of z values to zero. Standard t-tests showed that mean of correlation coefficient was significantly greater than zero in both tasks ($p_{same\ cue} = 0.0000001$, $p_{different\ cue} = 0.0000001$) indicating that participants performed well when reaching to the targets. The correlations were still significant ($p_{same\ cue} = 0.0000004$, $p_{different\ cue} = 0.0000004$) when absolute values for the distance were used, showing that amplitude of reach performance was also modulated.

To further quantify participants' performance, we calculated the absolute error (AE) and the variable error (VE) in the horizontal dimension for each participant in each task (*Same cue* or *Different cue*), respectively. The AE was the absolute value of the distance

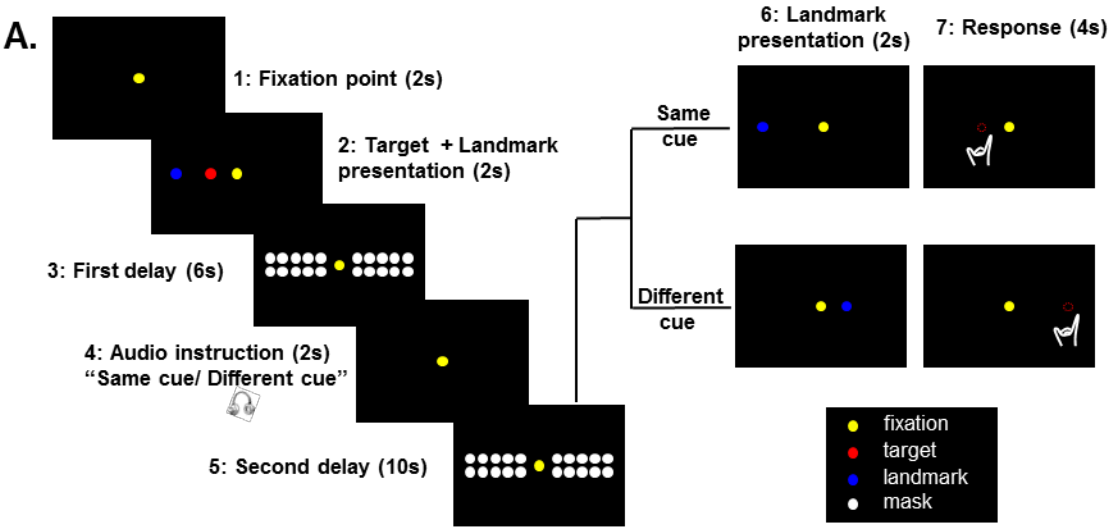
A.
1: Fixation point (2s)
2: Target + Landmark presentation (2s)
3: First delay (6s)
4: Audio instruction (2s)
"Same cue/ Different cue"
5: Second delay (10s)
6: Landmark presentation (2s)
7: Response (4s)
Same cue
Different cue
fixation
target
landmark
mask

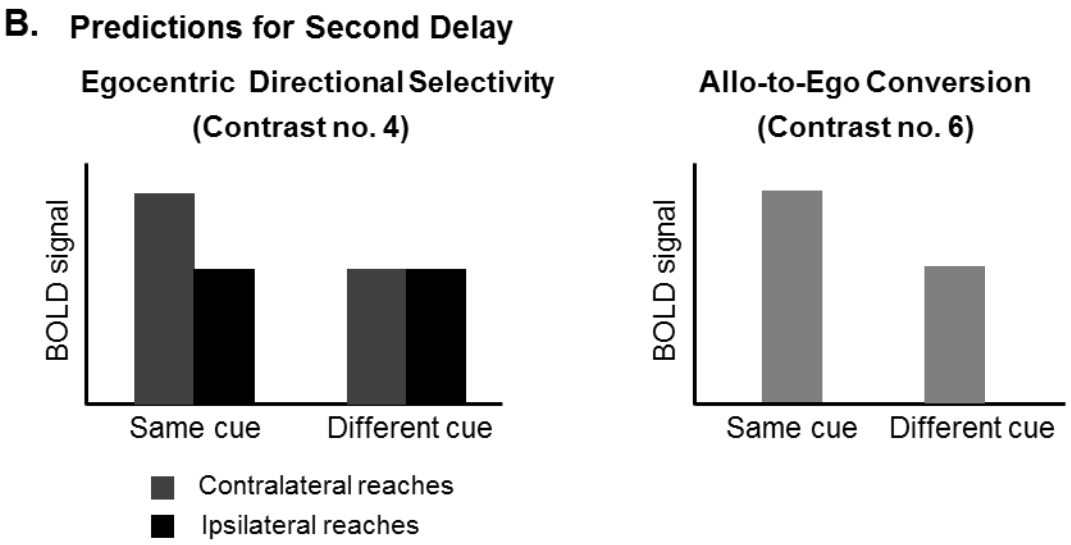
B. Predictions for Second Delay
Egocentric Directional Selectivity
(Contrast no. 4)
Allo-to-Ego Conversion
(Contrast no. 6)
BOLD signal
Same cue
Different cue
Contralateral reaches
Ipsilateral reaches

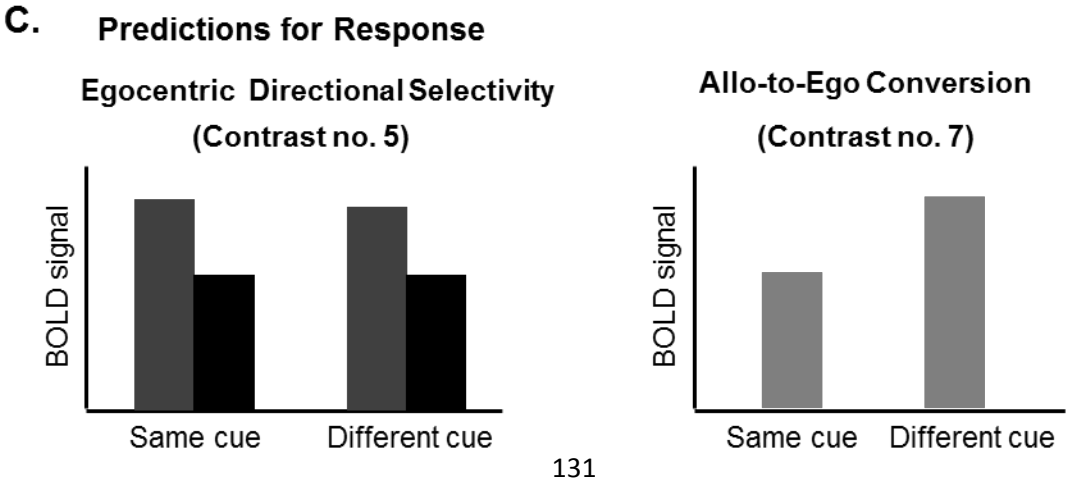
C. Predictions for Response
Egocentric Directional Selectivity
(Contrast no. 5)
Allo-to-Ego Conversion
(Contrast no. 7)
BOLD signal
Same cue
Different cue

Figure 4.1 Experimental paradigm and predicted BOLD signal changes during the second delay and response phases. ***A***, Illustration of the experimental paradigm. The displayed visual stimuli are the same for the two tasks: Same cue and Different cue. The critical difference between the two tasks is the early opportunity where the allocentric to egocentric conversion occurs. In the Same cue task the Allo-Ego conversion happens during the Second delay following a verbal cue; in contrast, in the Different cue task this conversion emerges during the Response following a visual cue of re-presented landmark at a new location. ***B***, Predictions for second delay. We expected that egocentric directional selectivity (reaches relative to midline) would be revealed by higher activation for contralateral than ipsilateral reaches in the Same cue task (left panel), and that areas involved in the Allo-Ego conversion would elicit higher activation in the Same cue task compared to the Different cue task during second delay (right panel). ***C,*** Predictions for response. We expected that egocentric directional selectivity (reaches relative to midline) would be revealed by higher activation for contralateral than ipsilateral reaches in both Different cue and Same cue tasks (left panel), and a reversed pattern of BOLD signal changes between the two tasks during response, i.e., higher activity in the Different cue task compared to the Same cue task (right panel).

between the reach target location and the endpoint of a reach movement, representing the amount by which the target was missed. The VE was calculated by taking the standard deviation of the constant reach errors, representing the variability of reach endpoints around the average endpoint. The across-subject means of AE were 1.29 ± 0.08 cm for the *Same cue* task and 1.41 ± 0.08 cm for the *Different cue* task. The across-subject means of VE were 1.30 ± 0.08 cm for the *Same cue* task and 1.32 ± 0.07 for the *Different cue* task. There was no significant difference between the errors in these two tasks [AE: $t_{(11)} = 1.71$, $p = 0.11$; VE: $t_{(11)} = 0.30$, $p = 0.77$].

Imaging parameters

This study was conducted at the neuroimaging center at York University using a 3-T whole body MRI system (Siemens Magnetom TIM Trio, Erlangen, Germany). The posterior half of a 12-channel head coil (6 channels) was placed at the back of the head in conjunction with a 4-channel flex coil covering the anterior part of the head. The former was tilted at an angle of 20° to allow a reach-to-touch movement to the touch screen as well as the direct viewing of the stimuli.

Functional data were acquired using an EPI (echo-planar imaging) sequence (repetition time [TR] = 2000 ms; echo time [TE] = 30 ms; flip angle [FA] = 90°; field of view [FOV] = 192 mm × 192 mm, matrix size = 64 × 64 leading to in-slice resolution of 3 mm × 3 mm; slice thickness = 3.5 mm, no gap; 35 transverse slices angled at approximately 25° covering the whole brain). The slices were collected in ascending and interleaved order. During each experimental session, a T1-weighted anatomical reference volume was acquired

using a MPRAGE sequence (TR = 1900 ms; TE = 2.52 ms; inversion time TI = 900ms; FA = 9°; FOV=256 mm× 256 mm× 192 mm, voxel size = 1 × 1 × 1 mm^3).

Preprocessing

Data were analyzed using the Brain Voyager QX 2.2 software (Brain Innovation, Maastricht, the Netherlands). The first 2 volumes of each fMRI scan were discarded to avoid T1 saturation effects. For each functional run, slice scan time correction (cubic spline), temporal filtering (removing frequencies < 2 cycles/run) and 3D motion correction (trilinear/sinc) were performed. The 3D motion correction was performed aligning each volume to the volume of the functional scan closest to the anatomical scan. Following inspection of the 3D motion correction parameters, the runs showing abrupt head motion exceeding 1 mm or 1° were discarded. Four runs (one from each of four participants) were discarded from the analyses due to head motion exceeding our set threshold. The six motion correction parameters were added to our general linear model (GLM) as predictors of no interest. The functional run closest to the anatomical image for each participant was co-registered to the anatomical image. Functional data were then mapped into standard Talairach space, using the spatial transformation parameters from each participant's anatomical image. Subsequently, functional data was spatially smoothed using a FWHM of 8mm.

Data analyses

For each participant, we used a GLM that included 19 predictors. Specifically, one predictor was used for the *Target and Landmark presentation* phase (2 s or 1 volume). In the

First delay phase, we used 8 predictors (6 s or 3 volumes), one for each experimental condition (see "Experimental paradigm and predictors"). In the *Verbal instruction phase*, we used one predictor (2 s or 1 volume). In the *Second Delay* phase, we used 4 predictors (10 s or 5 volumes), one for each experimental condition (see "Experimental paradigm and predictors"). In the *Landmark presentation* phase, we used one predictor (2 s or 1 volume). In the *Response* phase, we used 4 predictors, (4 s or 2 volumes), one for each experimental condition (see "Experimental paradigm and predictors"). Each predictor was derived from a rectangular wave function convolved with a standard hemodynamic response function (HRF), the Brain Voyager QX's default double-gamma HRF. In addition, we added six motion correction parameters and errors made in eye and reach data as confound predictors.

Voxelwise analyses

We performed contrasts on beta weights (β) using a group random effects (RFX) GLM where percentage signal change transformation had been performed. As described above, our questions were aimed at exploring brain areas involved in converting allocentric coding of remembered targets into egocentric representation for reaching movements during the second delay and response phases. Before examining these questions we performed three comparisons in the first delay phase to confirm some assumptions about our data. First, we directly compared the two tasks using Contrast no. 1 [First delay: (Same cue > Different cue)] to confirm that there was no difference yet in the *Same cue* vs. *Different cue* trials as expected here since these instructions were not yet given. We also performed directional contrasts from our previous study (Chen et al., 2014) to confirm a lack of egocentric reach plans using Contrast no. 2: [First delay: (Reach Right of Midline > Reach Left of Midline)],

as expected during allocentric memory before reach direction was specified, and to confirm allocentric target coding using Contrast 3: [First delay:(Target Left of Landmark > Target right of Landmark)].

Subsequently, we tested our hypothesis that the Allo-Ego conversion occurred in the second delay phase in the *Same cue* task, but only during the response phase in the *Different cue* task in the present study (Figure 4.1 B, C, left panels). As described above, this was confirmed by examining the first appearance of directional selectivity in brain areas known to encode contralateral reach targets in egocentric coordinates (here, reach relative to midline). In particular, we performed Contrast no. 4: [Second delay: (Reach Right of Midline > Reach Left of Midline)], and Contrast no. 5: [Response: (Reach Right of Midline > Reach Left of Midline)] on each of the two tasks.

Finally, we investigated the brain areas involved in the conversion of allocentric to egocentric target representation for reach. As illustrated in Figure 4.1 B and C (right panels), we hypothesized that areas that process the Allo-Ego conversion would show higher activation for the *Same cue* task versus the *Different cue* task in the second delay phase after the audio cue. In addition, there would be higher activation for the *Different cue* task as compared to the *Same cue* task in the response phase after the visual cue of re-displayed landmark. These hypotheses were tested by Contrast no. 6: [Second delay: (Same cue > Different cue)], and Contrast no. 7: [Response: (Different cue > Same cue)].

Both contrasts 6 and 7 were aimed at identifying regions involved in the Allo-Ego conversion. However, these conversions occurred at different times within the trial and were prompted by different type of cues (verbal instruction vs. visual presentation). As a result these contrasts could also contain activity related to the sensory modality (visual or verbal)

that was used for the instructions. Therefore, to identify the specific areas involved in the Allo-Ego conversion of target representations, regardless of the order or type of available cues we performed Contrast no. 8: a conjunction between Contrast 6 and Contrast 7.

Activation maps for group voxelwise results are overlaid on the average anatomical MRI from twelve participants. In order to correct for multiple comparisons, we performed a cluster threshold correction (Forman et al., 1995) using BrainVoyager's cluster-level statistical threshold estimator plug-in. This algorithm uses Monte Carlo simulations (1000 iterations) to estimate the probability of a number of contiguous voxels being active purely due to chance while taking into consideration the average smoothness of the statistical maps. Areas that did not survive a cluster threshold correction were excluded from further analyses. The estimated minimum cluster size was 16 voxels (3 mm^3) for a total volume of 432 mm^3 for Contrast nos. 4 and 5, and 26 voxels (3 mm^3) for a total volume of 702 mm^3 for Contrast nos. 3, 6 and 7. From each area, we extracted β weights from each individual participant to perform further comparisons using paired-sample t-tests.

Statistical Analyses

We first performed one comparison of LL vs. RL on the result of Contrast no. 3 to confirm allocentric coding of reach targets in the first delay phase for both tasks. The second comparisons on the results of Contrast nos. 4 and 5 were aimed at testing whether the egocentric reach directional selectivity (reach relative to midline) only occurred in the task where the allocentric coding of remembered targets could be converted to egocentric representations. Therefore, we performed the following two comparisons: Same cue: RM vs. LM, Different cue: RM vs. LM in the second delay and response phase, respectively.

Subsequently, a Bonferroni correction was applied to these two comparisons (corrected p = 0.025). The last comparisons on the results of Contrast nos. 6 and 7 was aimed at investigating brain areas involved in the All-Ego conversion by showing activation differences between the two tasks. Therefore, we performed one comparison of Same cue vs. Different cue. The results on β weights are plotted in bar graphs in Figures 4.2 - 4.6 to illustrate significant differences between conditions or tasks at the corrected p-value, unless specified (see Results). In the β weight plots, square brackets were used to indicate that results were non-independent of the selection criteria. The time course data from each of the identified brain areas that were specifically involved in Allo-Ego conversion were shown in line graphs in Figure 4.7 B.

4.4 RESULTS

We had two main purposes for our experimental design. First, we wanted to examine whether the behavioral result showing that the brain performs an Allo-Ego conversion at the first possible opportunity was also reflected in neural activity (Chen et al., 2011). We did so by identifying the first appearance of egocentric coding in reach areas after the presentation of an allocentrically coded target. Second, we wanted to identify the brain areas that were directly involved in this conversion. Our design employed two different cues for an Allo-Ego conversion at two different times, an audio cue (right before the second delay phase, only valid after the *Same cue* instruction) or a visual cue (right before the response phase, valid in the *Different cue* task). After confirming the presence of allocentric coding in the first delay phase, we analyzed egocentric reach directional selectivity in the second delay and response phases to confirm the occurrence of Allo-Ego conversion at the first opportunity, and then

made comparisons between the two tasks to investigate cortical mechanisms for this conversion. The cortical areas along with their corresponding acronyms identified by these contrasts are listed in Table 4.1.

Brain Activation during the First Delay Phase

During the first delay phase, there should be no difference between the *Same cue* and *Different cue* tasks because these cues had not yet been given. Similarly, there should be no egocentric reach-direction selectivity because the subjects did not yet know which direction they were going to reach. Our voxelwise analyses confirmed that during this phase, there was no active voxel when the two tasks were compared using Contrast no. 1 [Frist delay: (Same cue > Different cue), and no significant egocentric reach coding revealed by Contrast no. 2 [First delay: (Reach Right of Midline > Reach Left of Midline)]. However, one should expect allocentric coding of target direction during the first delay in both tasks, similar to what we observed in the memory delay of our previous experiment (Chen et al., 2014). We confirmed this by using Contrast no. 3: [First delay: (Target Left of Landmark > Target Right of Landmark)], in which we collapsed data from both the left and right reach target locations relative to midline and both *Same cue* and *Different cue* tasks. As illustrated in Figure 4.2, areas right ITG ($t_{(11)}$ =7.06, p = 0.00002) and left IOG ($t_{(11)}$ =4.26, p = 0.001) showed higher activation for reach targets to left versus right of the landmark. The Talairach coordinates of the brain areas are reported in Table 4.2. This is generally consistent with our previous result in reach study (Chen et al., 2014), and it confirms the original allocentric coding in this phase. Having confirmed these assumptions, we then examined the novel hypotheses in this study.

Table 4.1 Acronyms for brain areas from voxelwise analyses

Acronyms	Names of brain areas
AG	angular gyrus
*a*MTG	anterior middle temporal gyrus
*a*Precuneus	anterior precuneus
IFG	inferior frontal gyrus
IOG	inferior occipital gyrus
ITG	inferior temporal gyrus
LG	lingual gyrus
MFG	middle frontal gyrus
*p*IPS	posterior intraparietal sulcus
LOtG	lateral occipitotemporal gyrus
MFG	middle frontal gyrus
mIPS	midposterior intraparietal sulcus
MOG	middle occipital gyrus
PMd	dorsal premotor cortex
*p*MTG	posterior middle temporal gyrus
*p*IOG	posterior inferior occipital gyrus
*p*IPS	posterior intraparietal sulcus
Pre-SMA	presupplementary motor area
SMG	supramarginal gyrus
SOG	superior occipital gyrus

Contrast no. 3: (First delay)

Target Left of Landmark >

Target Right of Landmark >

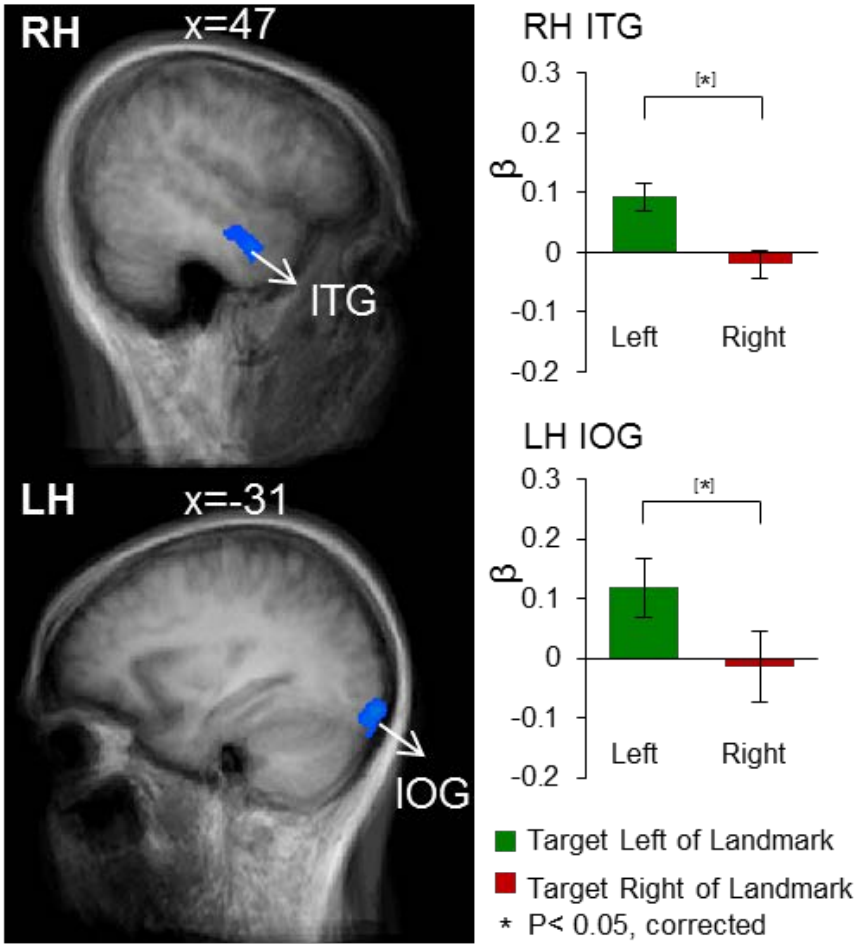

Figure 4.2 Voxelwise statistical map and activation levels for each area using Contrast no.3. [First delay: (Target Left of Landmark > Target Right of Landmark)], Left panel, activation map overlaid on the averaged anatomical image from all participants. Right panel, bar graphs show the β weights for the two conditions in each area. * Significant difference between two conditions for $p < 0.05$, [ ] non-independent of the criteria used to select the area. Error bars indicate 95% confidence intervals.

Allo-Ego Conversion: First Appearance of Egocentric Directional Selectivity

Based on our previous psychophysical study, we predicted that egocentric reach coding would first appear in the second delay of our paradigm in the *Same cue* task , and would first appear in the response phase of our *Different cue* task. We tested these predictions using Contrast no. 4 [Second delay: (Reach Right of Midline > Reach Left of Midline)] (Figure 4.3) and Contrast no. 5 [Response: (Reach Right of Midline > Reach Left of Midline)] (Figure 4.4 A and B) for each task. The Talairach coordinates of these brain areas are reported in Table 4.2.

As shown in Figure 4.3, during the second delay, Contrast no. 4 revealed contralateral reach directional selectivity in left posterior intraparietal sulcus (*p*IPS) ($t_{(11)}$ =4.61, p = 0.001), superior occipital gyrus (SOG) ($t_{(11)}$ =3.78, p = 0.003), middle occipital gyrus (MOG) ($t_{(11)}$ =3.97, p = 0.002) and inferior occipital gyrus (IOG) ($t_{(11)}$ =3.55, p = 0.005) in the *Same cue* task. Egocentric directional selectivity was not observed in the right hemisphere (not shown). In addition, significant egocentric direction specificity was never observed during the second delay in the *Different cue* task. These findings confirm the predictions shown in Figure 4.1 B, left panel.

In contrast, as predicted in Figure 4.1 C, left panel, egocentric directional selectivity was observed in both tasks during the response phase using Contrast no. 5 (Figure 4.4 A, B). In particular, as shown in Figure 4.4 A, areas Precuneus (*Different cue*: $t_{(11)}$ =5.66, p = 0.0001; *Same cue*: $t_{(11)}$ =3.91, p = 0.002), cuneus (*Different cue*: $t_{(11)}$ =3.69, p = 0.004; *Same cue*: $t_{(11)}$ =4.14, p = 0.002), calcarine (*Different cue*: $t_{(11)}$ =3.49, p = 0.005; *Same cue*: $t_{(11)}$ =4.79, p = 0.0006), lingual gyrus (LG) (*Different cue*: $t_{(11)}$ =4.23, p = 0.001; *Same cue*: $t_{(11)}$ =7.47, p = 0.00001), SOG (*Different cue*: $t_{(11)}$ =2.82, p = 0.016; *Same cue*: $t_{(11)}$ =4.74, p =

0.0006), MOG (*Different cue*: $t_{(11)}$ =3.30, p = 0.007; *Same cue*: $t_{(11)}$ =6.81, p = 0.00003) and IOG (*Different cue*: $t_{(11)}$ =2.97, p = 0.013; *Same cue*: $t_{(11)}$ =3.84, p = 0.003) in the left hemisphere showed higher activation for reaches made to the right versus left of midline for the both tasks, except left *p*IPS showed this pattern in the *Different cue* task only ($t_{(11)}$ =3.20, p = 0.008). Similarly, as illustrated in Figure 4.4 B, calcarine (*Different cue*: $t_{(11)}$ =3.72, p = 0.003; *Same cue*: $t_{(11)}$ =5.31, p = 0.0003) and LG (*Different cue*: $t_{(11)}$ =3.11, p = 0.01; *Same cue*: $t_{(11)}$ =4.04, p = 0.002) in the right hemisphere showed higher activation for reaches to the left versus right of midline in both tasks, except right *p*Precuneus showed this activity pattern in the *Same cue* task only ($t_{(11)}$ =3.60, p = 0.004).

In summary, contralateral reach directional selectivity was observed in occipital-parietal areas at the first appearance of a cue to the egocentric location of the allocentrically-defined target for reaches; in the second delay for the *Same cue* task, and in the response phase for the *Different cue* task. This confirmed that allocentric to egocentric conversion of reach target occurred as soon as possible, consistent with previous psychophysical study (Chen et al., 2011). Further, our results suggested that this Allo-Ego conversion could arise with use of a verbal or a visual cue, as shown in our *Same cue* task during the second delay phase and in our *Different cue* task during the response phase. We next tried to identify the areas of the brain that might be directly involved in producing this conversion.

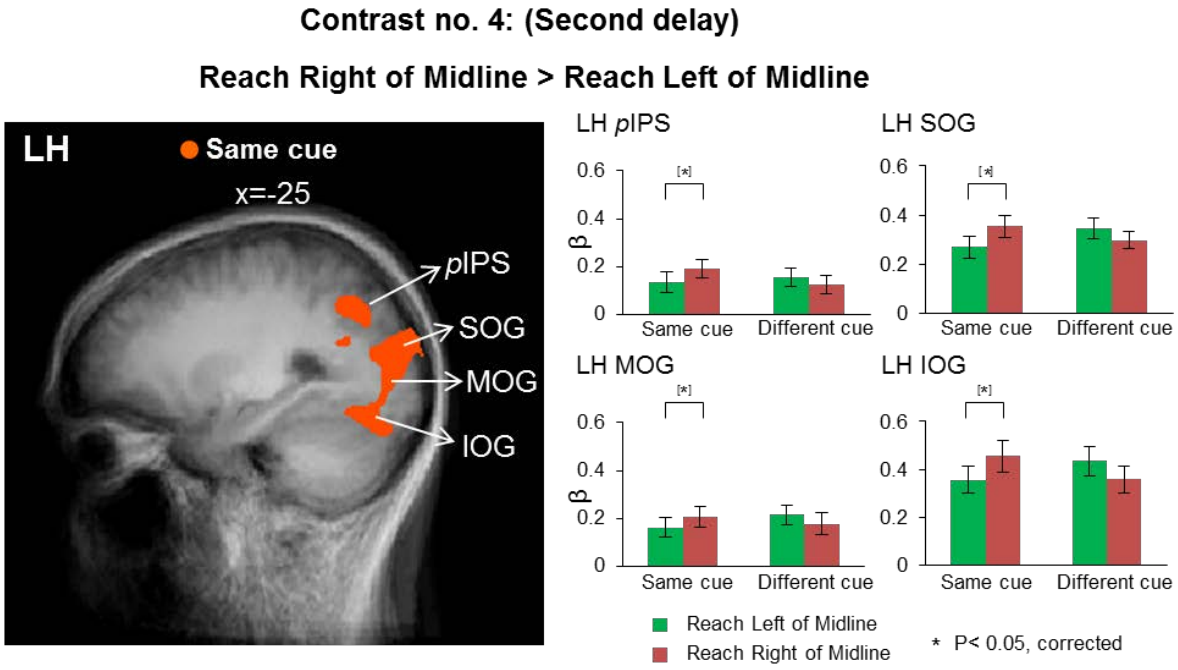

Figure 4.3 Voxelwise statistical map and activation levels for each area using Contrast no.3. [First delay: (Target Left of Landmark > Target Right of Landmark)], Left panel, activation map overlaid on the averaged anatomical image from all participants. Right panel, bar graphs show the β weights for the two conditions in each area. Legends as in Figures 4.2.

Contrast no. 5: (Response)

A. **Reach Right of Midline > Reach Left of Midline**

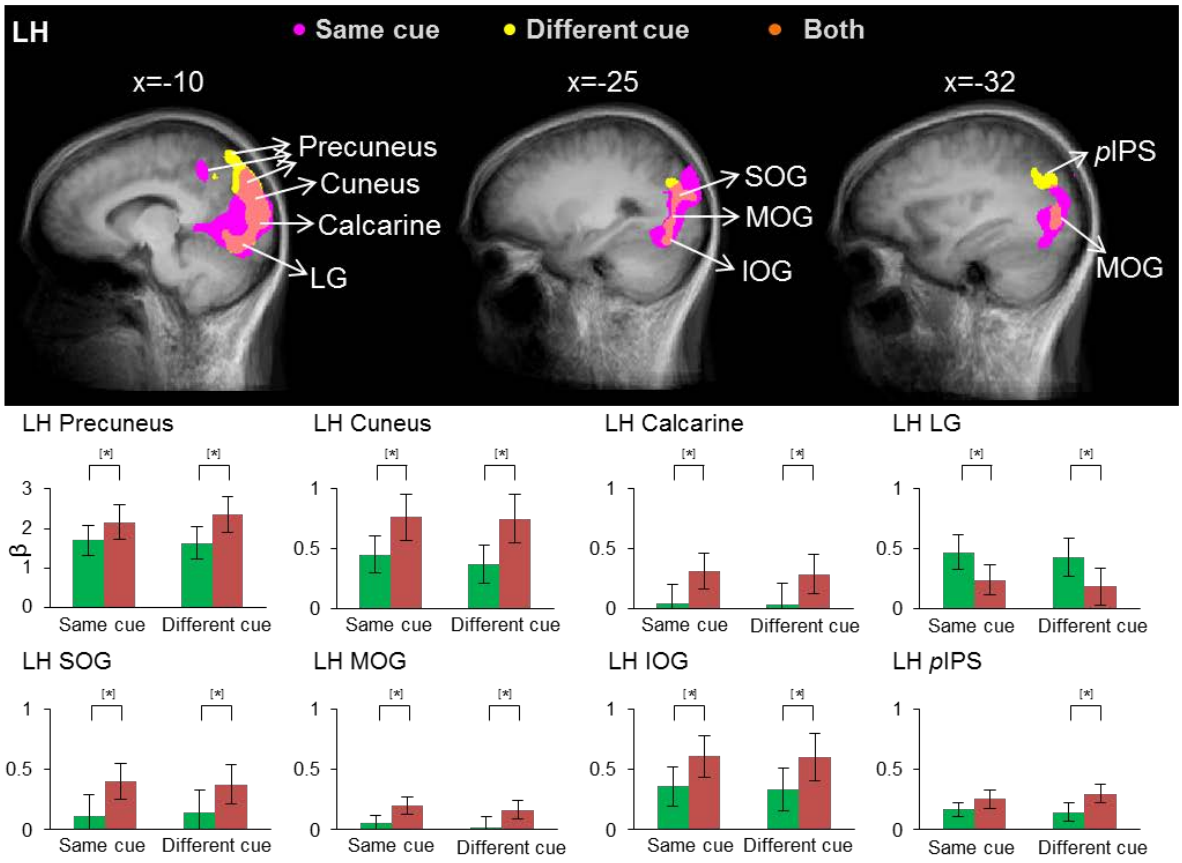

B. **Reach Left of Midline > Reach Right Midline**

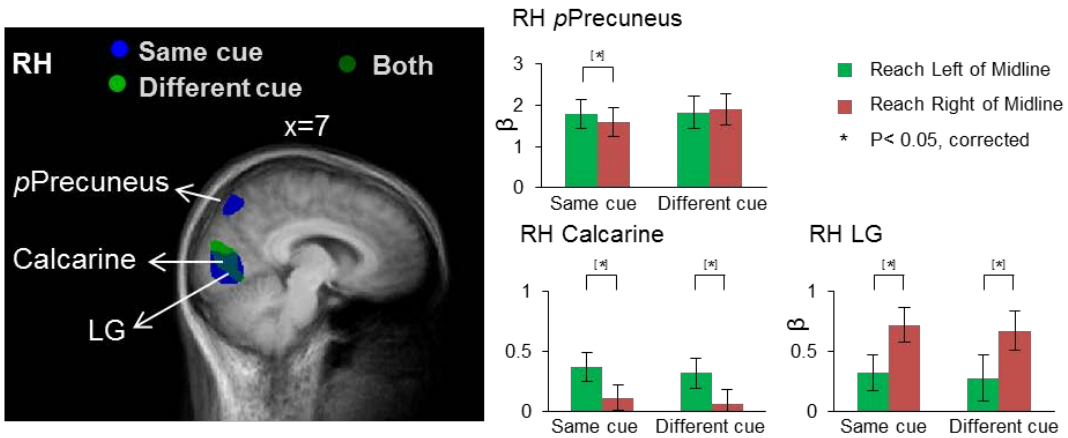

Figure 4.4 Voxelwise statistical map and activation levels for each area using Contrast no. 5. ***A,*** [Response: (Reach Right of Midline > Reach Left of Midline)]. Top panel, activation map overlaid on the averaged anatomical image from all participants. Pink represents voxels activated in the Same cue task. Yellow represents voxels activated in the Different cue task. Orange represents voxels activated in both tasks. Bottom panel, bar graphs show the β weights for each condition in each area. ***B,*** [Response: (Reach Left of Midline > Reach Right of Midline)]. Left panel, activation map overlaid on the averaged anatomical image from all participants. Blue represents voxels activated in the Same cue task. Light green represents voxels activated in the Different cue task. Dark green represents voxels activated in both tasks. Right panel, bar graphs show the β weights for each condition in each area. Legends as in Figures 4.2.

Table 4.2 Talairach coordinates and number of voxels for contrast nos. 3, 4, 5

Brain areas	Talairach coordinates			No. of voxels
	x	y	z	
Contrast no. 3				
First delay: Target Left of Landmark > Target Right of Landmark				
Both tasks:				
RH ITG	47	-4	19	288
LH IOG	-31	-89	-13	423
Contrast no. 4				
Second delay: Reach Right of Midline > Reach Left of Midline				
Same cue task:				
LH *p*IPS	-29	-64	37	430
LH SOG	-25	-87	18	512
LH MOG	-25	-85	4	383
LH IOG	-25	-73	-12	500
Contrast no. 5				
Response: Reach Right of Midline > Reach Left of Midline				
Both tasks:				
LH Precuneus	-8	-81	39	488
LH Cuneus	-9	-86	25	514
LH Calcarine	-5	-88	7	459
LH LG	-10	-75	-11	512
LH SOG	-25	-80	20	283
LH MOG	-32	-77	4	510
LH IOG	-25	-73	-12	250
Different cue task:				
LH *p*IPS	-32	-67	30	428
Response: Reach Left of Midline > Reach Right of Midline				
Both tasks:				
RH Calcarine	7	-75	5	506
RH LG	10	-70	-8	404
Same cue task:				
RH *p*Precuneus	8	-71	50	467

Allo-Ego Conversion during the Second Delay Phase

To investigate brain areas involved in the Allo- Ego conversion during second delay, we used Contrast no. 6 [Second delay: (Same cue > Different cue)] to directly compare activations of the *Same cue* task versus the *Different cue* task. The areas revealed by this contrast would be related to converting allocentric coding to egocentric representation in the *Same cue* task where subjects could anticipate they would reach to the original target location.

The brain areas revealed by this contrast are shown on horizontal and sagittal slices and the β weights are plotted in bar graphs (Figure 4.5). The Talairach coordinates of these brain areas are reported in Table 4.3. In particular, we found higher activation for *Same cue* versus *Different cue* in bilateral anterior Precuneus (*a*Precuneus) (LH: $t_{(11)}$ =3.64, p = 0.004; RH: $t_{(11)}$ =3.72, p = 0.003), left angular gyrus (AG) ($t_{(11)}$ =3.38, p = 0.006) and inferior frontal gyrus (IFG) ($t_{(11)}$ =3.65, p = 0.004), right posterior Precuneus (*p*Precuneus) ($t_{(11)}$ =2.69, p = 0.02), supramarginal gyrus (SMG) ($t_{(11)}$ =2.66, p = 0.022), middle frontal gyrus (MFG) ($t_{(11)}$ =3.32, p = 0.007), anterior middle temporal gyrus (*a*MTG) ($t_{(11)}$ =5.21, p = 0.0003) and posterior middle temporal gyrus (*p*MTG) ($t_{(11)}$ =2.73, p = 0.02).

In summary, we found several areas in posterior parietal cortex and a few areas in frontal and temporal cortex showing higher activation in the *Same cue* task than the *Different cue* task during the second delay phase when the verbal instruction for the former task had signaled the egocentric location of the allocentrically-defined target. These became our first set of candidate areas for the Allo-Ego conversion, based on a relatively early verbal cue before a memory/planning phase.

Contrast no. 6: (Second delay)

Same cue > Different cue

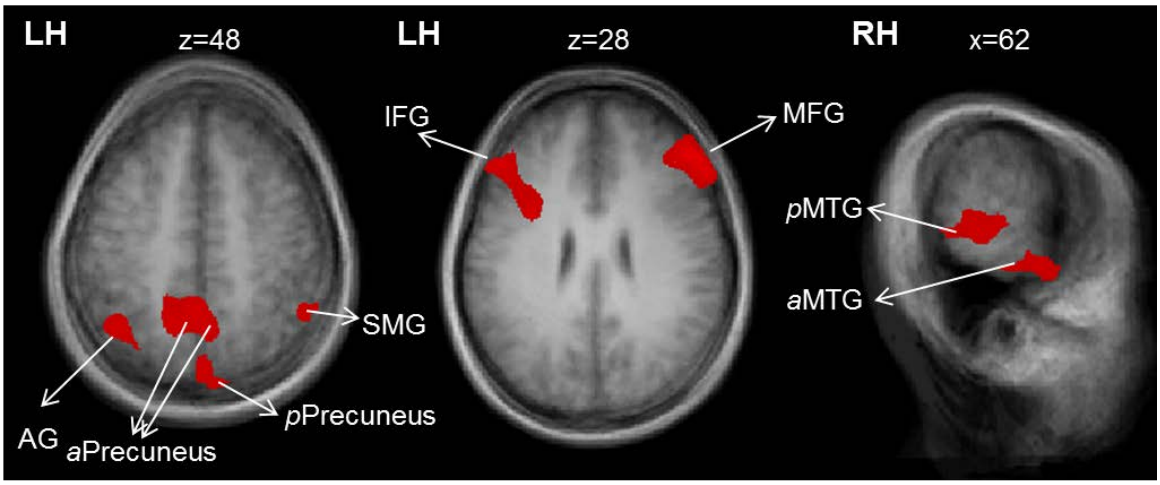

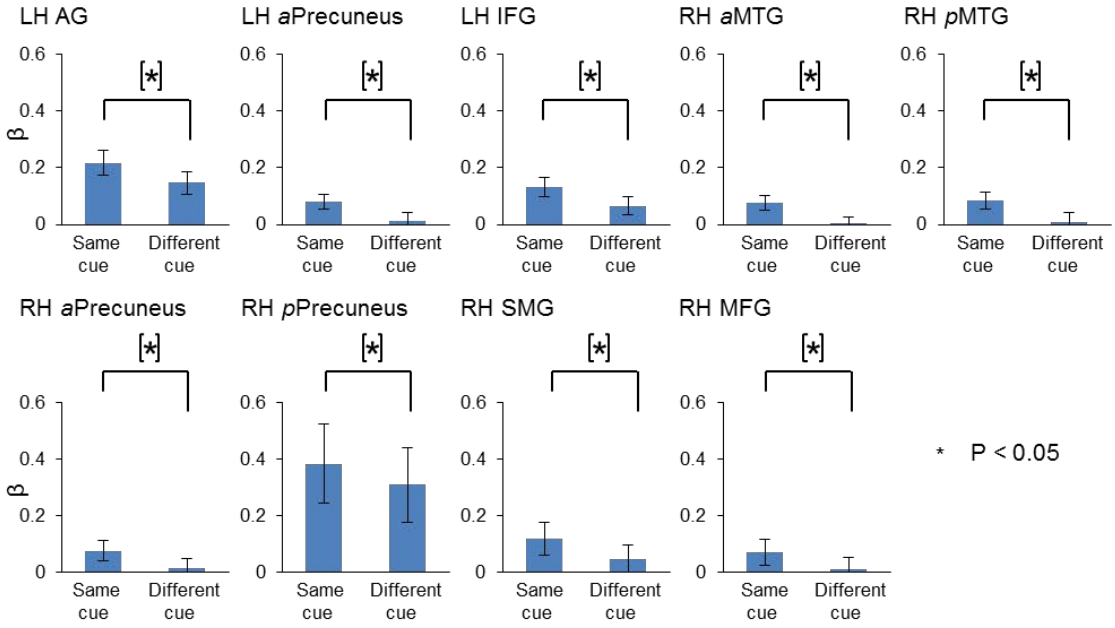

Figure 4.5 Voxelwise statistical map and activation levels for each area using Contrast no. 6. [Second delay: (Same cue > Different cue)], Top panel, activation map overlaid on the averaged anatomical image from all participants. Bottom panel, bar graphs show the β weights for the two tasks in each area. Legends as in Figures 4.2.

Allo-Ego Conversion during the Response Phase

Next, we examined the areas that would process the Allo-Ego conversion of target representation in the *Different cue* task during the response phase where the final target location for reach was indicated by using the visual cue of re-displayed allocentric landmark. We used Contrast no. 7 [Response: (Different cue > Same cue)], in which activation in the *Different cue* task was directly compared to that in the *Same cue* task. The activation map is shown on the horizontal slices and the β weights are plotted in bar graphs (Figure 4.6). The Talairach coordinates of these brain areas are reported in Table 4.3.

This contrast revealed areas showing higher activation for *Different cue* versus *Same cue* in bilateral *p*Precuneus (LH: $t_{(11)}$ =5.05, p = 0.0004; RH: $t_{(11)}$ =3.93, p = 0.002), dorsal premotor cortex (PMd) (LH: $t_{(11)}$ =3.05, p = 0.011; RH: $t_{(11)}$ =3.61, p = 0.004) and presupplementary motor area (Pre-SMA) (LH: $t_{(11)}$ =2.92, p = 0.014; RH: $t_{(11)}$ =2.90, p = 0.014), left AG ($t_{(11)}$ =2.77, p = 0.018), right SMG ($t_{(11)}$ =3.39, p = 0.006) and MFG ($t_{(11)}$ =3.10, p = 0.01).

In summary, this result demonstrated that several areas in a parietofrontal network showed higher activation in the *Different cue* task than the *Same cue* task during the response phase, after the egocentric location for a reach movement was specified by the visual presentation of the new allocentric landmark. These became our second set of candidate areas for the Allo-Ego conversion, based on a relatively late visual cue before motor execution. This comparison had an additional advantage over the previous comparison: since egocentric coding was established in both Same / Different instructions, the different activations observed here should not be due to overall differences in the amount of egocentric activation.

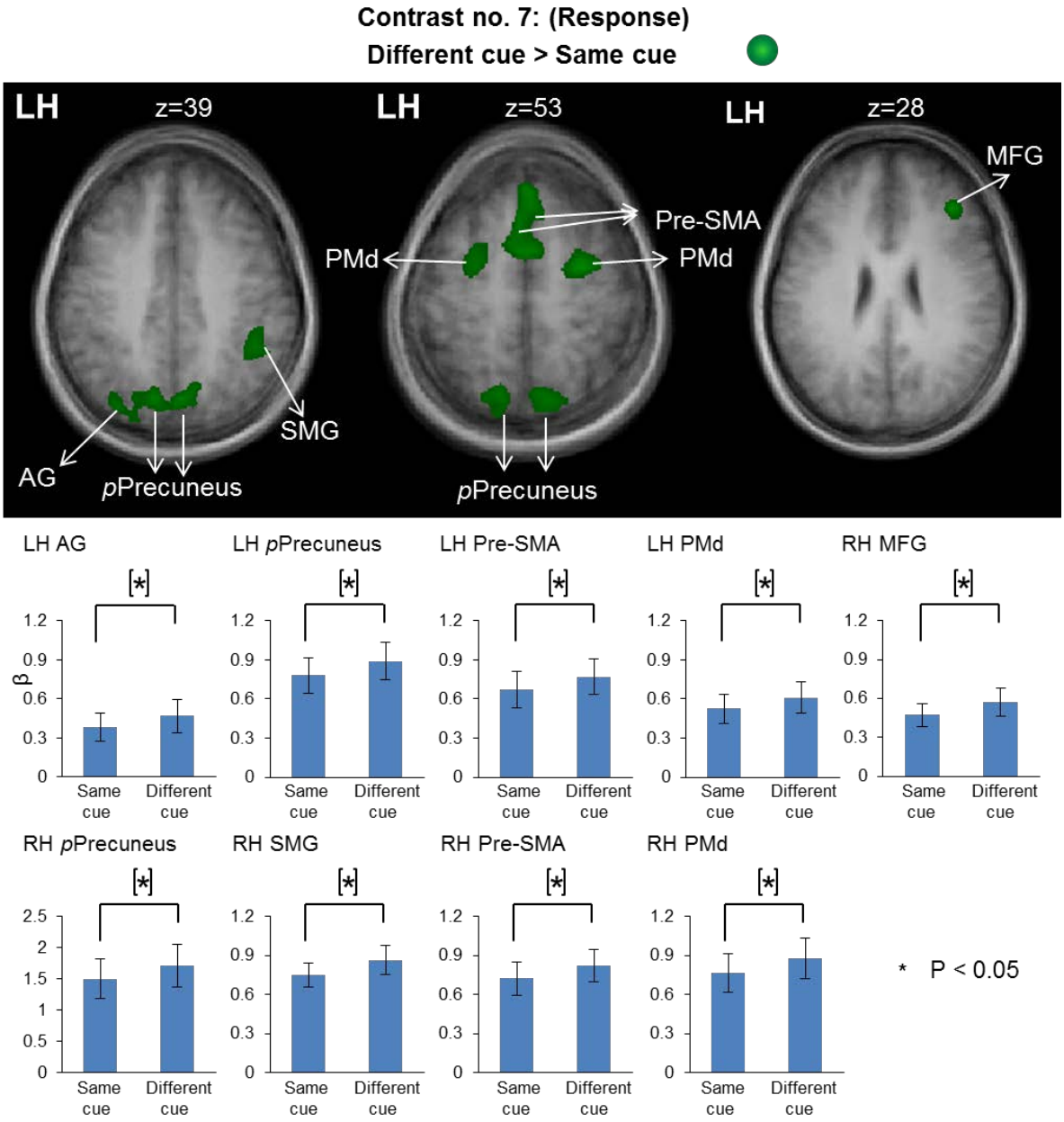

Figure 4.6 Voxelwise statistical map and activation levels for each area using Contrast no. 7. [Response: (Different cue > Same cue)], Top panel, activation map overlaid on the averaged anatomical image from all participants. Bottom panel, bar graphs show the β weights for the two tasks in each area. Legends as in Figures 4.2.

Table 4.3 Talairach coordinates and number of voxels for contrast nos. 6, 7

Brain areas	Talairach coordinates			
	x	y	z	No. of voxels
Contrast no. 6				
Second delay: Same cue > Different cue				
LH *a*Precuneus	-5	-46	47	506
RH *a*Precuneus	3	-52	47	507
LH AG	-38	-56	48	502
LH IFG	-47	27	27	512
RH *p*Precuneus	2	-69	42	431
RH SMG	47	-48	48	292
RH MFG	37	32	27	506
RH *a*MTG	62	-5	-18	501
RH *p*MTG	62	-32	-5	319
Contrast no. 7				
Response: Different cue > Same cue				
LH Pre-SMA	-2	8	52	510
RH Pre-SMA	1	7	52	454
LH PMd	-26	-3	53	491
RH PMd	25	-3	53	510
LH *p*Precuneus	-10	-72	43	498
RH *p*Precuneus	3	-52	47	506
LH AG	-31	-70	40	350
RH SMG	41	-44	42	511
RH MFG	37	32	27	418

Specific Brain Areas for Allocentric to Egocentric Conversion of Reach Target Representations

Contrasts nos. 6 and 7 should include areas involved in the Ego-Allo conversion, but might also include other types of activity such as auditory processing and egocentric target memory (contrast 6 from second delay) and residual visual processing (contrast 7 from the response phase). In addition, differences might arise simply from the timing of these two contrasts relative to initial target presentation and final motor execution. To filter out these extraneous elements and focus on the common areas involved in Allo-Ego conversion, we used Contrast no. 8, a conjunction analysis between Contrast nos. 6 and 7.

As shown in Figure 4.7 A, our conjunction analysis revealed four areas in PPC and frontal cortex, including right *p*Precuneus and SMG, left AG and MFG. To illustrate the change of activation related to remembered target representations through the three phases (first delay, second delay, response) between the two tasks, we plotted time course data from each of the four areas in Figure 4.7 B. These four specific "conversion" areas showed a consistent pattern of activation change. First, all four areas showed a trimodal activation pattern: during the first delay following target presentation, during the second delay following the task instruction (same/different), and during the response following the final cue presentation / go signal. In each case, the peak response occurred during the response phase, suggesting a link to behavior. Importantly, there was no activation difference between the two tasks during first delay (as should be expected because the tasks did not different at this point), but we found higher activation in the *Same cu*e task than the *Different cue* task during the second delay, and then a reverse pattern during the response (as expected for

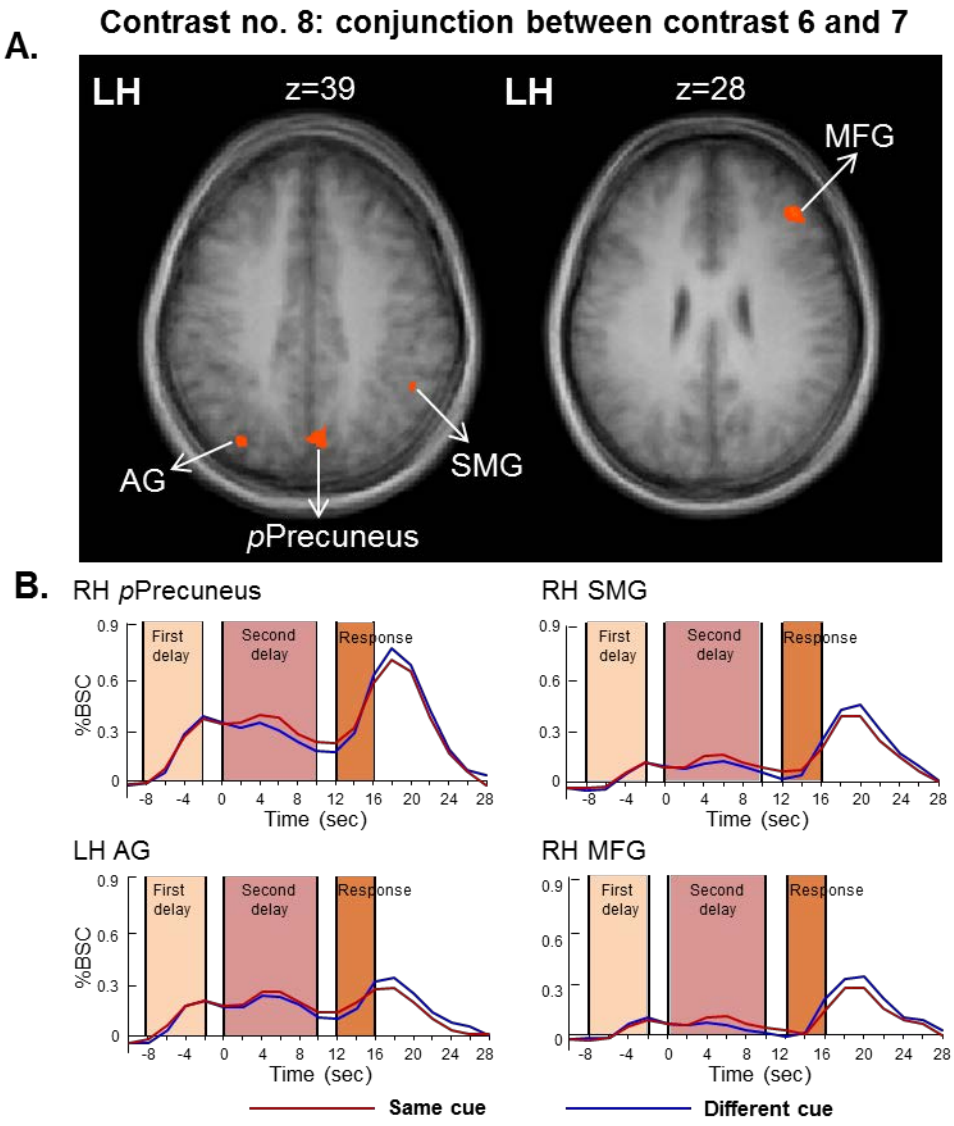

Figure 4.7 Voxelwise statistical map and time courses for each area using Contrast no. 8, a conjunction between contrast nos. 6 and 7. Top panel, activation map overlaid on the averaged anatomical image from all participants. Bottom panel, time course data in line graphs show averaged % BSC for the two tasks from each area.

areas that met the criteria imposed by our conjunction analysis). However, the time courses additionally confirmed that these instruction-related differences always initiated 4-6 seconds after the relevant verbal or visual instruction (provided in the gaps between the three phases), as expected for an instruction-related response when one accounts for sensory, cognitive, and hemodynamic delays. In other words, these four areas were clearly task-related and their task-dependent responses occurred at times consistent with our hypotheses for sites involved in the Allo-Ego conversion.

In summary, we identified four areas – *p*Precuneus, AG, SMG and MFG – that were specifically involved in the conversion of allocentric to egocentric target representations for reach at the first opportunity. This suggests that specific areas of PPC and frontal cortex are involved in converting allocentrically-defined target locations into the egocentric representations for targets and/or reach plans.

4.5 DISCUSSION

In the present study, we used an fMRI design to investigate the brain areas involved in allocentric to egocentric conversion of reach target representations, and tested when this happens in response to different sensory / cognitive cues. First, our data confirmed the original allocentric representations of reach targets in IOG and ITG during the first delay in accordance with our previous finding (Chen et al., 2014). Second, our results confirmed the early Allo-Ego conversion observed in our previous psychophysical study (Chen et al., 2011), by showing that egocentric reach directional selectivity arises within the brain at the first opportunity, regardless of the nature of the cue that triggers this event. Most importantly, we identified four specific areas in PPC and frontal cortex involved in converting allocentric

coding of target location to egocentric representation. These findings are graphically summarized in Figure 8, which compares the cortical areas involved in allocentric directional selectivity, Allo-Ego conversion, and egocentric reach direction selectivity, during the three major phases of our event-related design.

Egocentric Reach Directional Selectivity in the Second Delay and Response Phases

Previous human imaging studies have indicated egocentric directional selectivity of reach coding in PPC (Medendorp et al., 2003; Medendorp et al., 2005b; Fernandez-Ruiz et al., 2007; Beurze et al., 2009; Bernier and Grafton, 2010b; Chen et al., 2014), and target coding in occipital cortex (Chen et al., 2014). A psychophysical study has shown that conversion of allocentric to egocentric representation happens as soon as possible (Chen et al., 2011). To test this early conversion, we first confirmed the unique presence of allocentric coding in our first delay phases similar to that observed in our previous fMRI study (Chen et al., 2014), and then performed analysis of egocentric reach directional selectivity in both tasks during the second delay and response phase, respectively. We found that left *p*IPS, SOG, MOG and IOG showed a preference for contralateral reach direction (relative to gaze/midline) during the second delay in the *Same cue* task where a verbal instruction ("Same cue") had indicated the location of re-displayed visual landmark, allowing the subject to infer the future location of the target location. In addition, egocentric directional selectivity was observed in Precuneus, *p*IPS, cuneus, calcarine, LG, SOG, MOG and IOG during the response phase in the *Different cue* task where the visual cue of re-presented landmark provided the final target location for reach. The results in the response phase

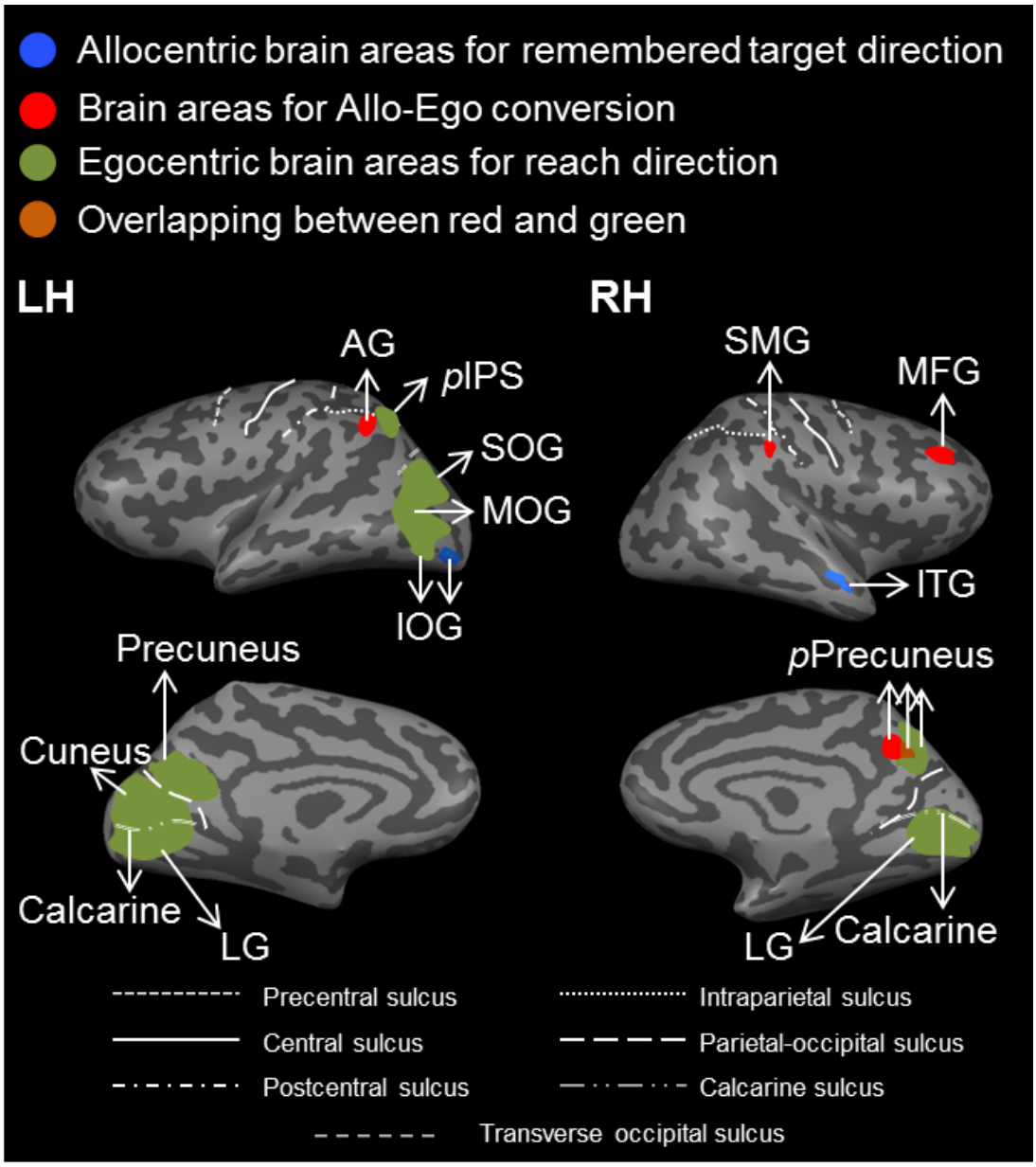
Allocentric brain areas for remembered target direction
Brain areas for Allo-Ego conversion
Egocentric brain areas for reach direction
Overlapping between red and green
LH
RH
AG
pIPS
SOG
MOG
IOG
SMG
MFG
ITG
Precuneus
Cuneus
Calcarine
LG
pPrecuneus
LG
Calcarine
Precentral sulcus
Central sulcus
Postcentral sulcus
Intraparietal sulcus
Parietal-occipital sulcus
Calcarine sulcus
Transverse occipital sulcus

Figure 4.8 Summary of cortical areas displayed on the inflated brain of one representative participant. Blue represents areas showing allocentric coding from Contrast no. 3 (Figure 4.2). Red represents areas involved in Allo-Ego conversion from Contrast no. 8 (Figure 4.7). Green represents areas showing egocentric reach directional selectivity from Contrast no. 4 and 5 (Figures 4.3, 4.4). Brown illustrates the overlapping area between red and green.

showed overlapping areas for egocentric reach directional selectivity in both tasks, suggesting that those areas could be involved in reach target representation and/or the early aspects of reach planning in egocentric coordinates. These two functions could not be disentangled with the current design; a comparison with previous studies shows overlap with occipital-parietal areas thought to be involved in both of these processes (Astafiev et al., 2003; Beurze et al., 2007; Fernandez-Ruiz et al., 2007; Chen et al., 2014). Our results further demonstrated that either visual information or spatial information inferred from a verbal cue could be used as a cue to process the early conversion of allocentric to egocentric representations.

Specific Areas Involved in the Allo-Ego Conversion

By using a conjunction analysis between Contrast no. 6 (second delay phase) and Contrast no. 7 (response phase), we were able to identify the specific areas most likely to be involved in converting allocentric coding to egocentric representation at the first opportunity regardless of the tasks and available cues. We found four areas, three in PPC (*p*Precuneus, AG and SMG) and one in lateral frontal cortex (MFG).

Regarding the role played by PPC in reach planning and control, a number of human imaging studies have focused on the two distinct subregions, medial intraparietal sulcus (mIPS) and superior parieto-occipital cortex (SPOC) (Medendorp et al., 2003; Grefkes et al., 2004; Prado et al., 2005; Beurze et al., 2007; Levy et al., 2007; Beurze et al., 2009). The SPOC is a special area situated more medial-posterior within Precuneus. A recent human neuroimaging study showed that Precuneus was involved in coding of motor goal for reach and could play a different role than SPOC (Gertz and Fiehler, 2015). Our results further

showed that Precuneus, not SPOC, is involved in converting reach targets encoded in allocentric coordinates into egocentric representation as soon as the reach target location was provided. This is consistent with the complexity of the Precuneus functions from previous studies such as automatically coding allocentric targets in large background coordinates (Uchimura et al., 2015) and processing spatial information for motor imagery (Cavanna and Trimble, 2006). It has been demonstrated that AG plays an important role in planning reaches with the specific effector (contralateral hand) (Fernandez-Ruiz et al., 2007; Koch et al., 2008; Vesia et al., 2010). Another area in the inferior parietal lobule, SMG is relatively less characterized in human reach. Previous studies using Transcranial Magnetic Stimulation (TMS) and fMRI demonstrated that SMG is involved in planning a goal-oriented hand movement with no effect on movement execution (Tunik et al., 2008), and processing a salient target for a target-detection response (Menon et al., 1997). Our finding of SMG in the Allo-Ego conversion could be related to the early stage of converting the relevant reach target encoded in allocentric coordinates into egocentric coding for the later stage of movement control. Unlike the well-studied PPC in reach planning, only a few studies have shown the function of lateral frontal cortex in processing relevant information for action (Tanji and Hoshi, 2008). Our findings indicate that right MFG is involved in the Allo-Ego conversion of targets for reach movements.

Taken together, by directly comparing the *Same cue* task to the *Different cue* task, we found three areas in PPC, one in the dorsomedial region (Precuneus), two (AG, SMG) in inferior parietal lobule, and one in lateral frontal cortex (MFG), that are related to allocentric to egocentric conversion of target representation. Note that this is different from the typical parieto-frontal network for reach planning and execution found in previous studies (Andersen

et al., 1993; Andersen et al., 1998; Batista et al., 1999; Connolly et al., 2007). This finding provides further insight into the different roles played by subdivisions of the PPC and frontal cortex in spatial coding and transformation for reach control.

Additional Task-Specific Activity in the Second Delay and Response Phases

In addition to the four areas described above, several other areas emerged in our comparisons between the *Same / Different cue* tasks including *a*Precuneus, IFG and MTG during the second delay, and PMd and Pre-SMA during the response, further suggesting that these areas could play multiple roles in the current reach task rather than converting allocentric coding to egocentric representation of targets for reaching movements. For example, during the second delay the higher activation observed in MTG could be related to its role in working memory (Olson et al., 2006a; Olson et al., 2006b; Axmacher et al., 2007; Ezzyat and Olson, 2008). Indeed, in our paradigm participants had to remember the converted egocentric information. Higher activation observed in IFG could be related to its involvement in orienting attention to visual targets (Japee et al., 2015), which might have occurred in the second delay phase for the *Same cue* task where Allo-Ego conversion of target representation took place. On the other hand, the higher activity revealed in PMd and Pre-SMA could be associated with their role in reaching plan and execution during the response phase (Kawashima et al., 1994; Van Oostende et al., 1997; Lee et al., 1999; Hoshi and Tanji, 2000; Toni et al., 2001; Hoshi and Tanji, 2006; Batista et al., 2007), suggesting that the Allo-Ego conversion and motor planning co-exist in the *Different cue* task. Interestingly, we found little directional selectivity in frontal cortex during the response phase of this task (and our previous allocentric reach task), compared to a purely egocentric

reach task (Chen et al., 2014). This suggests that the early use of allocentric codes also has an influence on the spatial coding of reach execution, even after the Ego-Allo conversion.

In conclusion**,** our results confirmed that the original allocentric representations of reach targets are converted into egocentric plan at the first possible opportunity, and that this conversion could occur when either a visual or a verbal instruction is used as the cue for the Allo-Ego conversion. More importantly, our results implicate four specific areas in PPC and frontal cortex involved in the Allo-Ego conversion for reach, regardless of the timing of this conversion within the task or the instruction modality.

CHAPTER FIVE

GENERAL DISCUSSION

5.1 Summary

My fMRI studies are the first to investigate neural mechanisms for allocentric coding of target memory for reaches and saccades, and directly compare allocentric vs. egocentric mechanisms. In addition, the neural substrates involved in allo-to-ego conversion of reach target representation are first examined. The results showed that different cortical substrates are involved in allocentric vs. egocentric target memory for saccadic (Chapter three) as well as reaching movements (Chapter two). Moreover, allocentric neural substrates for the remembered target coding for reaches and saccades are different, suggesting the effector-dependent (hand vs. eye) mechanisms for allocentric coding. Results from the third study (Chapter four) identified four brain areas, three in PPC and one in frontal cortex, that are specifically involved in converting allocentrically-defined reach targets within the ventral stream to egocentric plans at the first possible opportunity. Taken together, my findings are in general consistent with the theories of functional specialization related to the dorsal and ventral visual streams, indicating that both streams are involved in spatial coding for movements, but in different ways. The dorsal stream mostly relies on egocentric reference frames, whereas the ventral stream is more related to the allocentric reference frames for spatial processing.

These findings will help to explain what is going on in the brain for spatial coding during aiming movements, especially encoding target location in allocentric reference frames, which can further contribute to clinical applications. For instance, if the "egocentric" brain areas are damaged by a stroke, the “allocentric areas” might still be able to accommodate action. In these patients, rehabilitation therapies designed to enhance the use of allocentric information could reinforce recovery. Moreover, strategies developed to enhance

allocentric reliance might be useful for normal elderly with degraded egocentric function during normal ageing.

5.2 Distinction between allocentric coding in aiming movements and spatial navigation

Overall, the main goal of my studies was to investigate neural substrates involved in encoding remembered target location for two types of aiming movements, reaching and saccades. There is another common movement, navigating in the environment, where spatial coding, especially in allocentric coordinates must be needed. For instance one finds his way to drive a car to a supermarket via paths with different buildings on it. How our brain is processing the spatial information when navigating has become an interesting topic for researchers, especially the allocentric navigation, which has been investigated in laboratory using virtual environments along with some neuroimaging techniques in humans (Burgess et al., 2002; Shelton and Gabrieli, 2002; Rosenbaum et al., 2004; Epstein, 2008; Ekstrom et al., 2014; Robin et al., 2014). It was first proposed by Tolman (1948) that the brain creates a cognitive map of the environment for navigation such that the positions of objects in it are represented relative to each other on the map allocentrically. In general, this theory has been accepted by following studies showing medial temporal lobe (MTL), including hippocampus, parahippocampal cortex and entorhinal cortex, and retrosplenial cortex, involved in allocentric memory for navigation (Maguire, 1997; Maguire et al., 1997; Aguirre et al., 1998; Epstein and Kanwisher, 1998). Subsequent research has a more focus on the role of hippocampus in allocentric memory for spatial navigation by testing normal humans or patients with selective damage to it (Astur et al., 2002; Kumaran and Maguire, 2005;

Maguire et al., 2006; Bartsch et al., 2010; Goodrich-Hunsaker et al., 2010; Maguire and Mullally, 2013).

Compared to the results for spatial navigation, I did not find hippocampus or other brain areas in MTL showing allocentric coding of remembered target location for reaches and saccades. This would reflect the differences in allocentric neural mechanisms for spatial navigation where a cognitive map for a large-scale space is constructed (Ekstrom et al., 2014) versus the location of one target represented relative to a specified landmark for aiming movements (e.g., reaches, saccades), as investigated in my studies. This is consistent with the implications that the involvement of MTL, or particularly hippocampus in allocentric memory of spatial coding are spatial scale-dependent (Wolbers and Wiener, 2014).

5.3 Comparison to other senses for spatial coding

In my studies, I focused on the neural mechanisms for processing visuospatial information of targets for reaching and saccadic eye movements. As we know, in the real world there are multiple sensory modalities such as vision, audition and smell available to receive spatial information. Evidence from electrophysiological studies has indicated some classic higher-order cortical areas that are involved in multisensory integration including intraparietal sulcus and superior temporal sulcus (Ghazanfar and Schroeder, 2006; Simon, 2008). Among those, the spatial integration of visual-auditory information takes places in eye-centered reference frames in posterior parietal cortex (PPC) as well as superior colliculus (Andersen, 1997; Stein and Stanford, 2008), followed by further coordinate transformations to head- or should-centered frames for motor response (Cohen and Anderson, 2004).

Although neural mechanisms for visuospatial coding have been widely studies, those for auditory spatial coding are much less investigated, especially for allocentric representation.

Results from neurophysiological studies suggest that multiple reference frames such as eye-, head-centered and allocentric may be used in auditory spatial coding in PPC (Andersen et al., 1999). In particular, lateral intraparietal area (LIP) encodes and maintains auditory stimuli in eye-centered coordinates for saccadic movements (Stricanne et al., 1996); on the other hand, parietal reach region (PRR) is responsible for the spatial coding of auditory targets in eye-centered coordinates for reaching movements (Cohen and Andersen, 2000). Taken together, the results have suggested that neurons in PPC represent target location in eye-centered reference frames, regardless of the modality of sensory stimuli (i.e., visual or auditory). By employing neuroimaging, electroencephalography or magnetoencephalography techniques, several recent studies have investigated the neural mechanisms underlying the auditory spatial coding in humans (Maeder et al., 2001; Zimmer et al., 2006; Lewald et al., 2008; Altmann et al., 2009; Getzmann and Lewald, 2010; Lewald and Getzmann, 2011). Results from those studies have suggested that PPC, anterior and posterior temporal cortex, dorsolateral prefrontal cortex and inferior frontal cortex are involved in human auditory spatial coding. Other neuroimaging studies in humans have showed overlapping areas such as intraparietal sulcus (IPS) and frontal cortex, involved in auditory and visual spatial coding for motion discrimination tasks (Lewis et al., 2000), target selection tasks (Jiang and Kanwisher, 2003) and audiospatial working-memory tasks (Tark and Curtis, 2009). To my knowledge, there is no research investigating the neural mechanisms for auditory spatial processing of targets in allocentric reference frames as well as the directional selectivity in egocentric reference frames. However, based on the results

from my studies for spatial specificity of visual targets in the two reference frames and the literature reviewed above, I would expect similar neural substrates for encoding auditory target location to those for the coding of visual targets. There might be some brain areas specifically involved in auditory spatial coding, such as the posterior and lateral superior temporal lobe (Deouell et al., 2006; Altmann et al., 2012).

5.4 Subcortical mechanisms for saccade target coding

Neurophysiological studies have shown that besides cortical regions including lateral intraparietal sulcus (LIP), supplementary (SEF) and frontal eye fields (FEF), subcortical structures, such as superior colliculus (SC) and basal ganglia, also play critical roles in the egocentric saccadic system (Munoz, 2002). The functions and structures of SC in nonhuman primates for the control of eye movements have been well studied. The SC encodes saccade target location in an eye-centered reference frame (Klier et al., 2001), and the remembered target location is continuously updated across intervening eye movements (Dash et al., 2014). The structure of SC consists of superficial and intermediate layers. The former contains visual neurons that receive visual inputs directly from retina and visual cortices (Schiller and Malpeli, 1977; Pollack and Hickey, 1979; Fries and Distel, 1983; Rodieck and Watanabe, 1993; Abel et al., 1997); the latter receives inputs from cortical regions such as FEF and LIP as well as other subcortical regions such as substantia nigra of basal ganglia (Astruc, 1971; Leichnetz et al., 1981; Lynch et al., 1985; Hikosaka et al., 2000). There are two types of visuomovement neurons in the intermediate layers, buildup and burst, which have different functions in the control of saccade movements (Munoz and Wurtz, 1995). In particular, the buildup neurons have the characteristics of predictive response, i.e., discharge continuously

from stimulus onset to saccade initiation, suggesting their role in the process of saccade preparation (Basso and Wurtz, 1998; Horwitz and Newsome, 2001); in contrast, the burst neurons show strong activity before and during saccade generation, suggesting their involvement in saccade execution (Basso and Wurtz, 1998; McPeek and Keller, 2002).

In comparison to the neurophysiological studies, much less is known about the functions of SC in humans. The factors that have limited the use of functional brain imaging techniques to investigate the human SC include its small size, deep location and the noise arising from vascular structures close to it (Poncelet et al., 1992; Guimaraes et al., 1998). Recently, a few fMRI studies observed saccade-related activity in human SC in visual search tasks (Himmelbach et al., 2007) and in centrifugal saccade tasks (Krebs et al., 2010). Further, an fMRI study aiming at investigating the response of human SC associated with the saccade preparatory revealed increased activation in SC during saccade preparation and execution, which is consistent with the characteristics of visuomovement neurons in the intermediate layer of the nonhuman primate SC (Furlan et al., 2015). Based on the literature, I did not expect to observe activity in SC during the delay phase of my saccade study (study 2). The reason is that the final location of the target for a saccade was not provided during the delay so that no saccade preparation could be made. However, activity in SC would be observed during the response phase. The reason for the absence of activation in SC could be related to the used head coil, the positioned slices and the applied sequence for image acquisition in my study where only the images of cortical areas were ensured.

5.5 Additional considerations about allocentric coding and allo-to-ego conversion

In my experimental designs, I used a landmark as the allocentric cue and gave participants a clear instruction to ensure that the target location was represented relative to the allocentric cue (i.e., in the allocentric reference frames) in the allocentric tasks. In addition, I analyzed participants' behavior performance, which further confirmed the coding of target location in the allocentric coordinates in the allocentric tasks. Therefore, I believe that my allocentric tasks are allocentric, i.e., the distance and the direction of the target with respect to the allocentric cue had to be taken into account for the representation of the target location in the allocentric tasks. Recently, it is argued that allocentric coding may depend on egocentric reference frames (Filimon, 2015). I do not agree with Fillimon in that spatial relationships between the target and the allocentric cue had to be computed in the allocentric conditions, even though it could be possible to use egocentric comparison of the two stimuli. However, there was no egocentric directional selectivity observed in the allocentric tasks of my studies, suggesting allocentric coding was independent of egocentric reference frames, at least in my designs. The literature from behavioral, neuropsychological and neuroimaging studies have also provided evidence supporting different neural mechanisms related to the two reference frames (egocentric, allocentric) as well as both frames existing for target coding (Culham et al., 2003; Krigolson and Heath, 2004; Hay and Redon, 2006; Schenk, 2006; Zaehle et al., 2007; Chen et al., 2011; Thaler and Goodale, 2011b). It has been indicated that in real situations where egocentric and allocentric cues are available, the brain can combine the two cues for target coding, based on the relative weighting between them (Byrne and Crawford, 2010).

In my third study, I identified specific areas involved in the early allo-to-ego conversion of remembered reach targets by investigating egocentric directional selectivity at gaze-centered reference frames. Of course, there are other types of egocentric frames of reference such as head, should and hand. In order to perform reaching movements, eye-head-hand transformations are needed (Crawford et al., 2004; Crawford et al., 2011). Based on the goal of my third study, I did not attempt to differentiate those egocentric reference frames, instead focused on the earlier stage of converted egocentric target representations in the common gaze-centered coordinates. As suggested, the position of the hand is represented in gaze-centered reference frames in PPC, even when it is not visible, thus the hand-target comparison occurs in gaze-centered coordinates within PPC as well (Buneo et al., 2002). The identified three areas (precuneus, AG and SMG) within PPC for the allo-to-ego conversion of reach target representations are generally consistent with this suggestion. Except for those common areas in PPC during both delay and response phases, observed activity in other frontal regions, for instance dorsal premotor area (PMd) during the response phase is accordance with the function of PMd for encoding reach plans at shoulder-centered coordinates (Caminiti et al., 1991; Johnson et al., 1996; Shen and Alexander, 1997).

5.6 Future directions

Following the finding of four specific areas in parietal and frontal cortex for the conversion of allocentric to egocentric reach target representation, immediate questions are whether the four areas play a similar or a different role in the early Allo-Ego conversion, and how these areas are interconnected and coordinated. Future investigations can be performed by using TMS over each of these areas with a well designed experimental paradigm to

determine their role in the allocentric to egocentric conversion of reach target representations, or by combining TMS with the technique of diffusion tensor imaging (DTI) to examine the functional interconnections among these regions.

In addition, as shown in my saccade study, the cortical mechanisms for the allocentric coding of saccade target memory are different from those for reach target memory (from the first study), suggesting effector-dependent allocentric mechanisms for reaches versus saccades. Therefore, another intriguing question is whether the brain also uses different neural mechanisms for Allo-Ego conversion of saccade target representations as compared to reach target representations. To answer this question, future studies can use a similar behavioural paradigm to that for the reach study (Chen et al., 2011) to test if the early Allo-Ego conversion also happens for saccadic eye movements. An fMRI design similar to that in my third study then can be employed to further investigate the underlying neural mechanisms.

REFERENCES

Abel PL, O'Brien BJ, Lia B, Olavarria JF (1997) Distribution of neurons projecting to the superior colliculus correlates with thick cytochrome oxidase stripes in macaque visual area V2. J Comp Neurol 377:313-323.

Abrams RA, Davoli CC, Du F, Knapp WH, 3rd, Paull D (2008) Altered vision near the hands. Cognition 107:1035-1047.

Aguirre GK, Zarahn E, D'Esposito M (1998) Neural components of topographical representation. Proc Natl Acad Sci U S A 95:839-846.

Altmann CF, Wilczek E, Kaiser J (2009) Processing of auditory location changes after horizontal head rotation. J Neurosci 29:13074-13078.

Altmann CF, Getzmann S, Lewald J (2012) Allocentric or craniocentric representation of acoustic space: an electrotomography study using mismatch negativity. PLoS One 7:e41872.

Ances BM, Leontiev O, Perthen JE, Liang C, Lansing AE, Buxton RB (2008) Regional differences in the coupling of cerebral blood flow and oxygen metabolism changes in response to activation: implications for BOLD-fMRI. Neuroimage 39:1510-1521.

Andersen RA (1997) Multimodal integration for the representation of space in the posterior parietal cortex. Philos Trans R Soc Lond B Biol Sci 352:1421-1428.

Andersen RA, Buneo CA (2002) Intentional maps in posterior parietal cortex. Annu Rev Neurosci 25:189-220.

Andersen RA, Snyder LH, Li CS, Stricanne B (1993) Coordinate transformations in the representation of spatial information. Curr Opin Neurobiol 3:171-176.

Andersen RA, Snyder LH, Batista AP, Buneo CA, Cohen YE (1998) Posterior parietal areas specialized for eye movements (LIP) and reach (PRR) using a common coordinate frame. Sensory Guidance of Movement 218:109-128.

Andersen RA, Shenoy KV, Snyder LH, Bradley DC, Crowell JA (1999) The contributions of vestibular signals to the representations of space in the posterior parietal cortex. Ann N Y Acad Sci 871:282-292.

Astafiev SV, Shulman GL, Stanley CM, Snyder AZ, Van Essen DC, Corbetta M (2003) Functional organization of human intraparietal and frontal cortex for attending, looking, and pointing. J Neurosci 23:4689-4699.

Astruc J (1971) Corticofugal connections of area 8 (frontal eye field) in Macaca mulatta. Brain Res 33:241-256.

Astur RS, Taylor LB, Mamelak AN, Philpott L, Sutherland RJ (2002) Humans with hippocampus damage display severe spatial memory impairments in a virtual Morris water task. Behav Brain Res 132:77-84.

Axmacher N, Mormann F, Fernandez G, Cohen MX, Elger CE, Fell J (2007) Sustained neural activity patterns during working memory in the human medial temporal lobe. J Neurosci 27:7807-7816.

Bandettini PA, Cox RW (2000) Event-related fMRI contrast when using constant interstimulus interval: theory and experiment. Magn Reson Med 43:540-548.

Bandettini PA, Wong EC, Hinks RS, Tikofsky RS, Hyde JS (1992) Time course EPI of human brain function during task activation. Magn Reson Med 25:390-397.

Barbas H, Pandya DN (1987) Architecture and frontal cortical connections of the premotor cortex (area 6) in the rhesus monkey. J Comp Neurol 256:211-228.

Bartsch T, Schonfeld R, Muller FJ, Alfke K, Leplow B, Aldenhoff J, Deuschl G, Koch JM (2010) Focal lesions of human hippocampal CA1 neurons in transient global amnesia impair place memory. Science 328:1412-1415.

Basso MA, Wurtz RH (1998) Modulation of neuronal activity in superior colliculus by changes in target probability. J Neurosci 18:7519-7534.

Batista AP, Buneo CA, Snyder LH, Andersen RA (1999) Reach plans in eye-centered coordinates. Science 285:257-260.

Batista AP, Santhanam G, Yu BM, Ryu SI, Afshar A, Shenoy KV (2007) Reference frames for reach planning in macaque dorsal premotor cortex. J Neurophysiol 98:966-983.

Bays PM, Husain M (2007) Spatial remapping of the visual world across saccades. Neuroreport 18:1207-1213.

Belliveau JW, Kennedy DN, Jr., McKinstry RC, Buchbinder BR, Weisskoff RM, Cohen MS, Vevea JM, Brady TJ, Rosen BR (1991) Functional mapping of the human visual cortex by magnetic resonance imaging. Science 254:716-719.

Bernier P-M, Grafton ST (2010a) Human Posterior Parietal Cortex Flexibly Determines Reference Frames for Reaching Based on Sensory Context. Neuron 68:776-788.

Bernier PM, Grafton ST (2010b) Human posterior parietal cortex flexibly determines reference frames for reaching based on sensory context. Neuron 68:776-788.

Beurze SM, de Lange FP, Toni I, Medendorp WP (2007) Integration of target and effector information in the human brain during reach planning. J Neurophysiol 97:188-199.

Beurze SM, de Lange FP, Toni I, Medendorp WP (2009) Spatial and effector processing in the human parietofrontal network for reaches and saccades. J Neurophysiol 101:3053-3062.

Beurze SM, Toni I, Pisella L, Medendorp WP (2010) Reference frames for reach planning in human parietofrontal cortex. J Neurophysiol 104:1736-1745.

Blangero A, Ota H, Delporte L, Revol P, Vindras P, Rode G, Boisson D, Vighetto A, Rossetti Y, Pisella L (2007) Optic ataxia is not only 'optic': impaired spatial integration of proprioceptive information. Neuroimage 36 Suppl 2:T61-68.

Blurton SP, Raabe M, Greenlee MW (2012) Differential cortical activation during saccadic adaptation. J Neurophysiol 107:1738-1747.

Bradshaw MF, Watt SJ (2002) A dissociation of perception and action in normal human observers: the effect of temporal-delay. Neuropsychologia 40:1766-1778.

Bridgeman B, Peery S, Anand S (1997) Interaction of cognitive and sensorimotor maps of visual space. Percept Psychophys 59:456-469.

Brouwer AM, Knill DC (2007) The role of memory in visually guided reaching. J Vis 7:6 1-12.

Brown MR, Goltz HC, Vilis T, Ford KA, Everling S (2006) Inhibition and generation of saccades: rapid event-related fMRI of prosaccades, antisaccades, and nogo trials. Neuroimage 33:644-659.

Brown MR, DeSouza JF, Goltz HC, Ford K, Menon RS, Goodale MA, Everling S (2004) Comparison of memory- and visually guided saccades using event-related fMRI. J Neurophysiol 91:873-889.

Bruce CJ, Goldberg ME, Bushnell MC, Stanton GB (1985) Primate frontal eye fields. II. Physiological and anatomical correlates of electrically evoked eye movements. J Neurophysiol 54:714-734.

Buckner RL, Bandettini PA, O'Craven KM, Savoy RL, Petersen SE, Raichle ME, Rosen BR (1996) Detection of cortical activation during averaged single trials of a cognitive task using functional magnetic resonance imaging. Proc Natl Acad Sci U S A 93:14878-14883.

Buneo CA, Jarvis MR, Batista AP, Andersen RA (2002) Direct visuomotor transformations for reaching. Nature 416:632-636.

Burgess N (2006) Spatial memory: how egocentric and allocentric combine. Trends Cogn Sci 10:551-557.

Burgess N, Maguire EA, O'Keefe J (2002) The human hippocampus and spatial and episodic memory. Neuron 35:625-641.

Burgess N, Spiers HJ, Paleologou E (2004) Orientational manoeuvres in the dark: dissociating allocentric and egocentric influences on spatial memory. Cognition 94:149-166.

Burnod Y, Baraduc P, Battaglia-Mayer A, Guigon E, Koechlin E, Ferraina S, Lacquaniti F, Caminiti R (1999) Parieto-frontal coding of reaching: an integrated framework. Exp Brain Res 129:325-346.

Busan P, Barbera C, Semenic M, Monti F, Pizzolato G, Pelamatti G, Battaglini PP (2009) Effect of transcranial magnetic stimulation (TMS) on parietal and premotor cortex during planning of reaching movements. PLoS One 4:e4621.

Byrne P, Becker S (2008) A principle for learning egocentric-allocentric transformation. Neural Comput 20:709-737.

Byrne PA, Crawford JD (2010) Cue reliability and a landmark stability heuristic determine relative weighting between egocentric and allocentric visual information in memory-guided reach. J Neurophysiol 103:3054-3069.

Byrne PA, Cappadocia DC, Crawford JD (2010) Interactions between gaze-centered and allocentric representations of reach target location in the presence of spatial updating. Vision Res 50:2661-2670.

Caminiti R, Johnson PB, Galli C, Ferraina S, Burnod Y (1991) Making Arm Movements within Different Parts of Space - the Premotor and Motor Cortical Representation of a Coordinate System for Reaching to Visual Targets. Journal of Neuroscience 11:1182-1197.

Carrozzo M, Stratta F, McIntyre J, Lacquaniti F (2002) Cognitive allocentric representations of visual space shape pointing errors. Exp Brain Res 147:426-436.

Cavanna AE, Trimble MR (2006) The precuneus: a review of its functional anatomy and behavioural correlates. Brain 129:564-583.

Cavina-Pratesi C, Goodale MA, Culham JC (2007) FMRI reveals a dissociation between grasping and perceiving the size of real 3D objects. PLoS One 2:e424.

Cavina-Pratesi C, Monaco S, Fattori P, Galletti C, McAdam TD, Quinlan DJ, Goodale MA, Culham JC (2010) Functional magnetic resonance imaging reveals the neural substrates of arm transport and grip formation in reach-to-grasp actions in humans. J Neurosci 30:10306-10323.

Chakrabarti S, Martinez-Vazquez P, Gail A (2014) Synchronization patterns suggest different functional organization in parietal reach region and dorsal premotor cortex. J Neurophysiol 112:3138-3153.

Chen Y, Byrne P, Crawford JD (2011) Time course of allocentric decay, egocentric decay, and allocentric-to-egocentric conversion in memory-guided reach. Neuropsychologia 49:49-60.

Chen Y, Monaco S, Byrne P, Yan X, Henriques DY, Crawford JD (2014) Allocentric versus Egocentric Representation of Remembered Reach Targets in Human Cortex. J Neurosci 34:12515-12526.

Cohen YE, Andersen RA (2000) Reaches to sounds encoded in an eye-centered reference frame. Neuron 27:647-652.

Cohen YE, Andersen RA (2002) A common reference frame for movement plans in the posterior parietal cortex. Nat Rev Neurosci 3:553-562.

Cohen YE, Anderson RA (2004) Multimodal spatial representations in the primate parietal lobe. In: Crossmodal space and crossmodal attention (Spence C, Driver J, eds), pp 99-121. Oxford: Oxford University Press.

Colby CL (1998) Action-oriented spatial reference frames in cortex. Neuron 20:15-24.

Colby CL, Duhamel JR, Goldberg ME (1995) Oculocentric spatial representation in parietal cortex. Cereb Cortex 5:470-481.

Coluccia E, Mammarella IC, De Beni R, Ittyerah M, Cornoldi C (2007) Remembering object position in the absence of vision: egocentric, allocentric, and egocentric decentred frames of reference. Perception 36:850-864.

Committeri G, Galati G, Paradis AL, Pizzamiglio L, Berthoz A, LeBihan D (2004) Reference frames for spatial cognition: different brain areas are involved in viewer-, object-, and landmark-centered judgments about object location. J Cogn Neurosci 16:1517-1535.

Connolly JD, Andersen RA, Goodale MA (2003) FMRI evidence for a 'parietal reach region' in the human brain. Exp Brain Res 153:140-145.

Connolly JD, Goodale MA, Menon RS, Munoz DP (2002) Human fMRI evidence for the neural correlates of preparatory set. Nat Neurosci 5:1345-1352.

Connolly JD, Goodale MA, Cant JS, Munoz DP (2007) Effector-specific fields for motor preparation in the human frontal cortex. Neuroimage 34:1209-1219.

Connolly JD, Goodale MA, DeSouza JF, Menon RS, Vilis T (2000) A comparison of frontoparietal fMRI activation during anti-saccades and anti-pointing. J Neurophysiol 84:1645-1655.

Cordova A, Gabbard C, Cacola P (2012) Visual landmarks and response delay in estimates of reach. Percept Mot Skills 115:535-543.

Cornelissen FW, Kimmig H, Schira M, Rutschmann RM, Maguire RP, Broerse A, Den Boer JA, Greenlee MW (2002) Event-related fMRI responses in the human frontal eye fields in a randomized pro- and antisaccade task. Exp Brain Res 145:270-274.

Crammond DJ, Kalaska JF (1996) Differential relation of discharge in primary motor cortex and premotor cortex to movements versus actively maintained postures during a reaching task. Exp Brain Res 108:45-61.

Crawford JD, Medendorp WP, Marotta JJ (2004) Spatial transformations for eye-hand coordination. J Neurophysiol 92:10-19.

Crawford JD, Henriques DY, Medendorp WP (2011) Three-dimensional transformations for goal-directed action. Annu Rev Neurosci 34:309-331.

Crowe DA, Averbeck BB, Chafee MV (2008) Neural ensemble decoding reveals a correlate of viewer- to object-centered spatial transformation in monkey parietal cortex. J Neurosci 28:5218-5228.

Culham JC, Kanwisher NG (2001) Neuroimaging of cognitive functions in human parietal cortex. Curr Opin Neurobiol 11:157-163.

Culham JC, Cavina-Pratesi C, Singhal A (2006) The role of parietal cortex in visuomotor control: what have we learned from neuroimaging? Neuropsychologia 44:2668-2684.

Culham JC, Danckert SL, DeSouza JF, Gati JS, Menon RS, Goodale MA (2003) Visually guided grasping produces fMRI activation in dorsal but not ventral stream brain areas. Exp Brain Res 153:180-189.

Curtis CE, D'Esposito M (2006) Selection and maintenance of saccade goals in the human frontal eye fields. J Neurophysiol 95:3923-3927.

Dale AM, Buckner RL (1997) Selective averaging of rapidly presented individual trials using fMRI. Hum Brain Mapp 5:329-340.

Dash S, Yan X, Wang H, Crawford JD (2014) Continuous updating of visuospatial memory in superior colliculus during slow eye movements. Curr Biol 25:267-274.

Dassonville P, Schlag J, Schlag-Rey M (1995) The use of egocentric and exocentric location cues in saccadic programming. Vision Res 35:2191-2199.

Deneve S, Pouget A (2003) Basis functions for object-centered representations. Neuron 37:347-359.

Deouell LY, Parnes A, Pickard N, Knight RT (2006) Spatial location is accurately tracked by human auditory sensory memory: evidence from the mismatch negativity. Eur J Neurosci 24:1488-1494.

DeSouza JF, Menon RS, Everling S (2003) Preparatory set associated with pro-saccades and anti-saccades in humans investigated with event-related FMRI. J Neurophysiol 89:1016-1023.

DeSouza JF, Dukelow SP, Gati JS, Menon RS, Andersen RA, Vilis T (2000) Eye position signal modulates a human parietal pointing region during memory-guided movements. J Neurosci 20:5835-5840.

di Pellegrino G, Frassinetti F (2000) Direct evidence from parietal extinction of enhancement of visual attention near a visible hand. Curr Biol 10:1475-1477.

Diedrichsen J, Werner S, Schmidt T, Trommershauser J (2004) Immediate spatial distortions of pointing movements induced by visual landmarks. Percept Psychophys 66:89-103.

Disbrow EA, Slutsky DA, Roberts TP, Krubitzer LA (2000) Functional MRI at 1.5 tesla: a comparison of the blood oxygenation level-dependent signal and electrophysiology. Proc Natl Acad Sci U S A 97:9718-9723.

Duhamel JR, Colby CL, Goldberg ME (1992a) The updating of the representation of visual space in parietal cortex by intended eye movements. Science 255:90-92.

Duhamel JR, Colby CL, Goldberg ME (1992b) The Updating of the Representation of Visual Space in Parietal Cortex by Intended Eye-Movements. Science 255:90-92.

Duhamel JR, Bremmer F, BenHamed S, Graf W (1997) Spatial invariance of visual receptive fields in parietal cortex neurons. Nature 389:845-848.

Duncan J, Owen AM (2000) Common regions of the human frontal lobe recruited by diverse cognitive demands. Trends Neurosci 23:475-483.

Ekstrom AD, Arnold AE, Iaria G (2014) A critical review of the allocentric spatial representation and its neural underpinnings: toward a network-based perspective. Front Hum Neurosci 8:803.

Elliott D, Madalena J (1987) The influence of premovement visual information on manual aiming. Q J Exp Psychol A 39:541-559.

Enright JT (1995) The Nonvisual Impact of Eye Orientation on Eye-Hand Coordination. Vision Research 35:1611-1618.

Epstein R, Kanwisher N (1998) A cortical representation of the local visual environment. Nature 392:598-601.

Epstein RA (2008) Parahippocampal and retrosplenial contributions to human spatial navigation. Trends Cogn Sci 12:388-396.

Eskandar EN, Assad JA (1999) Dissociation of visual, motor and predictive signals in parietal cortex during visual guidance. Nat Neurosci 2:88-93.

Ezzyat Y, Olson IR (2008) The medial temporal lobe and visual working memory: comparisons across tasks, delays, and visual similarity. Cogn Affect Behav Neurosci 8:32-40.

Fabbri S, Caramazza A, Lingnau A (2012) Distributed sensitivity for movement amplitude in directionally tuned neuronal populations. J Neurophysiol 107:1845-1856.

Faillenot I, Sakata H, Costes N, Decety J, Jeannerod M (1997) Visual working memory for shape and 3D-orientation: a PET study. Neuroreport 8:859-862.

Fattori P, Breveglieri R, Marzocchi N, Filippini D, Bosco A, Galletti C (2009) Hand orientation during reach-to-grasp movements modulates neuronal activity in the medial posterior parietal area V6A. J Neurosci 29:1928-1936.

Fernandez-Ruiz J, Goltz HC, DeSouza JF, Vilis T, Crawford JD (2007) Human parietal "reach region" primarily encodes intrinsic visual direction, not extrinsic movement direction, in a visual motor dissociation task. Cereb Cortex 17:2283-2292.

Fiehler K, Wolf C, Klinghammer M, Blohm G (2014) Integration of egocentric and allocentric information during memory-guided reaching to images of a natural environment. Front Hum Neurosci 8:636.

Filimon F (2010) Human cortical control of hand movements: parietofrontal networks for reaching, grasping, and pointing. Neuroscientist 16:388-407.

Filimon F (2015) Are All Spatial Reference Frames Egocentric? Reinterpreting Evidence for Allocentric, Object-Centered, or World-Centered Reference Frames. Front Hum Neurosci 9:648.

Filimon F, Nelson JD, Hagler DJ, Sereno MI (2007) Human cortical representations for reaching: mirror neurons for execution, observation, and imagery. Neuroimage 37:1315-1328.

Filimon F, Nelson JD, Huang RS, Sereno MI (2009) Multiple parietal reach regions in humans: cortical representations for visual and proprioceptive feedback during on-line reaching. J Neurosci 29:2961-2971.

Fink GR, Dolan RJ, Halligan PW, Marshall JC, Frith CD (1997) Space-based and object-based visual attention: shared and specific neural domains. Brain 120 (Pt 11):2013-2028.

Fink GR, Marshall JC, Shah NJ, Weiss PH, Halligan PW, Grosse-Ruyken M, Ziemons K, Zilles K, Freund HJ (2000) Line bisection judgments implicate right parietal cortex and cerebellum as assessed by fMRI. Neurology 54:1324-1331.

Fogassi L, Gallese V, Fadiga L, Luppino G, Matelli M, Rizzolatti G (1996) Coding of peripersonal space in inferior premotor cortex (area F4). J Neurophysiol 76:141-157.

Forman SD, Cohen JD, Fitzgerald M, Eddy WF, Mintun MA, Noll DC (1995) Improved assessment of significant activation in functional magnetic resonance imaging (fMRI): use of a cluster-size threshold. Magn Reson Med 33:636-647.

Fries W, Distel H (1983) Large layer VI neurons of monkey striate cortex (Meynert cells) project to the superior colliculus. Proc R Soc Lond B Biol Sci 219:53-59.

Furlan M, Smith AT, Walker R (2015) Activity in the human superior colliculus relating to endogenous saccade preparation and execution. J Neurophysiol 114:1048-1058.

Gagnon D, O'Driscoll GA, Petrides M, Pike GB (2002) The effect of spatial and temporal information on saccades and neural activity in oculomotor structures. Brain 125:123-139.

Gail A, Andersen RA (2006) Neural dynamics in monkey parietal reach region reflect context-specific sensorimotor transformations. J Neurosci 26:9376-9384.

Gail A, Klaes C, Westendorff S (2009) Implementation of spatial transformation rules for goal-directed reaching via gain modulation in monkey parietal and premotor cortex. J Neurosci 29:9490-9499.

Galati G, Lobel E, Vallar G, Berthoz A, Pizzamiglio L, Le Bihan D (2000) The neural basis of egocentric and allocentric coding of space in humans: a functional magnetic resonance study. Exp Brain Res 133:156-164.

Galletti C, Battaglini PP, Fattori P (1993) Parietal neurons encoding spatial locations in craniotopic coordinates. Exp Brain Res 96:221-229.

Galletti C, Kutz DF, Gamberini M, Breveglieri R, Fattori P (2003) Role of the medial parieto-occipital cortex in the control of reaching and grasping movements. Experimental Brain Research 153:158-170.

Gallivan JP, McLean DA, Valyear KF, Pettypiece CE, Culham JC (2011) Decoding action intentions from preparatory brain activity in human parieto-frontal networks. J Neurosci 31:9599-9610.

Gauthier I, Tarr MJ, Moylan J, Skudlarski P, Gore JC, Anderson AW (2000) The fusiform "face area" is part of a network that processes faces at the individual level. J Cogn Neurosci 12:495-504.

Gaymard B, Ploner CJ, Rivaud S, Vermersch AI, Pierrot-Deseilligny C (1998) Cortical control of saccades. Exp Brain Res 123:159-163.

Gentilucci M, Fogassi L, Luppino G, Matelli M, Camarda R, Rizzolatti G (1988) Functional organization of inferior area 6 in the macaque monkey. I. Somatotopy and the control of proximal movements. Exp Brain Res 71:475-490.

Gertz H, Fiehler K (2015) Human posterior parietal cortex encodes the movement goal in a pro-/anti-reach task. J Neurophysiol 114:170-183.

Getzmann S, Lewald J (2010) Effects of natural versus artificial spatial cues on electrophysiological correlates of auditory motion. Hear Res 259:44-54.

Ghazanfar AA, Schroeder CE (2006) Is neocortex essentially multisensory? Trends Cogn Sci 10:278-285.

Goldberg ME, Bruce CJ (1990) Primate frontal eye fields. III. Maintenance of a spatially accurate saccade signal. J Neurophysiol 64:489-508.

Goodale MA, Milner AD (1992) Separate visual pathways for perception and action. Trends Neurosci 15:20-25.

Goodale MA, Haffenden A (1998) Frames of reference for perception and action in the human visual system. Neurosci Biobehav Rev 22:161-172.

Goodrich-Hunsaker NJ, Livingstone SA, Skelton RW, Hopkins RO (2010) Spatial deficits in a virtual water maze in amnesic participants with hippocampal damage. Hippocampus 20:481-491.

Gottlieb JP, Kusunoki M, Goldberg ME (1998) The representation of visual salience in monkey parietal cortex. Nature 391:481-484.

Greenlee MW, Magnussen S, Reinvang I (2000) Brain regions involved in spatial frequency discrimination: evidence from fMRI. Exp Brain Res 132:399-403.

Grefkes C, Ritzl A, Zilles K, Fink GR (2004) Human medial intraparietal cortex subserves visuomotor coordinate transformation. Neuroimage 23:1494-1506.

Grosbras MH, Lobel E, Van de Moortele PF, LeBihan D, Berthoz A (1999) An anatomical landmark for the supplementary eye fields in human revealed with functional magnetic resonance imaging. Cereb Cortex 9:705-711.

Guimaraes AR, Melcher JR, Talavage TM, Baker JR, Ledden P, Rosen BR, Kiang NY, Fullerton BC, Weisskoff RM (1998) Imaging subcortical auditory activity in humans. Hum Brain Mapp 6:33-41.

Hagler DJ, Jr., Riecke L, Sereno MI (2007) Parietal and superior frontal visuospatial maps activated by pointing and saccades. Neuroimage 35:1562-1577.

Harrison SA, Tong F (2009) Decoding reveals the contents of visual working memory in early visual areas. Nature 458:632-635.

Hartje W, Ettlinger G (1973) Reaching in light and dark after unilateral posterior parietal ablations in the monkey. Cortex 9:346-354.

Hawkins KM, Sayegh P, Yan X, Crawford JD, Sergio LE (2013) Neural Activity in Superior Parietal Cortex during Rule-based Visual-motor Transformations. Journal of Cognitive Neuroscience 25:436-454.

Hay L, Redon C (2006) Response delay and spatial representation in pointing movements. Neurosci Lett 408:194-198.

Heath M (2005) Role of limb and target vision in the online control of memory-guided reaches. Motor Control 9:281-311.

Henderson JM (2003) Human gaze control during real-world scene perception. Trends Cogn Sci 7:498-504.

Henderson JM, Hollingworth A (1999) The role of fixation position in detecting scene changes across saccades. Psychological Science 10:438-443.

Henderson JM, Weeks PA, Hollingworth A (1999) The effects of semantic consistency on eye movements during complex scene viewing. Journal of Experimental Psychology-Human Perception and Performance 25:210-228.

Henriques DY, Klier EM, Smith MA, Lowy D, Crawford JD (1998) Gaze-centered remapping of remembered visual space in an open-loop pointing task. J Neurosci 18:1583-1594.

Hikosaka O, Takikawa Y, Kawagoe R (2000) Role of the basal ganglia in the control of purposive saccadic eye movements. Physiol Rev 80:953-978.

Himmelbach M, Erb M, Karnath HO (2007) Activation of superior colliculi in humans during visual exploration. BMC Neurosci 8:66.

Honda M, Wise SP, Weeks RA, Deiber MP, Hallett M (1998) Cortical areas with enhanced activation during object-centred spatial information processing - A PET study. Brain 121:2145-2158.

Horwitz GD, Newsome WT (2001) Target selection for saccadic eye movements: prelude activity in the superior colliculus during a direction-discrimination task. J Neurophysiol 86:2543-2558.

Hoshi E, Tanji J (2000) Integration of target and body-part information in the premotor cortex when planning action. Nature 408:466-470.

Hoshi E, Tanji J (2006) Differential involvement of neurons in the dorsal and ventral premotor cortex during processing of visual signals for action planning. J Neurophysiol 95:3596-3616.

Howard IP, Templeton WB (1966) Human spatial orientation. London: Wiley.

Hu Y, Eagleson R, Goodale MA (1999) The effects of delay on the kinematics of grasping. Exp Brain Res 126:109-116.

Huettel S, Song AW, McCarthy G (2008) Functional magnetic resonance imaging. Sunderland: Sinauer Associates.

Humphreys GW (1983) Reference frames and shape perception. Cogn Psychol 15:151-196.

Isoda M, Tanji J (2002) Cellular activity in the supplementary eye field during sequential performance of multiple saccades. J Neurophysiol 88:3541-3545.

Japee S, Holiday K, Satyshur MD, Mukai I, Ungerleider LG (2015) A role of right middle frontal gyrus in reorienting of attention: a case study. Front Syst Neurosci 9:23.

Jiang Y, Kanwisher N (2003) Common neural substrates for response selection across modalities and mapping paradigms. J Cogn Neurosci 15:1080-1094.

Johnson PB, Ferraina S, Bianchi L, Caminiti R (1996) Cortical networks for visual reaching: Physiological and anatomical organization of frontal and parietal lobe arm regions. Cerebral Cortex 6:102-119.

Kakei S, Hoffman DS, Strick PL (1999) Muscle and movement representations in the primary motor cortex. Science 285:2136-2139.

Kakei S, Hoffman DS, Strick PL (2001) Direction of action is represented in the ventral premotor cortex. Nat Neurosci 4:1020-1025.

Kakei S, Hoffman DS, Strick PL (2003) Sensorimotor transformations in cortical motor areas. Neurosci Res 46:1-10.

Kalaska JF, Crammond DJ (1992) Cerebral Cortical Mechanisms of Reaching Movements. Science 255:1517-1523.

Kalaska JF, Scott SH, Cisek P, Sergio LE (1997) Cortical control of reaching movements. Current Opinion in Neurobiology 7:849-859.

Kanwisher N, McDermott J, Chun MM (1997) The fusiform face area: a module in human extrastriate cortex specialized for face perception. J Neurosci 17:4302-4311.

Karn KS, Moller P, Hayhoe MM (1997) Reference frames in saccadic targeting. Exp Brain Res 115:267-282.

Kastner S, DeSimone K, Konen CS, Szczepanski SM, Weiner KS, Schneider KA (2007) Topographic maps in human frontal cortex revealed in memory-guided saccade and spatial working-memory tasks. J Neurophysiol 97:3494-3507.

Kawashima R, Roland PE, O'Sullivan BT (1994) Fields in human motor areas involved in preparation for reaching, actual reaching, and visuomotor learning: a positron emission tomography study. J Neurosci 14:3462-3474.

Klier EM, Wang H, Crawford JD (2001) The superior colliculus encodes gaze commands in retinal coordinates. Nat Neurosci 4:627-632.

Koch G, Fernandez Del Olmo M, Cheeran B, Schippling S, Caltagirone C, Driver J, Rothwell JC (2008) Functional interplay between posterior parietal and ipsilateral motor cortex revealed by twin-coil transcranial magnetic stimulation during reach planning toward contralateral space. J Neurosci 28:5944-5953.

Konen CS, Mruczek RE, Montoya JL, Kastner S (2013) Functional organization of human posterior parietal cortex: grasping- and reaching-related activations relative to topographically organized cortex. J Neurophysiol 109:2897-2908.

Koyama M, Hasegawa I, Osada T, Adachi Y, Nakahara K, Miyashita Y (2004) Functional magnetic resonance imaging of macaque monkeys performing visually guided saccade tasks: comparison of cortical eye fields with humans. Neuron 41:795-807.

Kravitz DJ, Saleem KS, Baker CI, Mishkin M (2011) A new neural framework for visuospatial processing. Nat Rev Neurosci 12:217-230.

Krebs RM, Schoenfeld MA, Boehler CN, Song AW, Woldorff MG (2010) The Saccadic Re-Centering Bias is Associated with Activity Changes in the Human Superior Colliculus. Front Hum Neurosci 4:193.

Krigolson O, Heath M (2004) Background visual cues and memory-guided reaching. Hum Mov Sci 23:861-877.

Krigolson O, Clark N, Heath M, Binsted G (2007) The proximity of visual landmarks impacts reaching performance. Spat Vis 20:317-336.

Kumaran D, Maguire EA (2005) The human hippocampus: cognitive maps or relational memory? J Neurosci 25:7254-7259.

Kurata K (1991) Corticocortical inputs to the dorsal and ventral aspects of the premotor cortex of macaque monkeys. Neurosci Res 12:263-280.

Kurata K (1994) Information processing for motor control in primate premotor cortex. Behav Brain Res 61:135-142.

Kwong KK, Belliveau JW, Chesler DA, Goldberg IE, Weisskoff RM, Poncelet BP, Kennedy DN, Hoppel BE, Cohen MS, Turner R, et al. (1992) Dynamic magnetic resonance imaging of human brain activity during primary sensory stimulation. Proc Natl Acad Sci U S A 89:5675-5679.

Land M, Mennie N, Rusted J (1999) The roles of vision and eye movements in the control of activities of daily living. Perception 28:1311-1328.

Land MF, Hayhoe M (2001) In what ways do eye movements contribute to everyday activities? Vision Res 41:3559-3565.

Lee KM, Chang KH, Roh JK (1999) Subregions within the supplementary motor area activated at different stages of movement preparation and execution. Neuroimage 9:117-123.

Leff AP, Scott SK, Rothwell JC, Wise RJ (2001) The planning and guiding of reading saccades: a repetitive transcranial magnetic stimulation study. Cereb Cortex 11:918-923.

Leichnetz GR, Spencer RF, Hardy SG, Astruc J (1981) The prefrontal corticotectal projection in the monkey; an anterograde and retrograde horseradish peroxidase study. Neuroscience 6:1023-1041.

Lemay M, Stelmach GE (2005) Multiple frames of reference for pointing to a remembered target. Exp Brain Res 164:301-310.

Levy I, Schluppeck D, Heeger DJ, Glimcher PW (2007) Specificity of human cortical areas for reaches and saccades. Journal of Neuroscience 27:4687-4696.

Lewald J, Getzmann S (2011) When and where of auditory spatial processing in cortex: a novel approach using electrotomography. PLoS One 6:e25146.

Lewald J, Riederer KA, Lentz T, Meister IG (2008) Processing of sound location in human cortex. Eur J Neurosci 27:1261-1270.

Lewis JW, Beauchamp MS, DeYoe EA (2000) A comparison of visual and auditory motion processing in human cerebral cortex. Cereb Cortex 10:873-888.

Lindner A, Iyer A, Kagan I, Andersen RA (2010) Human posterior parietal cortex plans where to reach and what to avoid. J Neurosci 30:11715-11725.

Logothetis NK (2008) What we can do and what we cannot do with fMRI. Nature 453:869-878.

Logothetis NK, Guggenberger H, Peled S, Pauls J (1999) Functional imaging of the monkey brain. Nat Neurosci 2:555-562.

Lynch JC, Graybiel AM, Lobeck LJ (1985) The differential projection of two cytoarchitectonic subregions of the inferior parietal lobule of macaque upon the deep layers of the superior colliculus. J Comp Neurol 235:241-254.

Maeder PP, Meuli RA, Adriani M, Bellmann A, Fornari E, Thiran JP, Pittet A, Clarke S (2001) Distinct pathways involved in sound recognition and localization: a human fMRI study. Neuroimage 14:802-816.

Maguire EA (1997) Hippocampal involvement in human topographical memory: evidence from functional imaging. Philos Trans R Soc Lond B Biol Sci 352:1475-1480.

Maguire EA, Mullally SL (2013) The hippocampus: a manifesto for change. J Exp Psychol Gen 142:1180-1189.

Maguire EA, Frackowiak RS, Frith CD (1997) Recalling routes around london: activation of the right hippocampus in taxi drivers. J Neurosci 17:7103-7110.

Maguire EA, Nannery R, Spiers HJ (2006) Navigation around London by a taxi driver with bilateral hippocampal lesions. Brain 129:2894-2907.

Marr D, Nishihara HK (1978) Representation and recognition of the spatial organization of three-dimensional shapes. Proc R Soc Lond B Biol Sci 200:269-294.

Martinez-Trujillo JC, Medendorp WP, Wang H, Crawford JD (2004) Frames of reference for eye-head gaze commands in primate supplementary eye fields. Neuron 44:1057-1066.

McIntyre J, Stratta F, Lacquaniti F (1997) Viewer-centered frame of reference for pointing to memorized targets in three-dimensional space. J Neurophysiol 78:1601-1618.

McIntyre J, Stratta F, Lacquaniti F (1998) Short-term memory for reaching to visual targets: psychophysical evidence for body-centered reference frames. J Neurosci 18:8423-8435.

McKyton A, Zohary E (2007) Beyond retinotopic mapping: the spatial representation of objects in the human lateral occipital complex. Cereb Cortex 17:1164-1172.

McPeek RM, Keller EL (2002) Saccade target selection in the superior colliculus during a visual search task. J Neurophysiol 88:2019-2034.

Medendorp WP, Goltz HC, Vilis T (2005a) Remapping the remembered target location for anti-saccades in human posterior parietal cortex. J Neurophysiol 94:734-740.

Medendorp WP, Goltz HC, Vilis T (2006) Directional selectivity of BOLD activity in human posterior parietal cortex for memory-guided double-step saccades. J Neurophysiol 95:1645-1655.

Medendorp WP, Goltz HC, Vilis T, Crawford JD (2003) Gaze-centered updating of visual space in human parietal cortex. J Neurosci 23:6209-6214.

Medendorp WP, Goltz HC, Crawford JD, Vilis T (2005b) Integration of target and effector information in human posterior parietal cortex for the planning of action. J Neurophysiol 93:954-962.

Menon V, Ford JM, Lim KO, Glover GH, Pfefferbaum A (1997) Combined event-related fMRI and EEG evidence for temporal-parietal cortex activation during target detection. Neuroreport 8:3029-3037.

Merriam EP, Genovese CR, Colby CL (2003) Spatial updating in human parietal cortex. Neuron 39:361-373.

Merriam EP, Genovese CR, Colby CL (2007) Remapping in human visual cortex. J Neurophysiol 97:1738-1755.

Milner AD, Goodale MA (1995) The visual brain in action. Oxford: Oxford University Press.

Milner AD, Goodale MA (2006) The visual brain in action. Oxford: Oxford University Press.

Milner AD, Goodale MA (2008) Two visual systems re-viewed. Neuropsychologia 46:774-785.

Milner AD, Perrett DI, Johnston RS, Benson PJ, Jordan TR, Heeley DW, Bettucci D, Mortara F, Mutani R, Terazzi E, et al. (1991) Perception and action in 'visual form agnosia'. Brain 114 (Pt 1B):405-428.

Mohrmann-Lendla H, Fleischer AG (1991) The effect of a moving background on aimed hand movements. Ergonomics 34:353-364.

Monteon JA, Wang H, Martinez-Trujillo J, Crawford JD (2013) Frames of reference for eye-head gaze shifts evoked during frontal eye field stimulation. Eur J Neurosci 37:1754-1765.

Moscovitch C, Kapur S, Kohler S, Houle S (1995) Distinct neural correlates of visual long-term memory for spatial location and object identity: a positron emission tomography study in humans. Proc Natl Acad Sci U S A 92:3721-3725.

Mou W, McNamara TP, Rump B, Xiao C (2006) Roles of egocentric and allocentric spatial representations in locomotion and reorientation. J Exp Psychol Learn Mem Cogn 32:1274-1290.

Mountcastle VB, Lynch JC, Georgopoulos A, Sakata H, Acuna C (1975) Posterior parietal association cortex of the monkey: command functions for operations within extrapersonal space. J Neurophysiol 38:871-908.

Mullette-Gillman OA, Cohen YE, Groh JM (2005) Eye-centered, head-centered, and complex coding of visual and auditory targets in the intraparietal sulcus. J Neurophysiol 94:2331-2352.

Munoz DP (2002) Commentary: saccadic eye movements: overview of neural circuitry. Prog Brain Res 140:89-96.

Munoz DP, Wurtz RH (1995) Saccade-related activity in monkey superior colliculus. I. Characteristics of burst and buildup cells. J Neurophysiol 73:2313-2333.

Munoz DP, Everling S (2004) Look away: the anti-saccade task and the voluntary control of eye movement. Nat Rev Neurosci 5:218-228.

Murata A, Gallese V, Kaseda M, Sakata H (1996) Parietal neurons related to memory-guided hand manipulation. J Neurophysiol 75:2180-2186.

Muri RM, Iba-Zizen MT, Derosier C, Cabanis EA, Pierrot-Deseilligny C (1996) Location of the human posterior eye field with functional magnetic resonance imaging. J Neurol Neurosurg Psychiatry 60:445-448.

Muri RM, Gaymard B, Rivaud S, Vermersch A, Hess CW, Pierrot-Deseilligny C (2000) Hemispheric asymmetry in cortical control of memory-guided saccades. A transcranial magnetic stimulation study. Neuropsychologia 38:1105-1111.

Muri RM, Buhler R, Heinemann D, Mosimann UP, Felblinger J, Schlaepfer TE, Hess CW (2002) Hemispheric asymmetry in visuospatial attention assessed with transcranial magnetic stimulation. Exp Brain Res 143:426-430.

Neggers SF, Van der Lubbe RH, Ramsey NF, Postma A (2006) Interactions between ego- and allocentric neuronal representations of space. Neuroimage 31:320-331.

Obhi SS, Goodale MA (2005) The effects of landmarks on the performance of delayed and real-time pointing movements. Exp Brain Res 167:335-344.

Ogawa S, Tank DW, Menon R, Ellermann JM, Kim SG, Merkle H, Ugurbil K (1992) Intrinsic signal changes accompanying sensory stimulation: functional brain mapping with magnetic resonance imaging.

Olson CR (2003) Brain representation of object-centered space in monkeys and humans. Annu Rev Neurosci 26:331-354.

Olson CR, Gettner SN (1995) Object-centered direction selectivity in the macaque supplementary eye field. Science 269:985-988.

Olson CR, Gettner SN (1996) Brain representation of object-centered space. Curr Opin Neurobiol 6:165-170.

Olson CR, Gettner SN (1999) Macaque SEF neurons encode object-centered directions of eye movements regardless of the visual attributes of instructional cues. J Neurophysiol 81:2340-2346.

Olson CR, Tremblay L (2000) Macaque supplementary eye field neurons encode object-centered locations relative to both continuous and discontinuous objects. J Neurophysiol 83:2392-2411.

Olson IR, Moore KS, Stark M, Chatterjee A (2006a) Visual working memory is impaired when the medial temporal lobe is damaged. J Cogn Neurosci 18:1087-1097.

Olson IR, Page K, Moore KS, Chatterjee A, Verfaellie M (2006b) Working memory for conjunctions relies on the medial temporal lobe. J Neurosci 26:4596-4601.

Orban GA, Van Essen D, Vanduffel W (2004) Comparative mapping of higher visual areas in monkeys and humans. Trends Cogn Sci 8:315-324.

Pasternak T, Greenlee MW (2005) Working memory in primate sensory systems. Nat Rev Neurosci 6:97-107.

Paus T (1996) Location and function of the human frontal eye-field: a selective review. Neuropsychologia 34:475-483.

Paus T, Jech R, Thompson CJ, Comeau R, Peters T, Evans AC (1997) Transcranial magnetic stimulation during positron emission tomography: a new method for studying connectivity of the human cerebral cortex. J Neurosci 17:3178-3184.

Perenin MT, Vighetto A (1988) Optic ataxia: a specific disruption in visuomotor mechanisms. I. Different aspects of the deficit in reaching for objects. Brain 111 (Pt 3):643-674.

Pertzov Y, Avidan G, Zohary E (2011) Multiple reference frames for saccadic planning in the human parietal cortex. J Neurosci 31:1059-1068.

Pesaran B, Nelson MJ, Andersen RA (2006) Dorsal premotor neurons encode the relative position of the hand, eye, and goal during reach planning. Neuron 51:125-134.

Philbeck JW, Loomis JM, Beall AC (1997) Visually perceived location is an invariant in the control of action. Percept Psychophys 59:601-612.

Pierrot-Deseilligny C, Milea D, Muri RM (2004) Eye movement control by the cerebral cortex. Curr Opin Neurol 17:17-25.

Pierrot-Deseilligny C, Rivaud S, Gaymard B, Agid Y (1991) Cortical control of reflexive visually-guided saccades. Brain 114 (Pt 3):1473-1485.

Pierrot-Deseilligny C, Muri RM, Ploner CJ, Gaymard B, Rivaud-Pechoux S (2003) Cortical control of ocular saccades in humans: a model for motricity. Prog Brain Res 142:3-17.

Pitzalis S, Sereno M, Committeri G, Galati G, Fattori P, Galletti C (2006) A possible human homologue of the macaque V6A. Journal of Vision 6:536a.

Pollack JG, Hickey TL (1979) The distribution of retino-collicular axon terminals in rhesus monkey. J Comp Neurol 185:587-602.

Poncelet BP, Wedeen VJ, Weisskoff RM, Cohen MS (1992) Brain parenchyma motion: measurement with cine echo-planar MR imaging. Radiology 185:645-651.

Pouget A, Ducom JC, Torri J, Bavelier D (2002) Multisensory spatial representations in eye-centered coordinates for reaching. Cognition 83:B1-11.

Prado J, Clavagnier S, Otzenberger H, Scheiber C, Kennedy H, Perenin MT (2005) Two cortical systems for reaching in central and peripheral vision. Neuron 48:849-858.

Rayner K (1998) Eye movements in reading and information processing: 20 years of research. Psychol Bull 124:372-422.

Rayner K (2009) Eye movements and attention in reading, scene perception, and visual search. Q J Exp Psychol (Hove) 62:1457-1506.

Reed CL, Grubb JD, Steele C (2006) Hands up: attentional prioritization of space near the hand. J Exp Psychol Hum Percept Perform 32:166-177.

Robin J, Hirshhorn M, Rosenbaum RS, Winocur G, Moscovitch M, Grady CL (2014) Functional connectivity of hippocampal and prefrontal networks during episodic and spatial memory based on real-world environments. Hippocampus 25:81-93.

Rodieck RW, Watanabe M (1993) Survey of the morphology of macaque retinal ganglion cells that project to the pretectum, superior colliculus, and parvicellular laminae of the lateral geniculate nucleus. J Comp Neurol 338:289-303.

Rosenbaum RS, Ziegler M, Winocur G, Grady CL, Moscovitch M (2004) "I have often walked down this street before": fMRI studies on the hippocampus and other structures during mental navigation of an old environment. Hippocampus 14:826-835.

Rossetti Y, Pisella L, Vighetto A (2003) Optic ataxia revisited: Visually guided action versus immediate visuomotor control. Experimental Brain Research 153:171-179.

Ruff CC, Bestmann S, Blankenburg F, Bjoertomt O, Josephs O, Weiskopf N, Deichmann R, Driver J (2008) Distinct causal influences of parietal versus frontal areas on human visual cortex: evidence from concurrent TMS-fMRI. Cereb Cortex 18:817-827.

Russo GS, Bruce CJ (1996) Neurons in the supplementary eye field of rhesus monkeys code visual targets and saccadic eye movements in an oculocentric coordinate system. J Neurophysiol 76:825-848.

Sabes PN, Breznen B, Andersen RA (2002) Parietal representation of object-based saccades. J Neurophysiol 88:1815-1829.

Salmon E, Van der Linden M, Collette F, Delfiore G, Maquet P, Degueldre C, Luxen A, Franck G (1996) Regional brain activity during working memory tasks. Brain 119 (Pt 5):1617-1625.

Schall JD (1991) Neuronal activity related to visually guided saccades in the frontal eye fields of rhesus monkeys: comparison with supplementary eye fields. J Neurophysiol 66:559-579.

Schall JD, Thompson KG (1999) Neural selection and control of visually guided eye movements. Annu Rev Neurosci 22:241-259.

Schenk T (2006) An allocentric rather than perceptual deficit in patient D.F. Nat Neurosci 9:1369-1370.

Schiller PH, Malpeli JG (1977) Properties and tectal projections of monkey retinal ganglion cells. J Neurophysiol 40:428-445.

Schlag J, Schlag-Rey M (1985) Unit activity related to spontaneous saccades in frontal dorsomedial cortex of monkey. Exp Brain Res 58:208-211.

Schlag J, Schlag-Rey M (1987) Evidence for a supplementary eye field. J Neurophysiol 57:179-200.

Schluppeck D, Glimcher P, Heeger DJ (2005) Topographic organization for delayed saccades in human posterior parietal cortex. J Neurophysiol 94:1372-1384.

Schmidt T, Werner S, Diedrichsen J (2003) Spatial distortions induced by multiple visual landmarks: how local distortions combine to produce complex distortion patterns. Percept Psychophys 65:861-873.

Schutz I, Henriques DY, Fiehler K (2013) Gaze-centered spatial updating in delayed reaching even in the presence of landmarks. Vision Res 87:46-52.

Scott SH, Kalaska JF (1997) Reaching movements with similar hand paths but different arm orientations .1. Activity of individual cells in motor cortex. Journal of Neurophysiology 77:826-852.

Scott SH, Sergio LE, Kalaska JF (1997) Reaching movements with similar hand paths but different arm orientations .2. Activity of individual cells in dorsal premotor cortex and parietal area 5. Journal of Neurophysiology 78:2413-2426.

Seal J, Commenges D (1985) A quantitative analysis of stimulus- and movement-related responses in the posterior parietal cortex of the monkey. Exp Brain Res 58:144-153.

Sereno MI, Pitzalis S, Martinez A (2001) Mapping of contralateral space in retinotopic coordinates by a parietal cortical area in humans. Science 294:1350-1354.

Sergio LE, Kalaska JF (1998) Changes in the temporal pattern of primary motor cortex activity in a directional isometric force versus limb movement task. J Neurophysiol 80:1577-1583.

Sergio LE, Kalaska JF (2003) Systematic changes in motor cortex cell activity with arm posture during directional isometric force generation. J Neurophysiol 89:212-228.

Sergio LE, Hamel-Paquet C, Kalaska JF (2005) Motor cortex neural correlates of output kinematics and kinetics during isometric-force and arm-reaching tasks. J Neurophysiol 94:2353-2378.

Sharika KM, Ramakrishnan A, Murthy A (2014) Use of exocentric and egocentric representations in the concurrent planning of sequential saccades. J Neurosci 34:16009-16021.

Shelton AL, Gabrieli JD (2002) Neural correlates of encoding space from route and survey perspectives. J Neurosci 22:2711-2717.

Shen LM, Alexander GE (1997) Preferential representation of instructed target location versus limb trajectory in dorsal premotor area. Journal of Neurophysiology 77:1195-1212.

Silk TJ, Bellgrove MA, Wrafter P, Mattingley JB, Cunnington R (2010) Spatial working memory and spatial attention rely on common neural processes in the intraparietal sulcus. Neuroimage 53:718-724.

Simon SS (2008) Merging of the senses. Front Neurosci 2:13-14.

Sparks DL (1986) Translation of sensory signals into commands for control of saccadic eye movements: role of primate superior colliculus. Physiol Rev 66:118-171.

Sparks DL, Freedman EG, Chen LL, Gandhi NJ (2001) Cortical and subcortical contributions to coordinated eye and head movements. Vision Res 41:3295-3305.

Stein BE, Stanford TR (2008) Multisensory integration: current issues from the perspective of the single neuron. Nat Rev Neurosci 9:255-266.

Stricanne B, Andersen RA, Mazzoni P (1996) Eye-centered, head-centered, and intermediate coding of remembered sound locations in area LIP. J Neurophysiol 76:2071-2076.

Tanji J, Hoshi E (2008) Role of the lateral prefrontal cortex in executive behavioral control. Physiol Rev 88:37-57.

Tanne-Gariepy J, Rouiller EM, Boussaoud D (2002) Parietal inputs to dorsal versus ventral premotor areas in the macaque monkey: evidence for largely segregated visuomotor pathways. Exp Brain Res 145:91-103.

Tark KJ, Curtis CE (2009) Persistent neural activity in the human frontal cortex when maintaining space that is off the map. Nat Neurosci 12:1463-1468.

Tatler BW, Land MF (2011) Vision and the representation of the surroundings in spatial memory. Philos Trans R Soc Lond B Biol Sci 366:596-610.

Thaler L, Goodale MA (2011a) The role of online visual feedback for the control of target-directed and allocentric hand movements. J Neurophysiol 105:846-859.

Thaler L, Goodale MA (2011b) Neural substrates of visual spatial coding and visual feedback control for hand movements in allocentric and target-directed tasks. Front Hum Neurosci 5:92.

Thier P, Andersen RA (1996) Electrical microstimulation suggests two different forms of representation of head-centered space in the intraparietal sulcus of rhesus monkeys. Proc Natl Acad Sci U S A 93:4962-4967.

Tobler PN, Muri RM (2002) Role of human frontal and supplementary eye fields in double step saccades. Neuroreport 13:253-255.

Tolman EC (1948) Cognitive maps in rats and men. Psychol Rev 55:189-208.

Tomassini V, Jbabdi S, Klein JC, Behrens TE, Pozzilli C, Matthews PM, Rushworth MF, Johansen-Berg H (2007) Diffusion-weighted imaging tractography-based parcellation of the human lateral premotor cortex identifies dorsal and ventral subregions with anatomical and functional specializations. J Neurosci 27:10259-10269.

Toni I, Thoenissen D, Zilles K (2001) Movement preparation and motor intention. Neuroimage 14:S110-117.

Tunik E, Lo OY, Adamovich SV (2008) Transcranial magnetic stimulation to the frontal operculum and supramarginal gyrus disrupts planning of outcome-based hand-object interactions. J Neurosci 28:14422-14427.

Uchimura M, Kitazawa S (2013) Cancelling prism adaptation by a shift of background: a novel utility of allocentric coordinates for extracting motor errors. J Neurosci 33:7595-7602.

Uchimura M, Nakano T, Morito Y, Ando H, Kitazawa S (2015) Automatic representation of a visual stimulus relative to a background in the right precuneus. Eur J Neurosci 42:1651-1659.

Ungerleider LG, Mishkin M (1982) Two cortical visual systems. In: Analysis of visual behavior (Ingle DJ, Goodale MA, Mansfield RJW, eds), pp 549-586. Cambridge: MIT Press.

Van Oostende S, Van Hecke P, Sunaert S, Nuttin B, Marchal G (1997) FMRI studies of the supplementary motor area and the premotor cortex. Neuroimage 6:181-190.

Van Pelt S, Toni I, Diedrichsen J, Medendorp WP (2010) Repetition suppression dissociates spatial frames of reference in human saccade generation. J Neurophysiol 104:1239-1248.

Vergilino-Perez D, Fayel A, Lemoine C, Senot P, Vergne J, Dore-Mazars K (2012) Are there any left-right asymmetries in saccade parameters? Examination of latency, gain, and peak velocity. Invest Ophthalmol Vis Sci 53:3340-3348.

Vesia M, Crawford JD (2012) Specialization of reach function in human posterior parietal cortex. Exp Brain Res 221:1-18.

Vesia M, Prime SL, Yan X, Sergio LE, Crawford JD (2010) Specificity of human parietal saccade and reach regions during transcranial magnetic stimulation. J Neurosci 30:13053-13065.

Vindras P, Viviani P (1998) Frames of reference and control parameters in visuomanual pointing. J Exp Psychol Hum Percept Perform 24:569-591.

Vogeley K, Fink GR (2003) Neural correlates of the first-person-perspective. Trends Cogn Sci 7:38-42.

Weinrich M, Wise SP (1982) The premotor cortex of the monkey. J Neurosci 2:1329-1345.

Westendorff S, Klaes C, Gail A (2010) The cortical timeline for deciding on reach motor goals. J Neurosci 30:5426-5436.

Wexler M (2003) Voluntary head movement and allocentric perception of space. Psychol Sci 14:340-346.

Whitney D, Westwood DA, Goodale MA (2003) The influence of visual motion on fast reaching movements to a stationary object. Nature 423:869-873.

Wise SP, Weinrich M, Mauritz KH (1986) Movement-related activity in the premotor cortex of rhesus macaques. Prog Brain Res 64:117-131.

Wolbers T, Wiener JM (2014) Challenges for identifying the neural mechanisms that support spatial navigation: the impact of spatial scale. Front Hum Neurosci 8:571.

Wurtz RH, Albano JE (1980) Visual-motor function of the primate superior colliculus. Annu Rev Neurosci 3:189-226.

Yang Q, Kapoula Z (2004) TMS over the left posterior parietal cortex prolongs latency of contralateral saccades and convergence. Invest Ophthalmol Vis Sci 45:2231-2239.

Zaehle T, Jordan K, Wustenberg T, Baudewig J, Dechent P, Mast FW (2007) The neural basis of the egocentric and allocentric spatial frame of reference. Brain Res 1137:92-103.

Zimmer U, Lewald J, Erb M, Karnath HO (2006) Processing of auditory spatial cues in human cortex: an fMRI study. Neuropsychologia 44:454-461.

APPENDIX: Author Contributions

Chapter 2 (from Chen, Monaco, Byrne, Yan, Henriques, & Crawford, 2014)

- Created and designed the experiment: Ying Chen, J. Douglas Crawford
- Designed the experimental apparatus used in scanner: Ying Chen
- Recruited participants, set up the apparatus and collected data: Ying Chen
- Analyzed data: Ying Chen (assisted by Simona Monaco)
- Contributed materials and relevant analysis tools: Ying Chen, Simona Monaco, Xiaogang Yan, Denise Henriques, & J. Douglas Crawford
- Wrote the paper: Ying Chen (assisted by J. Douglas Crawford & Simona Monaco)

Chapter 3 (from Chen & Crawford, submitted / in review)

- Created and designed the experiment: Ying Chen, J. Douglas Crawford
- Recruited participants, set up the apparatus and collected data: Ying Chen
- Analyzed data: Ying Chen
- Contributed materials and relevant analysis tools: Ying Chen, J. Douglas Crawford
- Wrote the paper: Ying Chen (assisted by J. Douglas Crawford)

Chapter 4 (from Chen, Monaco, & Crawford, submitted / in review)

- Created and designed the experiment: Ying Chen, J. Douglas Crawford
- Recruited participants, set up the apparatus and collected data: Ying Chen
- Analyzed data: Ying Chen (some feedback provided by Simona Monaco)
- Contributed materials and relevant analysis tools: Ying Chen, Simona Monaco, &

J. Douglas Crawford

- Wrote the paper: Ying Chen (assisted by J. Douglas Crawford, some feedback provided by Simona Monaco)